

**ADVANCED POPULATION PHARMACOKINETIC MODELLING TO QUANTIFY  
SELECTED CHARACTERISTICS OF DRUGS**

Dissertation  
zur  
Erlangung des Doktorgrades (Dr. rer. nat.)  
der  
Mathematisch-Naturwissenschaftlichen Fakultät  
der  
Rheinischen Friedrich-Wilhelms-Universität Bonn

vorgelegt von

Khaled Mohammed Abdulwahab Abduljalil  
aus  
Taiz-Jemen

Bonn, Februar 2010

Angefertigt mit Genehmigung der Mathematisch-Naturwissenschaftlichen Fakultät  
der Rheinischen Friedrich-Wilhelms-Universität Bonn  
Am Pharmakologischem Institut der Universität zu Köln

1. Gutachter

Prof. Dr. Richard Süverkrüp  
Pharmazeutisches Institut der Universität Bonn,  
Pharmazeutische Technologie,  
Gerhard-Domagk-Straße  
53121 Bonn,  
Germany

2. Gutachter

Prof. med. Dr. Uwe Fuhr  
Klinikum der Universität zu Köln,  
Institut für Pharmakologie, Klinische Pharmakologie  
Gleueler Straße 24,  
50931 Köln  
Germany

Tag der Promotion: 26.07.2010

Erscheinungsjahr: 2010

**IN DER DISSERTATION EINGEBUNDEN:**

Zusammenfassung

Lebenslauf

For obtaining the doctorate degree in pharmacy  
Pharmaceutical Technology Section  
Department of Pharmacy,  
Faculty of Mathematics and Natural Science  
University of Bonn  
Germany

Doctoral Thesis 2010  
Department of Pharmacology  
University of Cologne  
Germany

To my parents

## Publications

This thesis is based on the following papers:

- **Abduljalil K**, Diestelhorst M, Doroshenko O, Lux A, Steinfeld A, Dinslage S, Süverkrüp R, Fuhr U. Modelling ocular pharmacokinetics of fluorescein administered as lyophilisate or conventional eye drops. *Eur J Clin Pharmacol*. 2008 May;64(5):521-9.
- **Abduljalil K**, Kinzig M, Bulitta J, Horkovics-Kovats S, Sörgel F, Rodamer M, Fuhr U. Modeling the autoinhibition of clarithromycin metabolism during repeated oral administration. *Antimicrob Agents Chemother*. 2009 Jul;53(7):2892-901.
- **Abduljalil K**, Frank D, Gaedigk A, Klaasse T, Tomalik-Scharte D, Jetter A, Jaehde U, Kirchheiner J, Fuhr U. Activity assessment for individual CYP2D6 alleles by population pharmacokinetics of dextromethorphan. To be submitted to *Clin Pharmacol Ther*
- **Abduljalil K**, Stehle S, Zadoyan G, Schwab M, Lazar A, Tomalik-Scharte D, Kirchheiner J, Gleiter C, Harenberg J, Wu W, Fuhr U. Prospective evaluation of the pharmacogenetics component in pharmacokinetics and pharmacodynamics of steady state phenprocoumon. To be submitted to *Clin Pharmacol Ther*

# CONTENTS

<b>1</b>	<b>INTRODUCTION.....</b>	<b>1</b>
1.1	GENERAL INTRODUCTION.....	1
1.2	AIM OF THE THESIS.....	3
1.3	OVERVIEW OF POPULATION APPROACHES.....	4
1.3.1	<i>Definitions.....</i>	4
1.3.2	<i>Theory of Population Approach.....</i>	5
1.3.3	<i>Software.....</i>	6
1.3.4	<i>Types of Models.....</i>	6
1.3.5	<i>Model Development and Evaluation Strategies.....</i>	7
1.3.6	<i>Properties of the Final Model.....</i>	8
1.4	POTENTIAL EXAMPLES OF MODELLING PHARMACOKINETIC-PHARMACODYNAMIC PROCESSES.....	8
1.4.1	<i>Absorption.....</i>	8
1.4.2	<i>Distribution.....</i>	10
1.4.3	<i>Clearance.....</i>	10
1.4.3.1	<i>Variability in renal clearance.....</i>	10
1.4.3.2	<i>Variability in hepatic clearance.....</i>	11
1.4.4	<i>Metabolites.....</i>	12
1.4.5	<i>Modelling Drug Response.....</i>	13
1.5	CHARACTERISTICS OF PROBE DRUGS.....	15
1.5.1	<i>Chemical Structures.....</i>	16
1.5.2	<i>Bioavailability of Fluorescein for Ocular Administration.....</i>	17
1.5.3	<i>Clarithromycin and Autoinhibition of Metabolism.....</i>	19
1.5.4	<i>The Use of Dextromethorphan as a CYP2D Phenotyping Drug.....</i>	22
1.5.5	<i>Understanding Variability in Phenprocoumon Response.....</i>	25
<b>2</b>	<b>MATERIALS AND METHODS.....</b>	<b>29</b>
2.1	FLUORESCHEIN DATA.....	30
2.1.1	<i>Clinical Studies and Ethical Conduct.....</i>	30
2.1.2	<i>Measurements and Variables.....</i>	30
2.2	CLARITHROMYCIN DATA.....	31
2.2.1	<i>Clinical Studies and Ethical Conduct.....</i>	31
2.2.2	<i>Measurements and Variables.....</i>	32
2.3	DEXTROMETHORPHAN DATA.....	33
2.3.1	<i>Clinical Studies and Ethical Conduct.....</i>	33
2.3.2	<i>Measurements and Variables.....</i>	33
2.4	PHENPROCOUMON DATA.....	35
2.4.1	<i>Clinical Studies and Ethical Conduct.....</i>	35
2.4.2	<i>Measurements and Variables.....</i>	35
2.5	DATA ANALYSIS.....	37
2.5.1	<i>Software.....</i>	37
2.5.2	<i>Model Justifications.....</i>	38
2.5.3	<i>Covariate Analyses.....</i>	39
2.5.4	<i>Statistical Models.....</i>	39
2.5.5	<i>Fluorescein Data Analysis.....</i>	40
2.5.6	<i>Clarithromycin Data Analysis.....</i>	41
2.5.7	<i>Dextromethorphan Data Analysis.....</i>	43
2.5.8	<i>Phenprocoumon Data Analysis.....</i>	44
<b>3</b>	<b>RESULTS.....</b>	<b>47</b>
3.1	FLUORESCHEIN.....	48
3.2	CLARITHROMYCIN.....	59
3.3	DEXTROMETHORPHAN.....	75
3.4	PHENPROCOUMON.....	90
<b>4</b>	<b>DISCUSSION.....</b>	<b>103</b>

4.1	FLUORESCEIN .....	104
4.2	CLARITHROMYCIN .....	106
4.3	DEXTROMETHORPHAN .....	109
4.4	PHENPROCOUMON .....	111
<b>5</b>	<b>CONCLUSIONS.....</b>	<b>115</b>
5.1	FLUORESCEIN .....	116
5.2	CLARITHROMYCIN .....	116
5.3	DEXTROMETHORPHAN .....	117
5.4	PHENPROCOUMON .....	117
<b>6</b>	<b>SUMMARY .....</b>	<b>118</b>
<b>7</b>	<b>REFERENCES:.....</b>	<b>120</b>
<b>8</b>	<b>ACKNOWLEDGMENTS .....</b>	<b>141</b>
<b>9</b>	<b>CURRICULUM VITAE.....</b>	<b>106</b>

# 1 INTRODUCTION

## 1.1 General Introduction

A drug profile is continuously refined and qualified with progressive understanding of its pharmacokinetics (PK) and pharmacodynamics (PD). Traditionally, understanding of PK [PD] behaviour has been based on fitting a mathematical model to data obtained from highly selected individuals. The obtained model should then give the opportunity to predict the extent and time course of the exposure [related to a pharmacological effect and adverse events] and to optimise therapeutic outcomes (Rowland and Tozer 1989; Derendorf et al. 2000; Gieschke and Steimer 2000). In fact, PK and PD are complex processes in nature with a high degree of variability due to the impact of a myriad of interactions that arise from differences in the pathophysiologic, demographic and/or genotypic characteristics between individuals, or over time within a given individual (Rowland and Tozer 1989). Unfortunately, such variability can potentially affect all PK and PD parameters estimates. The precise assessment of such variability is hampered by estimates of uncertainty (Bois 2001), which are basically due to a lack of knowledge on the variability stemming from various sources, including model simplifications or misspecifications (Nestorov 2001; Gueorguieva et al. 2005).

Pharmacokinetic and pharmacodynamic evaluations can be performed by modelling data either from each subject (“individual approach”) or from a group of individuals together (“population approach”). The individual approach requires intensive individual sampling to draw reliable conclusions; however, in many cases (and for ethical and/or clinical reasons), only limited samples are possible. For instance, the frequent withdrawal of blood *samples* may not be a feasible basis for PK/ PD investigations in the case of HIV-infected (Roos et al. 2008), anaemic (Vincent et al. 2006) or paediatric (Cole et al. 2006) populations. Furthermore, individual subjects provide insufficient information due to the fact that not all aspects are exhibited by all subjects or that the model specifications are simply not appropriate. For instance, it is common in pharmacokinetics that a one-compartment model can frequently fit plasma concentration data of a particular drug from some individuals, but a two-compartment model is needed to fit data from other individuals in the same study (Schoemaker and Cohen 1996; Bonate 2006). Considerable interindividual variability in plasma concentration levels (and consequently the therapeutic outcome) of many drugs like



## INTRODUCTION

antidepressants and anticoagulants has been recently explained by genetic and demographic factors (Lessard et al. 1999; Ma et al. 2004; Stehle et al. 2008). These examples show that the individual approach can mask an important PK characteristic that may have serious outcomes, especially if these drugs are of narrow therapeutic index or potentially interact with other drugs (Lessard et al. 1999; Hughes et al. 2004; Hung et al. 2005).

It has been recognized that the most effective tool to deal with these problems is the application of the population approach. The data provided by different subjects can be integrated (Schoemaker and Cohen 1996) and the subjects' characteristics can be co-analyzed to obtain adequate parameter estimates. Because of its ability to partly disentangle the uncertainty from the variability, the population approach can produce a general model of sensible parameter estimates, which differ randomly between individuals (Bois 2001). The obtained model should then enable description of the data for each and all individuals adequately (Sheiner and Ludden 1992; Ette et al. 2004). Extensive contextualization of the methodology and the applications of this approach in drug development are available (Gieschke and Steimer 2000; Ette, E.I. and Williams, P.J. 2007; Grasela et al. 2007).

For the current study, I shall provide a relevant framework of this approach and potential examples of its applications before embarking on modelling the drug probes of interest; fluorescein, clarithromycin, dextromethorphan and phenprocoumon. Although the context presented here will be illustrated with pharmacokinetics in most cases, the general principles are applicable to pharmacodynamics as well, unless stated otherwise.

## 1.2 Aim of the Thesis

The overall aim of the thesis was to quantify selected pharmacokinetic and/or pharmacodynamic characteristics of specific probe drugs utilizing the advantages of the population analysis approach. By accounting for the between-subject variability in the population approach, the final developed model is expected to carry great advantages compared to standard non-compartmental analysis. Simulation of final models outcomes in addition to prior information about respective drugs pharmacology were used to build a confidence about the utility of the presented models.

The specific aims are to:

- Compare the ocular pharmacokinetics of a lyophilisate formulation in relation to eye drops and to develop an empiric ocular population pharmacokinetic model describing concentrations in the cornea and anterior chamber adequately. Fluorescein sodium was selected as a probe drug because it is safe and extensively used as a diagnostic substance in ophthalmology and because local concentrations can be determined non-invasively by flurophotometry.
- Quantitatively describe the nonlinearity in the pharmacokinetics of clarithromycin in the presence of its active metabolite, 14(R)-hydroxy-clarithromycin and to better understand the time course of inhibition via population pharmacokinetic modelling. These data are important for a better understanding of the underlying processes and for the assessment of dose adjustments of clarithromycin and co-administered CYP3A4 substrates.
- Assess the activity of individual CYP2D6 alleles with regard to the clearance of dextromethorphan to dextrorphan. These data are needed for a better prediction of CYP2D6 activity from genotypes for respective dose adjustments of CYP2D6 substrates.
- Develop a general population PK/PD model for phenprocoumon that combines demographic and genetic covariates to explain the variability of the entire dose-exposure-response relationship. This information is a prerequisite for prediction of the individual optimal phenprocoumon dosing based on mechanistic rather than empirical considerations.

## 1.3 Overview of Population Approaches

### 1.3.1 Definitions

According to the definition of the US Food and Drug Administration (FDA), Population pharmacokinetics (PopPK) is “the study of the sources and correlates of variability in drug concentrations among individuals who are the target patient population receiving clinically relevant doses of a drug of interest”. Certain patient demographical, pathophysiological, and therapeutic features, such as body weight, age, excretory and metabolic functions, and the presence of other therapies, can regularly alter dose–concentration relationships (FDA 1999). However, there is currently no definition for population pharmacodynamics (PopPD) provided by the FDA. PopPD aims to interpret and describe the sources and correlates of variability in therapeutic outcome, in a quantitative fashion and in a target population receiving clinically relevant doses (Ette, E.I. and Williams, P.J. 2007). The Population Model is an elaborate statistical model which deals with identifying and quantifying the types, degrees and causes of differences within and between individuals, often depending on sparse pharmacokinetic/pharmacodynamic data (Williams and Ette 2007). The comprehensive field of drug evaluations that involves the development or estimation of pharmacokinetics, pharmacodynamics, linking pharmacodynamic–outcomes and disease progression models, is called pharmacometrics (Ette, E.I. and Williams, P.J. 2007).

In the arena of pharmacometrics, simulation is defined as the generation of data using certain types of mathematical and probabilistic models describing the behaviour of the system under study. It provides convincing objective evidence of the merits of a proposed study design and analysis (FDA 1999).

### 1.3.2 Theory of Population Approach

Within the framework of population nonlinear mixed effects models, and if the data come from  $j=1, \dots, N$  individuals, then the observed response of interest, e.g., plasma concentration, in an individual can be described as

$$Y_{ij} = f(\phi_j, x) + \varepsilon_{ij}$$

where the dependent variable  $Y_{ij}$  for  $i = 1, \dots, n_j$  is the response of interest (e.g. drug concentrations) of the  $j$ th subject. The symbol  $f$  stands for a function that predicts the response in the  $j$ th subject (e.g., one or several exponentials), which is a function of known quantities,  $x$  (time of observation, drug dose) and parameters,  $\phi$  (drug clearance, volume of distribution, rate constant). The quantities in  $x$  are known, because they are either measured or controlled, and therefore, are called “fixed effects”. The parameters in the  $\phi_i$  vector are called “fixed effect parameters” because they quantify the influence of the fixed effects on the dependent variable. The individual  $\phi_j$  is assumed to arise from some multivariate probability. The last part of the previous equation,  $\varepsilon_{ij}$  is the residual error of the model, i.e., the  $i$ th measurement of the difference between the observed and the predicted response in the  $j$ th subject. It is assumed to come from probability distributions with a mean of zero and the same (usually unknown) variance. If the distribution of  $\varepsilon_{ij}$  is assumed to be normal, with zero mean and uniform variance, then the maximum likelihood estimation reduces to ordinary least squares estimation. Although the function  $\phi_j$  will differ between individuals, it is realistic to assume that the set of model structural parameters is qualitatively the same for all individuals and that the parameters vary quantitatively among individuals. Mathematically this can be written as

$$\phi_j = g(\theta, z_j) + \eta_j$$

where  $g$  is a known function that describes the expected value of  $\phi_j$  as a function of individual specific covariates  $z_j$ , such as weight, age etc., and the vector of population parameters  $\theta$ . The symbol  $\eta_j$  represents the random variation of the individual parameter vectors around the population prediction. The  $\eta_j$  is usually assumed to be independent across individuals (i.e.,  $\eta_j, \eta_l$  are independent for  $j \neq l$ ) and follow a lognormal distribution with a median of 1 and a constant coefficient of variation. It does not follow that each  $\theta$  must have a corresponding  $\eta$ . Because this model describes the influence of both fixed and

random effects, it is called a “mixed effect model” (Sheiner and Beal 1980; Ette and Williams 2004; Bonate 2006).

### **1.3.3 Software**

Many software programs have been widely used in PopPK and PopPD such as NONMEM (Beal and Sheiner 1980), ADAPT (D’Argenio and Schumitzky 2008), and MONOLIX (Lavielle and Mentre 2007). These programs differ in the number of assumptions made regarding the statistical distribution of the estimated parameters (Aarons 1999; Bauer et al. 2007). They take either a parametric approach with strong assumptions (typically of a Gaussian distribution (Beal and Sheiner 1980; Lindstrom and Bates 1990) or Bayesian approach (Lunn et al. 2002)), a semiparametric view with relaxed assumption (Verotta et al. 1989; Wang, Y et al. 2008) or a nonparametric (no assumption) approach (Mallet et al. 1988; Jelliffe et al. 2000). During modelling, the program uses a minimization routine to fine-tune an initial set of model parameter estimates specified by the user. This process repeats through several iterations until the model has reached convergence.

### **1.3.4 Types of Models**

Population models are commonly classified into descriptive and predictive models according to their functions or to mechanistic and empirical models according to their principle.

Unlike predictive models, descriptive models are derived from certain data and cannot be extrapolated. For instance, the linear concentration-effect relationship may not be extrapolated beyond the range of observed concentrations but the  $E_{max}$ -type models can be used. The danger of extrapolating the descriptive model in this case could be a high incidence of side effects due to greater exposure of the drug (Gobburu 2004; Bonate 2006).

Likewise, mechanistic models allow direct and/or indirect linkage to physiological processes, whereas empiric models do not allow such relation. Mechanistic models, such as physiological-based pharmacokinetic models are based on physical and physiological principles and should have as many features of the system incorporated into the model as the data allow (Thakur 1991; Bonate 2006).

Actually, most known population models are said to be hybrid models, i.e., mechanistic in areas where the physiology and pharmacology of the system are understood and empirical in places that are still black boxes.

### **1.3.5 Model Development and Evaluation Strategies**

The process of model development usually begins with appropriate identification of the model structure based on physiological and mathematical bases that serve its usefulness (Ette et al. 2003; Bonate 2006). To identify the model appropriately, prior information regarding the model parameters and the influencing covariates are very helpful to specify and optimize the model structure (Maitre et al. 1991). Data visualization usually guides and determines the model building strategy, and hence directly influences the efficacy with which the final model is derived. Other means that guide model development should include objective function minimization and inclusion of random parameters and covariates (Ette and Ludden 1995; Jonsson et al. 2007).

Modelling both PK and PD data can be done either sequentially or simultaneously. In the sequential modelling, the PD is conditioned on the PK estimates. In the simultaneous model, the parameters are considered to be jointly distributed and the flow of information is bidirectional (Williams et al. 2001; Zhang et al. 2003a; Zhang et al. 2003b). Both approaches appear to provide similar results (Davidian and Giltinan 1993; Zhang et al. 2003a).

In many cases, a link model between PK and PD data provides the essential integrated step to arrive at an enlightened understanding of the dose-exposure-response relationship. This link can be described directly or indirectly by many models, e.g., mechanistic or empirical models (Williams et al. 2001; Williams and Ette 2007).

Once the model is developed, it should be evaluated for its reliability, potential misspecifications and for its stability (Ette et al. 2003; Bonate 2006). Reliability of a final model can be checked via the assessment of the uncertainty of the parameters and random effects (Ette et al. 1998; Williams et al. 2007). Mis-specifications and systematic error can be identified through goodness-of-fit plots, which include plots of predicted values, residuals and the possible impact of individuals' covariates. These plots provide helpful information about whether the model addresses all relevant aspects of data or whether part(s) of the model need(s) further attention (Logan 2003; Williams et al. 2007). In addition, visual predictive check plots and simulated graphics are also helpful to ensure adequate model performance (Post et al. 2008). Indeed, simulation has recently gained recognition as a useful tool for providing more informed and scientifically sound decision-making regarding the developed model and its logical implications (FDA 1999; Holford 2006; Williams and Ette 2007) and any future changes in the drug profile towards new dosing schedules (Hamberg et

al. 2007; Nomura et al. 2008). The final model stability can be assessed by its resistance to data change (Ette 1997; Williams et al. 2007) or by omitting a portion of the data and comparing the result of the reduced data set with those of the full data set (Zandvliet et al. 2005).

### **1.3.6 Properties of the Final Model**

The final model should at least be useful as “the true or right” model is unknown. For a population model to be useful, it should represent the interaction between the drug and the biological system. Since general effects in a clinical data set can be blurred by other sources of variation or by random effects, a useful model should provide a summary of the data in terms of the fixed effects and the nature and magnitude of the random effects. It should mimic the complexity of biological processes. A gross complex model is, in general, difficult to solve numerically, difficult to interpret and may falsely convey confidence in the study findings. On the other hand, a very simple model can lead to loss of information about the biological system. In these circumstances, balanced assumptions are needed for the model to be descriptive and the biological system or process to be predictive (Haefner 1996; Kimko and Duffull 2003; Bonate 2006). Thus, a useful model should also be simple, transparent, applicable, informative, descriptive, predictive, retrodictive and valid (Bonate 2006; Ette, E.I. and Williams, P.J. 2007).

## **1.4 Potential Examples of Modelling Pharmacokinetic-Pharmacodynamic Processes**

Serious clinical consequences can be caused by variability, which in most cases can lead to unexpected or unusual characteristics in drug profiles. These features cannot be quantified by simple tools of analysis and thus extensive work is required. To come up with a useful model based on plausible concepts, it is essential to describe this variability at the level of the underlying processes.

### **1.4.1 Absorption**

Drug absorption after oral administration is a highly variable process and an extremely complex phenomenon that depends upon the interaction between three types of variables;

## INTRODUCTION

(i) drug-specific variables, such as the physicochemical properties of the drug and its dosage form, etc, (ii) patient-specific variables, such as the (patho)physiology of the gastrointestinal tract, first pass effect, genetics, diet and concomitant drugs etc and (iii) population variables, such as the distribution of (patho)physiological factors (Petricoulo et al. 2007).

When efficacy and/or safety are related to maximum drug concentration, it may be important to describe the absorption phase accurately (Kleinbloesem et al. 1987; Bagli et al. 1996; Bagli et al. 1999). The occurrence of cardiotoxicity of fluoroquinolones, for instance, was related to their maximum concentration in plasma (Rubinstein and Camm 2002). The difficulty in dose adjustment of ophthalmic preparations may lead to potential ocular damage or systemic toxicity (Noecker et al. 2004; Fraunfelder 2006).

More often, drug plasma concentration profiles are irregular shortly after oral administration and cannot be interpreted easily with conventional models based on first- or zero-order absorption kinetics and lag time (Zhou 2003). In such cases, more complex models are needed, such as those based on Weibull function (Zhou 2003; Rousseau et al. 2004), inverse Gaussian input (Csajka et al. 2005; Wang, J et al. 2008), saturable time-constraint absorption model (Piotrovskij et al. 1994) or those based on the Erlang (Rousseau et al. 2004) or Gamma (Debord et al. 2001) distribution. Actually, absorption kinetics are best described by a physiologically-based modelling approach, which should take into account the fairly complex interaction between the drug and the (patho)physiological environment of the gastrointestinal tract (Agoram et al. 2001; Van de Waterbeemd et al. 2004; Willmann et al. 2004). However, development of such a model necessitates a large amount of data (Cai et al. 2006), which is seldom available in humans.

It is common in clinical studies that few samples are taken during the absorption phase making absorption kinetics difficult to be characterized with precision. In this case, the absorption rate constant is needed to be fixed to a value based upon prior knowledge from the literature (Bonate 2006) or a constant rate infusion is defined up to the first sample (Csajka et al. 2002). It should be noted that fixing absorption parameters could lead to biased estimates of disposition and elimination parameters (Booth and Gobburu 2003; Carlsson et al. 2005). Furthermore, inappropriate estimation of absorption parameter(s) may arise due to a high correlation or co-linearity with other model parameters (Suverkrup 1985; Wang and Reuning 1992; Wade et al. 1993). Other issues concerning absorption modelling are that both rate and extent of absorption can vary over the duration of a study (Csajka et



al. 2002; Higaki et al. 2008) and also absorption profiles in healthy subjects may be not appropriate for patient populations.

### **1.4.2 Distribution**

In general, interindividual variability in volume of distribution is less than that in other pharmacokinetic parameters (Breimer 1983). Most of the observed interindividual variability in drug distribution stems from differences in body size and composition, genetics, and/or alteration in protein binding due to pathophysiological changes or comedication (Banh et al. 2002; De Paepe et al. 2002; Sutherland 2005).

Part of this variability can be explained by one or more of subjects' covariates, such as body weight, age, gender, etc., (Holford, N H 2002; Conil et al. 2007). Actually, modelling variability in distribution may involve the application of physiological-based pharmacokinetic models, especially where tissue binding is the main issue to be addressed (as in the case for toxicokinetics (Bjorkman et al. 2001)). However, the application of these models remains limited, in part due to information deficit and uncertainty regarding model parameters (Fisher et al. 1998; Brightman et al. 2006; Levitt and Schoemaker 2006).

### **1.4.3 Clearance**

The most clinically useful parameter in drug therapy is clearance, because it reflects all the mechanisms of elimination and it is the only parameter that directly relates dose to the systemic drug exposure (AUC). Drug clearance is highly variable between individuals, hence its characterization provides the opportunity to optimize therapeutic regimens and to suggest dosage adjustments in specific conditions. This involves the recognition of different routes of elimination and situations in which drug clearance is commonly altered, such as hepatic or renal dysfunction.

#### **1.4.3.1 Variability in renal clearance**

For renally excreted drugs, gross changes in glomerular filtration or urine flow and/or pH will have a substantial effect on total clearance (Chiou 1986; Bonnacker et al. 1989) and may lead to either toxic effects or ineffective treatment (Rougier et al. 2003). Unlike plasma, which has a narrow pH range of 7.3 to 7.5, urine pH ranges from 4.5 to 8.5 and can influence drug re-absorption (Florence, A.T. and Attwood, D. 2006). Indeed, urine pH has been shown

to be a major determinant for the excretion of basic drugs like memantine [pKa=10.27] (Freudenthaler et al. 1998), flecainide [pKa = 9.3] (Hertrampf et al. 1991) and methoxyphenamine [pKa = 10.45] (Roy et al. 1987).

Recently, high inter-individual variability in renal clearance of ampicillin, famotidine, cephalexin, and metformin was partly explained by genetic variations in renal transporter expression (Yin et al. 2006; Wang, Z J et al. 2008).

### **1.4.3.2 Variability in hepatic clearance**

Drug metabolism mainly takes place in the liver and to a lesser degree in other tissues such as the small intestine, kidneys and lungs (Krishna and Klotz 1994; Fisher et al. 2001; Ding and Kaminsky 2003). Metabolizing enzymes are expressed with identical function and structure, but their abundance and activity varies from site to site (Lin and Lu 2001). This is recognized as an important source of PK and PD variability (McGilveray 2005; Garrido et al. 2006; Lehr et al. 2008). For example, there is a 20-fold difference in the abundance and activity of CYP enzymes in the liver compared to the small intestine (Thummel et al. 1996; Paine et al. 1997). Interindividual differences in protein levels within this group of oxidizing enzymes are approximately 5-fold for CYP2C and CYP3A4, 12-fold for CYP2E1, 20-fold for CYP1A2, and >50-fold for CYP2A6, CYP2B6, and CYP2D6 (Lin 2006).

Although most metabolizing enzymes are polymorphic, the major polymorphisms that have clinical implications are those related to the oxidation of drugs by CYP2D6, CYP2C9 and CYP2C19 (Sachse et al. 1997; Kirchheiner et al. 2004c; Ufer et al. 2004a; Henningsson et al. 2005; Sconce et al. 2005; Yukawa and Mamiya 2006; Gaedigk et al. 2008; Hirt et al. 2008), acetylation by N-acetyltransferase type 2 (Kinzig-Schippers et al. 2005; Luck et al. 2009), and S-methylation by thiopurine methyltransferase (Cuffari et al. 2004; Chrzanowska et al. 2006; Bosch 2008). Individuals who inherit an impaired ability to catalyze one or more of these enzymatic reactions may be at an increased risk of concentration-related adverse effects and toxicity upon administration of standard doses. The natural interpretation of this is that these subpopulations represent individuals who do or do not have particular signals for gene activity and so would be expected to exhibit differential drug disposition (Hamberg et al. 2007; Kaila et al. 2007).

Multiple distributions are required to describe such variability in order to account for each apparently distinct subpopulation (i.e., extensive or poor metabolizers). Based on such mixed distributions, this strategy will end up with a hierarchical or “mixture” model, with

highly accurate parameter estimates (*Grasmader et al. 2004; Kaila et al. 2007*). Mixture models assume that one or more subpopulations of individuals can exist rather than assuming that the entire population is best described by unimodal distributions for random effects (*Frame et al. 2003; Kaila et al. 2007; Lemenuel-Diot et al. 2007*). A complete and useful mixture population model should describe each of the sub-populations through sub-models that can be entirely different or share some features, including parameter values (*Frame et al. 2003; Hamberg et al. 2007; Kaila et al. 2007*). Mathematically, a model could be difficult to solve if the distribution is blended from more than one sub-population (*Lemenuel-Diot et al. 2007*) and misclassification could appear here, which is related to the overlapping region between each two adjacent distributions (*Kaila et al. 2007*).

#### **1.4.4 Metabolites**

It is well demonstrated that modelling only the parent drug data may not reveal the metabolic pathway properly and in most cases leads to an inappropriate description of the metabolic pathway (*Cosson et al. 2007; Lindauer et al. 2008*). This is because of missing information in the metabolite data set, such as the rate and extent of metabolism or the impact of covariates on the overall metabolic clearance (*Kerbusch et al. 2003; Hamberg et al. 2007; Hirt et al. 2008*). Modelling metabolites can also lead to refinement of the underlying mechanism of interactions (*Hassan et al. 1999; Huitema et al. 2001; de Jonge et al. 2005; Quinney et al. 2008*), improvement of the overall pharmacodynamic profile of the drug (*Garrido et al. 2006; Herd et al. 2007*) and increase applicability of the model (*Cosson et al. 2007; Lindauer et al. 2008*).

In reality, evaluating metabolite data is challenging, especially if the metabolite was not administered separately. This is because metabolite parameters depend heavily on parent data and many are unidentifiable. For example, if the volume of distribution of a metabolite is unknown a priori, then all the model parameters are globally unidentifiable and only the relative rate of systemic drug conversion to metabolite can be determined (*Evans et al. 2001; van der Marel et al. 2003*). In this case, the model should be simplified and fixing parameters to prior knowledge is necessary (*Black et al. 2003; Cosson et al. 2007; Levi et al. 2007*). If the link between the drug and its metabolite is not correctly specified, then the fit to the drug will suffer and the key correlations could be lost for the reasons mentioned above. If this is the case, then sequential fitting would seem a sensible alternative. Further

information about this linkage could also be obtained by deconvolution (Karol and Goodrich 1988; Weiss 1998).

Different models have been proposed to provide quantitative insight into factors determining the concentration-time curve of a metabolite following intravenous and/or oral administration of the precursor drug (Weiss 1988; Taft et al. 1997; Evans et al. 2001; Kerbusch et al. 2003). The number of metabolites for which parameters can be estimated is not limited (Evans et al. 2001; de Jonge et al. 2005).

### **1.4.5 Modelling Drug Response**

Clinicians have long been aware that patients may require very different doses of a drug to produce the same clinical response (Irwin 1964; Marchant 1981; Bagli et al. 1999; Kirchheiner et al. 2005). However, only since the advent of molecular biology has the contribution of genetics to drug response variability come into focus and explained some of the reasons behind this variability (Tucker 2000; Stehle et al. 2008). It is well known that genetic polymorphisms can cause variability in drug response as a result of varied drug metabolism (Scordo and Spina 2002; Lee 2007; Mega et al. 2009) and transporter (Bosch 2008; Choi and Song 2008; Pacanowski et al. 2008) and receptor activity (Muszkat 2007; Mahesh Kumar et al. 2008; Roskopf and Michel 2008; Werner et al. 2008). These parameters can also be modulated by many other demographic, pathophysiologic, environmental and/or subjective factors (Furst 1988; Lu 1998; Tucker 2000; El Desoky et al. 2006). The net worth of genetic knowledge increases significantly when it is integrated into PK and/or PD models. This has been proved to be one of the pivotal factors explaining large portion of interindividual variability (Schalekamp et al. 2007; Limdi et al. 2008; Stehle et al. 2008).

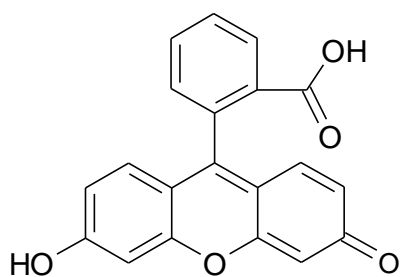
The clinical profiles of oral anticoagulants such as warfarin, acenocoumarol and phenprocoumon share the features of narrow therapeutic index and wide interindividual variability in exposure, which attenuate the dose-response relationship (Ansell 2003; Ufer 2005a; D'Andrea et al. 2008; Stehle et al. 2008). Variability in the extent of anticoagulation depends on not only CYP2C9 polymorphisms but also on polymorphisms associated with the vitamin K epoxide-reductase-complex (VKORC1). This suggests that genetics-based dose individualization will meet the general objective of optimizing safety and efficacy (Limdi et al. 2008; Qazim et al. 2008; Spreafico et al. 2008; Stehle et al. 2008). Taking the warfarin example, the development of a predictive dosage algorithm incorporating genetic factors

## INTRODUCTION

showed that 54% of the variance in warfarin dose could be explained by a combination of genetic (CYP2C9 and VKORC), clinical and demographic factors. Use of this algorithm resulted in more than a 50% decrease in the risk of adverse drug reactions (Hamberg et al. 2007; Gage et al. 2008). Further refinement of this model could lead to effective improvement in the use of warfarin as additional CYP4F2 variants have been recently reported to impact upon warfarin dose (Caldwell et al. 2008). These examples show how genetics have shed light on interindividual variability in response to drugs. They also represent cases in which gene penetrance and frequency are relatively high. For these reasons, identification, evaluation and management of drug response variability is a therapeutic premise. Finally, biomarkers such as the prothrombin time or the international normalized ratio (INR), blood glucose and protein adducts are also of significant value when they are related to a clinical response (Danhof et al. 2005).

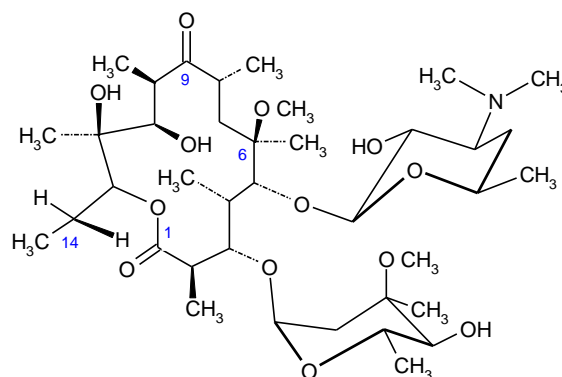
## 1.5 Characteristics of Probe Drugs

1.5.1 Chemical Structures



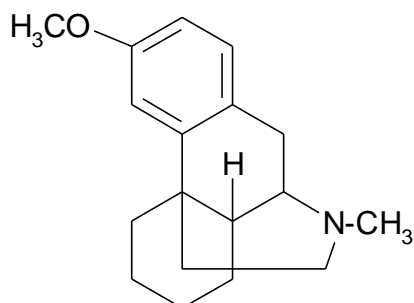
Fluorescein

Formula  $C_{20}H_{12}O_5$   
Mol. mass 332.306 g/mol



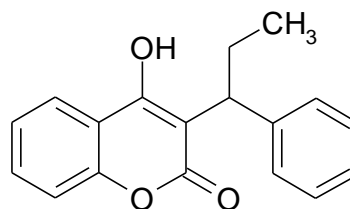
Clarithromycin

Formula  $C_{38}H_{69}NO_{13}$   
Mol. mass 747.953 g/mol



Dextromethorphan

Formula  $C_{18}H_{25}NO$   
Mol. mass 271.4 g/mol



Phenprocoumon

Formula  $C_{18}H_{16}O_3$   
Mol. mass 280.318 g/mol

Figure 1: Chemical structures of probe drugs

### 1.5.2 Bioavailability of Fluorescein for Ocular Administration

Fluorescein, usually as fluorescein sodium, is used extensively as a diagnostic tool in ophthalmology. For example, it is used to help diagnose corneal ulcers and infections, to examine the circulation through ocular tissues (Manivannan et al. 2005), to evaluate tear turnover (Mochizuki et al. 2009), and to measure the corneal permeability and transport of the blood-ocular barriers (Cunha-Vaz and Maurice 1967; Nelson 1995).

When a drug solution is instilled onto the cornea, it subjects to three processes: (1) corneal absorption into the eye, systemic absorption via conjunctiva and sclera, and a large volume is cleared out of the eye with the tears, of which a part is lost and a part is absorbed systemically (Ahmed and Patton 1985; Mitra 2003; Lee et al. 2004; Urtti 2006). As a result, drug absorption after topical instillation of a drug into the eye is incomplete. Indeed, not more than 5% of a dose instilled by eye drops enters the eye via the cornea (Schoenwald 1990; Chastain 2003).

Normally, the conjunctival fornix contains about 7–9  $\mu\text{L}$  of tears with a physiological tear flow of about 1  $\mu\text{L}/\text{min}$  (Mishima et al. 1966). Conventional ophthalmic bottles dispense drops of about 30–50  $\mu\text{L}$  (Davies 2000; Chastain 2003). The maximum volume that can be contained in the conjunctival fornix without overflow is about 30  $\mu\text{L}$  (Mishima et al. 1966). However, only about 10–15  $\mu\text{L}$  remains in the pre-corneal area, and the rest is spilled out immediately from the lids at the time of drug application (Mishima et al. 1966; Fraunfelder and Meyer 1987). Beyond the rapid loss of the additional volume, instillation of eye drops also stimulates lacrimation and increases the turnover rate by 25–30% (Macdonald and Maurice 1991). This reaction further decreases the contact time between the drug and the cornea. Finally, most eye-drop solutions contain preservatives that may cause local irritation or even toxic endothelial degeneration with long-term therapy (Noecker 2001; Pisella et al. 2002; Jaenen et al. 2007). Irritation increases blinking, which eliminates about 2  $\mu\text{l}$  per blink (of the physiological 7–9  $\mu\text{l}$ ) out through the puncta into the nasolacrimal duct (Maurice and Mishima 1984). For these reasons, 80% or more of the instilled drug is lost in the first 15–30 s via conjunctiva and lacrimal drainage and does not enter the eye (Patton and Francoeur 1978; Fraunfelder and Meyer 1987; Ahmed 2003; Chastain 2003). Generally, drainage limits the drug/pre-corneal contact time to about 5 min (Chastain 2003; Macha et al. 2003). This drainage mechanism causes the drug to be systemically absorbed by the nasal mucosa or by



## INTRODUCTION

the gastrointestinal tract (Lee and Robinson 1986; Chang and Lee 1987; Lang 1995). For instance, ocular bioavailability of timolol is about 11% (Urtti et al. 1990), while the rest is systemically absorbed, and a reduction of more than 60% of timolol systemic absorption was achieved after nasolacrimal occlusion in humans (Zimmerman et al. 1984). In rabbits, ocular versus systemic bioavailability was reported to be about 2.5 vs. 46% for levobunolol (Tang-Liu et al. 1987) and 9 vs. 74% for flurbiprofen (Tang-Liu et al. 1984), which implies that most of the drug dose is unavailable for efficacy. Topical instillation of more drops does not significantly improve the ocular bioavailability (Chrai et al. 1974; Patton and Francoeur 1978) but may increase systemic side effects of the drug, even to critical levels for some drugs such as beta blockers (Diamond 1997; Taniguchi and Kitazawa 1997; Hayreh et al. 1999).

To overcome eye-drop limitations, different drug delivery systems have been developed such as liposomes (Lee et al. 1985; Hathout et al. 2007), exoplants (Pontes de Carvalho et al. 2006), collagen shields (Reidy et al. 1990; Taravella et al. 1999), ocular inserts (Hornof et al. 2003), mucoadhesives (Davies et al. 1992) and lyophilisate (Diestelhorst et al. 1999; Suverkrup et al. 1999). These systems differ from each other in safety, possibility of dose adjustment and targeting, pre-corneal residence time, patient compliance, simplicity of use, and cost. Advantages and disadvantages of most delivery systems have been reported elsewhere (Mitra 2003). Lyophilisates (Figure 2) have recently been suggested to be a favorable formulation for delivering a drug into the eye (Diestelhorst et al. 1999; Dinslage et al. 2002; Lux et al. 2003; Steinfeld et al. 2004).



**Figure 2: Application of ophthalmic lyophilisate (Lux et al. 2003)**

## INTRODUCTION

The ophthalmic lyophilisate carrier system (OLCS) is prepared from a drop of a hydrophilic polymer solution, in which a drug is dissolved or dispersed and freeze-dried on the tip of a soft hydrophobic carrier strip. The drug is administered to the conjunctival fornix by wiping the lyophilisate over the lower eyelid. Upon contact with tear film and/or conjunctiva, the lyophilisate rapidly rehydrates and dissolves to release the incorporated substance (Diestelhorst et al. 1999). It is not washed out by immediate copious tear secretion (Suverkrup et al. 2004). Since the corneal contact time is increased and pre-corneal losses are reduced (Lux et al. 2003), ocular bioavailability of the active ingredient should be enhanced. Lyophilisate water content is less than 5% and thus too low for microbial growth or hydrolytic degradation of constituents. Therefore, neither preservatives nor buffer salts are required to ensure stability (Suverkrup et al. 2004). Clinical data from ophthalmic applications of this dosage form with fluorescein (Dinslage et al. 2002; Lux et al. 2003; Steinfeld et al. 2004), mitomycin C (Schraermeyer et al. 1999), and pilocarpine (Suverkrup et al. 1999) indicated a reduction of topical and systemic side effects, less discomfort, and more pronounced therapeutic effects compared to eye drops.

### **1.5.3 Clarithromycin and Autoinhibition of Metabolism**

Clarithromycin is a broad spectrum macrolide antibiotic and widely used for the treatment of upper and lower respiratory tract and other infections (Fernandes et al. 1986; Sturgill and Rapp 1992; Langtry and Brogden 1997). Clarithromycin interacts with many drugs on the level of intestinal and hepatic metabolizing enzymes CYP3A (Gorski et al. 1998; Rodvold 1999). This may change efficacy and tolerability of other co-administered CYP3A substrates. Clarithromycin is rapidly and nearly completely absorbed from the gastrointestinal tract (Ishii et al. 1998). Due to notable first pass metabolism, approximately 50% to 55% of an oral dose is bioavailable as clarithromycin in the systemic circulation (Chu et al. 1992a; Fraschini et al. 1993; Gorski et al. 1998). The free fraction of clarithromycin in plasma is about 0.3 in healthy volunteers (Chu, S Y et al. 1993; Traunmuller et al. 2007). Clarithromycin is widely distributed throughout the body with an apparent volume of distribution range from 126 to 306 litres (Chu, S et al. 1993; Rodvold 1999; Traunmuller et al. 2007). Approximately 22% of an oral dose is recovered as parent compound, 18% in the urine and 4% in the faeces (Davey

## INTRODUCTION

1991). The elimination half-life ( $t_{1/2}$ ) of clarithromycin is dose- and time-dependent, and ranges from 2.7 to 4.8 hours (Ferrero et al. 1990b; Chu et al. 1992b; Chu, S et al. 1993; Traunmuller et al. 2007). In healthy subjects, the average total body clearance ranges from 29 to 58 L/h and renal clearance from 6.7 to 12.8 L/h, depending on the amount and number of doses administered (Chu, S et al. 1993; Rodvold 1999). After single and multiple (7 doses) administration of 500 mg clarithromycin tablets, the apparent total body clearance was reported to decrease from 42.1 to 18.7 L/h (Chu, S et al. 1993; Traunmuller et al. 2007). As renal clearance does not change under these conditions, the nonlinearity is attributed to non-renal elimination mediated by cytochrome P450 metabolism (Chu, S et al. 1993). Clarithromycin is extensively metabolized into at least eight metabolites via three metabolic pathways; i.e. hydroxylation at the 14-position, N-demethylation and hydrolysis of the cladinose sugar. Secondary biotransformation was also evident (Ferrero et al. 1990b; Davey 1991; Yamamoto et al. 2004). Metabolic pathways of primary biotransformation are given below in Figure 3.

Clarithromycin hydroxylation at position 14 is stereospecific yielding the 14-hydroxy-(R)-epimer as the main metabolite, which accounts for 20% of the parent drug metabolism (Ferrero et al. 1990b; Davey 1991; Langtry and Brogden 1997). Indeed, this metabolite contributes significantly to the overall antimicrobial effect of clarithromycin (Martin et al. 2001; Yamamoto et al. 2004). Formation of this main metabolite, is predominantly mediated by CYP3A4 (Rodrigues et al. 1997; Bruce et al. 2001; Suzuki et al. 2003; Yamamoto et al. 2004) and was suggested to be capacity-limited, which may in part account for the nonlinearity observed in clarithromycin pharmacokinetics (Chu, S et al. 1993).

Clarithromycin is also a potent inhibitor of intestinal and hepatic CYP3A4 activity (Gorski et al. 1998; Pinto et al. 2005b) in a dose-dependent manner (Ushiyama et al. 2002). It has been classified as a mechanism-based inhibitor (Zhou et al. 2005). Based on in vitro models, clarithromycin was predicted to cause a reduction in the steady-state concentration of liver CYP3A4 to approximately 39% of initial level (Mayhew et al. 2000). The mechanism of this auto-inhibition was reported to be reversible (Hung et al. 2005; Pinto et al. 2005b), irreversible (Gorski et al. 1998; Bruce et al. 2001; Pinto et al. 2005a) and suicide inhibition mediated by formation of a metabolic intermediate complex (Mayhew et al. 2000).

## INTRODUCTION

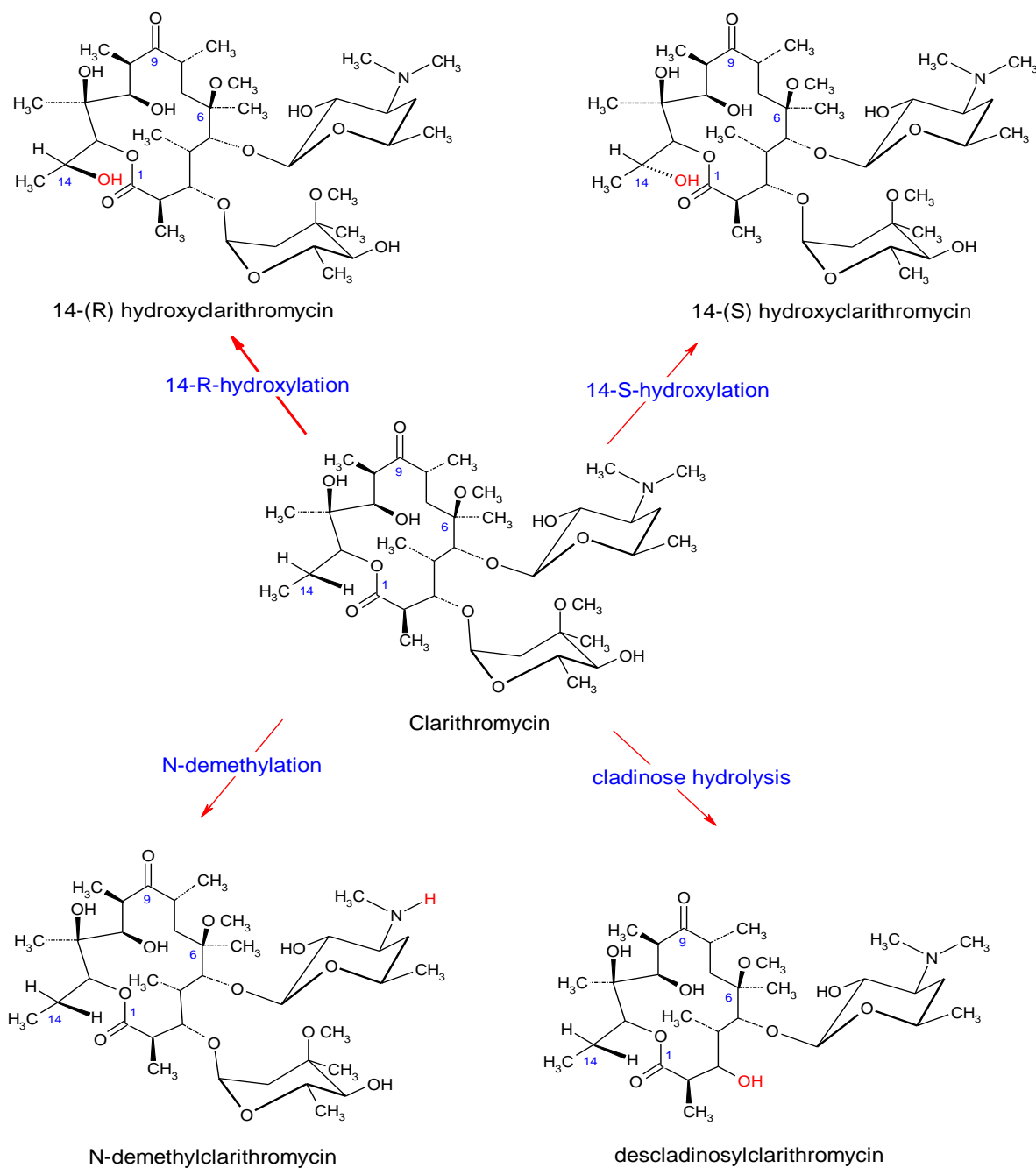


**Figure 3: Primary metabolic pathways of clarithromycin in man** (Ferrero et al. 1990a)

For clarithromycin the ratio of the area under free plasma concentration-time curve to the minimum inhibitory concentration ( $fAUC/MIC$ ) is considered as the most predictive PK/PD index (Craig et al. 2002; Tessier et al. 2002) and used to link the pharmacokinetic parameters to the most important antimicrobial pharmacodynamic parameter, i.e. minimum inhibitory concentration (MIC). Based on animal infection models, a derived target value of  $fAUC_{0-24\text{ plasma}}/MIC$  was assumed to be 35 h for clarithromycin (Craig et al. 2002; Tessier et al. 2002).

## INTRODUCTION

Actually, the adult dosage regimen of clarithromycin 500mg twice daily achieves an average area under the concentration-time curve of free drug  $fAUC_{0-24}$  of about  $5.85 \pm 1.79$  mg•h/litre in plasma (Traunmuller et al. 2007), which may provide sufficient efficacy as long as the MIC value does not exceed 0.25 to 1.0  $\mu\text{g/mL}$  (Rodvold 1999). However, this dosing regimen may be ineffective in the treatment of infections caused by pathogens with a drug MIC higher than  $1\mu\text{g/mL}$  in plasma, or higher than  $0.125 \mu\text{g/mL}$  in tissues where fAUC is lower, suggesting the need of administration of a higher dose (Noreddin et al. 2002; Traunmuller et al. 2007). Because of the nonlinear kinetics, it is difficult to predict fAUC changes achieved by higher doses.

### 1.5.4 The Use of Dextromethorphan as a CYP2D Phenotyping Drug

Dextromethorphan is an antitussive drug which is widely used to relieve non-productive cough associated with acute upper respiratory tract infection (Parvez et al. 1996; Lee et al. 2000). Its pharmacokinetics is characterised by a rapid absorption from the gastrointestinal tract ( $k_a = 2.6 \pm 0.9 \text{ h}^{-1}$ ) after oral administration and a large volume of distribution ranging from 1220 to 16491 Litres (Kazis et al. 1996; Moghadamnia et al. 2003). The apparent total clearance of dextromethorphan ranges from 75 L/hr to 4167 L/h (Kazis et al. 1996; Borges et al. 2005). Dextromethorphan undergoes rapid and extensive first-pass metabolism. Primary metabolic steps include formation of dextrorphan mainly by CYP2D6 and of 3-methoxymorphinan by CYP3A (Barnhart 1980; Jacqz-Aigrain et al. 1993; Moghadamnia et al. 2003). Both dextrorphan and 3-methoxymorphinan are further metabolized to 3-hydroxymorphinan by CYP3A4 and CYP2D6, respectively (Jacqz-Aigrain et al. 1993). A schematic description of dextromethorphan elimination pathways is given in Figure 4.

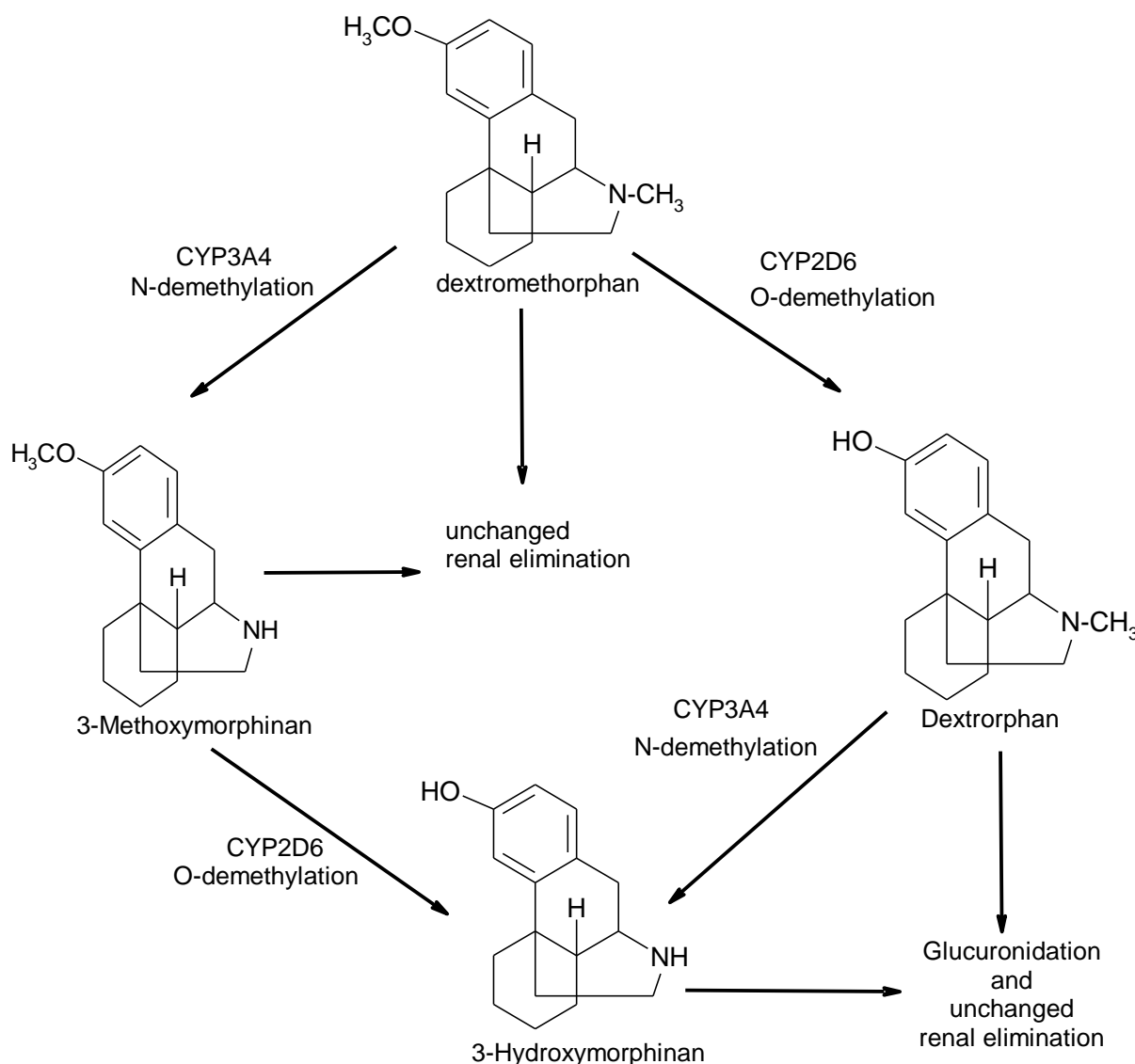


**Figure 4: Elimination pathways of dextromethorphan** (Yu, A and Haining, R L 2001)

The dominating metabolic pathway in the majority of the population is the conversion of dextromethorphan to dextrorphan by CYP2D6 (Kupfer et al. 1984; Yeh et al. 2003; Pope et al. 2004), contributing to more than 80% to the formation of dextrorphan (Schmider et al. 1997; Yu, A and Haining, R 2001; Moghadamnia et al. 2003). The selectivity of dextrorphan formation via CYP2D6, in addition to its favourable safety and availability, has made dextromethorphan a probe of choice for CYP2D6 phenotyping (Frank et al. 2007; Fuhr et al. 2007).

It is well known that CYP2D6 is a highly polymorphic enzyme. Today, more than 83 allelic variants have been described (Zhou et al. 2009). Because the overall disposition of dextromethorphan is highly dependent upon CYP2D6 activity (Nielsen et al. 1990; Zhang et

## INTRODUCTION

al. 1992; Sachse et al. 1997), these polymorphisms contribute to a wide interindividual variation in its plasma levels (Labbe et al. 2000; Pope et al. 2004) and response (Sachse et al. 1997; Abdul Manap et al. 1999; Labbe et al. 2000; Tucker 2000; Moghadamnia et al. 2003). For other CYP2D6 substrates such as antidepressants and antipsychotic drugs such variability can lead to failure of treatment in carriers of haplotypes coding for a very high CYP2D6 activity or may expose individuals with low activity haplotypes to a high risk of toxicity (poor metabolizers) (Seeringer and Kirchheiner 2008; Laika et al. 2009). For some opioids such as dihydrocodeine, codeine and tramadol, where the active metabolite is formed by CYP2D6, vice versa failure is associated with low activity and toxicity with high activity genotypes (Kirchheiner et al. 2007; Kirchheiner et al. 2008).

Because it is important to identify individuals at risk for therapeutic failure or adverse effects caused by aberrant CYP2D6 activity, different proposals have been made to establish simple useful systems for the prediction of CYP2D6 phenotype as a prerequisite to personalize therapy with CYP2D6 substrates based on genotype information (Kirchheiner et al. 2001). These systems suffer from potential pitfalls depending on the correctness of underlying assumptions which may compromise prediction accuracy. The classical procedure divided populations, usually based on the urinary metabolic ratio of dextrorphan over dextromethorphan and an arbitrary "cut-off" value, into poor and extensive metabolizers (Mahgoub et al. 1977; Eichelbaum et al. 1979), with poor metabolizers representing individuals carrying two non-functional CYP2D6 alleles. However, it is difficult to predict phenotype correctly of individuals who are heterozygous for an active CYP2D6 allele, as these individuals are characterized by a large variability in CYP2D6 phenotype (Bock et al. 1994). To account for heterozygosity and gene duplications, intermediate and ultra-rapid metabolizers subgroups have subsequently been introduced into the classification creating a polymodal distribution (Sachse et al. 1997; Kirchheiner et al. 2001; Heller et al. 2006; Rebsamen et al. 2008). Further refinement was required to account for decreased activity of the CYP2D6\*10 allele frequently occurring in Asians (Yue et al. 1998; Mihara et al. 1999). In addition, a semi-quantitative scoring system defining categories for CYP2D6 alleles have been developed (Kirchheiner et al. 2004a; Steimer et al. 2004). This system defined a CYP2D6 genotype score as the sum of the gene dose for both alleles, with 1 for fully functional alleles, 0.5 for reduced activity functional alleles, and zero for non-functional alleles (Steimer et al. 2004). Although these classifications have improved phenotype

predictions (Sachse et al. 1997), considerable variability within heterozygous groups has still been reported (Raimundo et al. 2000; Kirchheiner et al. 2001) and substantial overlap between intermediate and extensive metabolizer distributions has been observed (Gaedigk et al. 2008).

In the most recent scoring system, the so-called activity score system defined CYP2D6 genotype as the sum of presumed values assigned to individual alleles (Gaedigk et al. 2008). The phenotype scores were derived from urinary ratios of dextromethorphan. It assigned a value of 1, 0.5, and 0 for fully functional, reduced, and non-functional alleles Table 1.

**Table 1: The activity score model** (Gaedigk et al. 2008)

Value assigned to allele	Observed CYP2D6 alleles
0	*3, *4, *4xN, *5, *6, *7, *16, *36, *40, *42, *56B
0.5	*9, *10, *17, *29, *41, *45, *46
1	*1, *2, *35, *43, *45xN
2	*1xN, *2xN, *35xN

Obviously, the score activity system assumes identical metabolic activity for different alleles of in each group. This is, however, valid for defective CYP2D6 alleles such as \*4 and \*3, but the assumption for fully functional alleles, for example \*1 and \*2 alleles, to have identical activity is questionable. An in vitro study of rCYP2D6 enzyme supports this classification for some CYP2D6 probe drugs such as metoprolol and debrisoquine, but not for dextromethorphan, where the intrinsic clearance value of CYP2D6\*2 was half that of CYP2D6\*1 for dextromethorphan O-demethylation (Bapiro et al. 2002). These observations warrant further assessment of individual activity of each allele directly from plasma concentration time profile of CYP2D6 probes.

### 1.5.5 Understanding Variability in Phenprocoumon Response

Phenprocoumon is a coumarin derivative oral anticoagulant drug used for the prevention and treatment of arterial and venous thromboembolic disorders (Bourgain and Wright 1955). The maintenance dose ranges from 0.75 to 9 mg per day (Trenk et al. 1987). Phenprocoumon exerts its effect by inhibition of vitamin K epoxide reductase (VKOR), which



## INTRODUCTION

converts vitamin K from non-reduced to reduced form, leading to a decrease in prothrombin level (Hirsh et al. 1998). Its large interindividual pharmacokinetic variability and narrow therapeutic index render a close monitoring necessary (Schalekamp et al. 2007; Stehle et al. 2008).

Phenprocoumon is rapidly absorbed from the gastrointestinal tract with an absorption rate constant of  $2.5 \text{ h}^{-1}$  (Haustein and Huller 1994) and nearly complete bioavailability (Alberio 2003). It has a volume of distribution of 10 - 14.4 L (Haustein and Huller 1994; Masche et al. 1999). More than 99% of the drug is bound to plasma proteins (>99%) (Trenk et al. 1987; de Vries and Volker 1990) with a serum free fraction of about  $0.51 \pm 0.20 \%$  (Russmann et al. 2001). A long elimination half-life of about 5 days has been reported for phenprocoumon with a mean total apparent clearance of about 0.040-0.063 L/h (Kitteringham et al. 1984; Russmann et al. 2001; Kirchheiner et al. 2004c). About 40 % of the administered dose is excreted unchanged (Toon et al. 1985) and may be eliminated with the faeces (de Vries et al. 1988). The remainder of 60 % undergoes hepatic hydroxylation and conjugation (Toon et al. 1985). A schematic representation of phenprocoumon metabolic elimination pathways is given below in Figure 5.

The 4'-, 6-, 7-, and 8-hydroxy metabolites are the major metabolites formed mainly by CYP2C9 (He et al. 1999; Ufer et al. 2004c; Kammerer et al. 2005), however CYP3A4 and CYP2C8 may be involved to a less degree (Ufer 2005a). In comparison with other structurally and pharmacologically related drugs, warfarin or acenocoumarol, phenprocoumon metabolism is substantially less dependent on CYP2C9 activity (Kammerer et al. 2005; Ufer 2005a), most probably due to higher contribution of other CYP enzymes (Freedman and Olatidoye 1994; Ufer et al. 2004c) and the involvement of bile and urine excretion pathways (de Vries et al. 1988; Edelbroek et al. 1990).

## INTRODUCTION

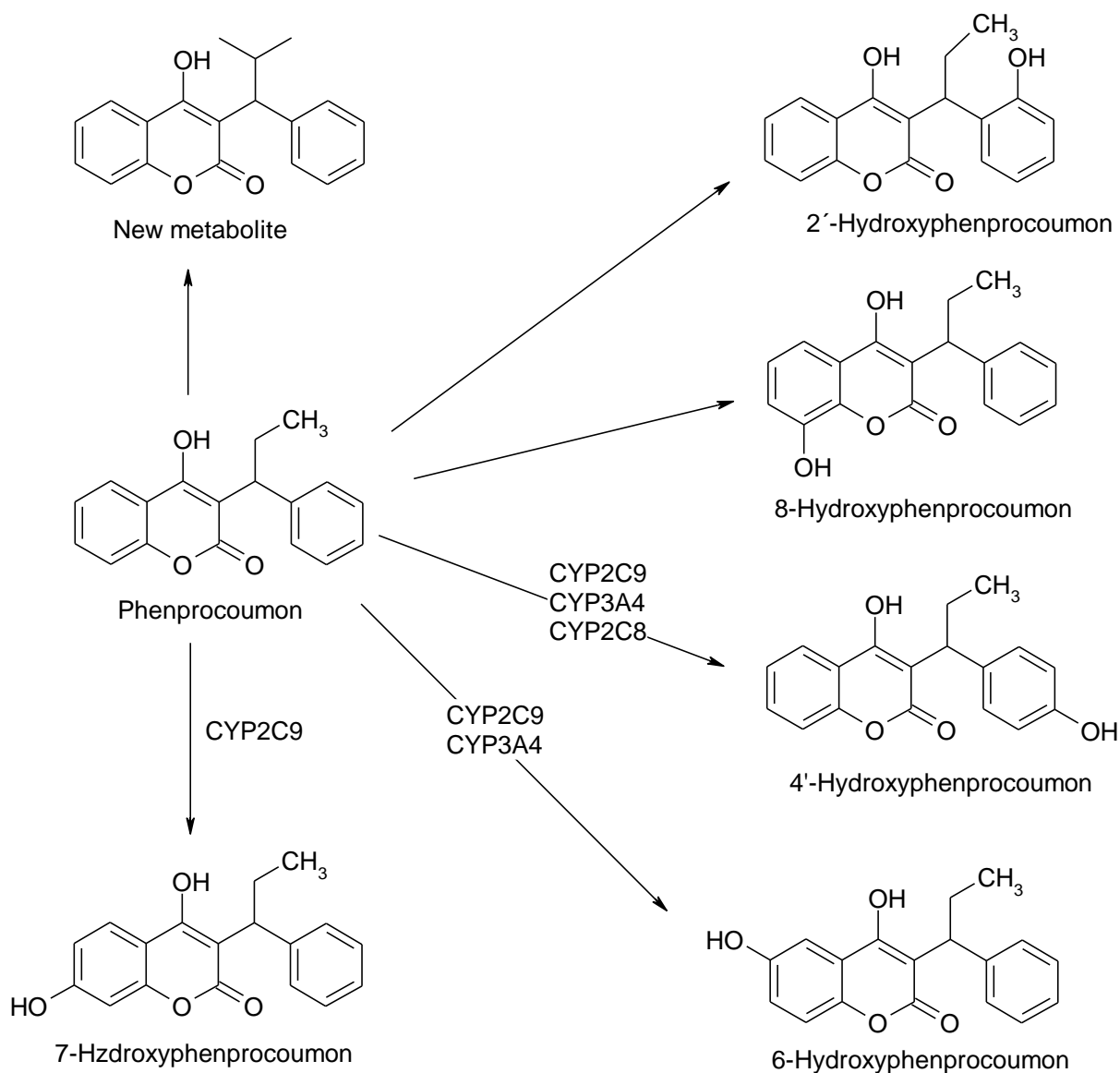


**Figure 5: Metabolic clearance pathways of phenprocoumon** (Stehle et al. 2008)

Previous studies have attributed a major part of interindividual differences in the pharmacokinetics of phenprocoumon to the genetic polymorphism of CYP2C9. A higher metabolic capacity was obtained for homozygous carriers of CYP2C9\*1/\*1 than CYP2C9\*2/\*3 or CYP2C9\*3/\*3 genotype (Kirchheiner et al. 2004c; Schalekamp et al. 2004; Ufer 2005b). In a study of 284 patients during a follow-up period of 6 months, carriers of CYP2C9\*2 or \*3 genotypes had an increased risk of phenprocoumon overanticoagulation compared with homozygous CYP2C9\*1/\*1 subjects (Schalekamp et al. 2004). Compared with homozygous carriers of CYP2C9\*1, patients homozygous for CYP2C9\*3 were estimated to need a 1.5-fold reduction in the mean dose phenprocoumon to achieve the same INR (Stehle et al. 2008).

## INTRODUCTION

On the other hand, polymorphism of the vitamin K epoxide reductase complex (VKORC1) was identified as an important factor to explain a major fraction in the variability between individuals in their response to warfarin (Wadelius et al. 2009), acenocoumarol (Schalekamp et al. 2006; Teichert et al. 2009), and phenprocoumon (Schalekamp et al. 2007; Werner et al. 2009). The increased risk of bleeding called for dose reduction in carriers of at least one T allele compared to those carrying CC homozygous (Reitsma et al. 2005; Schalekamp et al. 2007). Homozygous presence of the VKORC1 variant C1173T (\*2) allele was related to 1.9-fold lower empirical doses compared with the wild-type for phenprocoumon (Stehle et al. 2008). Furthermore, the differences in phenprocoumon dose requirements between patients with different CYP2C9 genotypes are modified by the VKORC1 genotype (Schalekamp et al. 2007), and being a carrier of a combination of CYP2C9\*3/\*3 and VKORC1 TT variants is associated with over-anticoagulation status. About 7.2% of the variability in phenprocoumon dose requirement was reported to be explained by the CYP2C9 genotype, while up to 28.7% of the variability was explained by the VKORC1 genotype. A combination of both genes in interaction with patient's age and sex explained up to 54.7% of variability in the mean dose requirement of phenprocoumon (Schalekamp et al. 2007).

Published studies drew their conclusions from pharmacokinetic studies in healthy populations or from direct determination of the effect of genetic variants on phenprocoumon dose requirements. Concentrations of phenprocoumon and its metabolites have not yet been measured for a better understanding of the genetic impact on dose-response relationships in patients. Indeed, this information is a prerequisite for prediction of the individual optimal phenprocoumon dose based on mechanistic rather than empirical considerations. While this has already been implemented for warfarin (Klein et al. 2009), a similar approach may be helpful also for phenprocoumon despite its lower dependence on CYP2C9 because its long elimination half-life of 106 - 150 hours (Kitteringham et al. 1984; Russmann et al. 2001) delays the effect of any dose adjustments.

## **2 MATERIALS AND METHODS**

## 2.1 Fluorescein Data

### 2.1.1 Clinical Studies and Ethical Conduct

Forty-four healthy volunteers were enrolled in three open-label, randomized, clinical studies that had been approved by the Ethics Committee of the University of Cologne. All participants gave their written informed consent. In studies 1, 2, and 3, sodium fluorescein 0.17% was applied to 10 (age range: 24–27 years), 22 (age range: 22–45 years), and 12 (age range: 23–33 years) subjects at the same doses as conventional, preservative-free 40- $\mu$ L eye drops (Fluoreszein 0.17% SE Thilo, Alcon, Germany) to one eye and as a fluorescein-containing lyophilisate to the fellow eye.

To prepare the lyophilisate, 170 mg sodium fluorescein was dissolved in 10 mL of a 1% hypromellose solution, filtered through a 0.22- $\mu$ m cellulose ester membrane and deposited in aliquots of 40  $\mu$ l on sterilized poly(tetrafluoroethylene) carrier strips by pipetting. The strips were frozen and lyophilized under aseptic conditions either in a water vapor permeable container in a conventional laboratory freeze-dryer (Christ alpha 2–4, Osterode, Germany) or they were snap-frozen by evacuation and freeze-dried directly in a small glass chamber; thereafter, they were packed aseptically in sterilized test tubes. The resulting lyophilisate was hemispherical in shape with a radius of approximately 2.3 mm. The method has been described in detail (Dinslage et al. 2002; Lux et al. 2003; Steinfeld et al. 2004; Suverkrup et al. 2004).

Lyophilized fluorescein was deposited on the lower conjunctival fornix by stripping the lyophilisate off the carrier in a wiping motion. The fluorescein dose was 68  $\mu$ g in studies 1 and 3, administered as a single eye drop (40  $\mu$ L) or as lyophilisate. In study 2, a triple dose (204  $\mu$ g) of fluorescein was given as a single lyophilisate application to one eye or as three conventional eye drops containing 68  $\mu$ g in 40  $\mu$ L each to the fellow eye, applied at 15-min intervals (0, 15 and 30 min) to avoid extensive immediate loss of the dose due to overflow. The rationale for the 204-mg dose in study 2 was to examine whether a three-fold higher single dose could be delivered into the eye when administered as a lyophilisate.

### 2.1.2 Measurements and Variables

Fluorescein concentrations in the cornea and anterior chamber were measured non-invasively by fluorophotometry (Fluorotron Master II, Ocumetrics, Palo Alto, CA, USA).

Measurement times were as follows: study 1, prior to the first dose and every 2 min up to 30 min after dosing; study 2, prior to the first dose and 15, 30, 45, 60, 120, 180, 240, 300, 360, 420 min after dosing; study 3, prior to the first dose and 15, 30, 45, 60, 120, 180 min after dosing.

## 2.2 Clarithromycin Data

### 2.2.1 Clinical Studies and Ethical Conduct

A total of twelve healthy Caucasian volunteers (7 men and 5 women; 19 – 40 years; 47.3 – 85.2 kg body weight; 157-182 cm body height) were enrolled into a single centre, open, randomized steady-state clinical study, which had been approved by the Ethics Committee of the Ministry of Health Clinic Hospital of the Republic of Moldavia, Chisinau, Republic of Moldavia. The study was conducted according to the revised version of the Declaration of Helsinki. All participants gave their written informed consent. Volunteers were non-smokers or ex-smokers between the age of 19 and 41 (mean and SD  $28 \pm 8$ ) years, their weight was between 45.1 and 86.1 kg ( $66.5 \pm 11.8$  kg), body height ranged between 150.0 to 186.0 cm ( $168.4 \pm 9.7$  cm). Participants were judged to be healthy as based on medical history, vital signs, complete physical examination, neurological assessment, and 12-lead electrocardiogram, clinical chemistry, hematology, urinalysis, and virological tests.

Each subject took an oral dose of 500 mg clarithromycin every 12 h for four consecutive days (a total of seven doses, each single dose was 500 mg per 10 mL of clarithromycin suspension equivalent to 500 mg clarithromycin, Klacid, Abbott B.V., Hoofddorp, Netherlands). Subjects took the drug in the fasting state with 240 mL low-carbonated calcium-poor mineral water. After each administration the subjects lay in bed for at least 3 hours. Consumption of alcohol was prohibited starting at 2 days, beverages or foods containing methylxanthines starting at 2 days, and grapefruit products starting at 7 days predose, respectively. From approximately 8 hours before until approximately 4 hour after each morning dose and from approximately 2.5 hours before until approximately 3 hours after each evening dose no food was allowed. Identical low fat food was given on all study days. No fluid intake from 1 hour before until 2 hours postdose (with exception of the fluid for study drug administration) was allowed. Thereafter, 120 mL of low-carbonated calcium-poor mineral water (room temperature) was

given every hour until 11 hours after morning administration. No extensive fluid intakes (>120 mL/hour) were allowed during nights.

### 2.2.2 Measurements and Variables

Blood samples were collected for quantification of clarithromycin and its 14(R)-hydroxyl metabolite immediately before administration and 0.33, 0.67, 1, 1.5, 2, 2.5, 3, 3.5, 4, 4.5, 5, 5.5, 6, 8, and 12 h after the first, third and seventh dose. Additionally, one sample each was taken immediately prior to the fifth and sixth dose. Plasma samples were analyzed by a validated LC-MS/MS assay at the institute of Biomedical and Pharmaceutical Research, Nürnberg-Heroldsberg.

Briefly, plasma samples (0.1 mL) were precipitated by addition of 200  $\mu$ L of acetonitrile containing the internal standard. After thorough mixing, the samples were centrifuged for 5 minutes at 3,280 g at approximately +4 °C, and the supernatant was diluted (1:1) with buffer. 15  $\mu$ L of each sample were chromatographed on a reversed-phase column (Waters Symmetry<sup>®</sup> C-8), eluted with an isocratic solvent system consisting of ammonium acetate buffer and acetonitrile (65/35,v/v, pH 4) and monitored by LC-MS/MS with a single reaction monitoring (SRM) method as follows: Precursor  $\rightarrow$  product ion for clarithromycin m/z 749  $\rightarrow$  m/z 158, m/z 765  $\rightarrow$  m/z 158 for 14(R)-hydroxy-clarithromycin and m/z 838  $\rightarrow$  m/z 679 for internal standard, all analyses were in positive mode. Under these conditions clarithromycin, 14(R)-hydroxy-clarithromycin and the internal standard were eluted after approximately 1.8, 0.8 and 2.0 minutes, respectively. The MacQuan software (version 1.6, PE Sciex, Thornhill, Ontario, Canada, 1991 - 1998) was used for evaluation of chromatograms.

Plasma samples were measured against a plasma calibration row prepared by adding the defined amounts of standard solution to drug-free human plasma. Spiked quality controls (SQC) were prepared for determination of interassay variation by the addition of defined amounts of the stock solution or the spiked control of higher concentration to defined amounts of tested drug-free human plasma. There was no interference observed in plasma, for clarithromycin, 14(R)-hydroxy-clarithromycin or the internal standard. Weighted linear regression ( $1/\text{concentration}^2$ ) was performed for calibration. Linearity of the calibration curve could be shown in human plasma between 0.00992  $\mu$ g/mL and 3.98  $\mu$ g/mL for

clarithromycin and between 0.0101 and 4.04 µg/mL for 14(R)-hydroxy-clarithromycin. Lower limits of quantification were identical with the lowest calibration levels.

The inter-day precision and the analytical recovery of the spiked quality control standards of clarithromycin in human plasma ranged from 3.0 to 4.4 % and were 99.9 % (3.07 µg/mL), 100.4 % (1.02 µg/mL), 100.3 % (0.0941 µg/mL) and 100.9 % (0.0267 µg/mL), respectively. The inter-day precision and the analytical recovery of the spiked quality control standards of 14(R)-hydroxy-clarithromycin in human plasma ranged from 6.3 to 6.8 % and were 100.1 % (3.04 µg/mL), 97.2 % (1.01 µg/mL), 95.5 % (0.0930 µg/mL) and 96.8 % (0.0264 µg/mL), respectively.

## 2.3 Dextromethorphan Data

### 2.3.1 Clinical Studies and Ethical Conduct

Data from a total of fifty healthy Caucasian male volunteers from 3 cocktail interaction studies were available for this evaluation; 16 in study A, 11 in study B, and 11 in study C (Klaassen et al. 2008; Tomalik-Scharte et al. 2009). Briefly, all studies were approved by the ethics committee of the Medical Faculty of the University of Cologne, Germany, and were conducted according to the revised version of the Declaration of Helsinki and corresponding European and international guidelines. All participants gave their written informed consent. The data evaluated in this study is from the reference period where each subject received a single oral dose of 30 mg dextromethorphan hydrobromide (one capsule of Hustenstillerratiopharm, ratiopharm, Ulm, Germany). Data from two subjects carrying rare CYP2D6 alleles were excluded from this evaluation (see below) and therefore 36 male subjects (18 – 49 years; 60 – 101 kg body weight; 171 – 195 cm body height) were enrolled in this evaluation.

### 2.3.2 Measurements and Variables

Blood samples were collected for quantification of dextromethorphan and dextrophan as follows:



## MATERIALS AND METHODS

*Study (A)* immediately before administration and 0.17, 0.5, 0.75, 1.0, 1.33, 2.0, 3.15, 4.25, 5.25, 6.0, 8.0, 10.0, 11.95, 14.0, 24.0 h after dosing;

*Study (B)* immediately before administration and 0.17, 0.33, 0.50, 1.0, 1.33, 1.67, 2.0, 2.5, 3.25, 3.95, 4.5, 5.25, 7.00, 10.00, 12.0, 16.0, 24.0 h after dosing;

*Study (C)* immediately before administration and 0.17, 0.33, 0.50, 0.75, 1.00, 1.33, 1.67, 2.0, 2.5, 3.25, 3.95, 4.13, 4.25, 4.5, 4.75, 5.0, 5.5, 6.5, 8.0, 10.0, 12.0 h after dosing.

For quantification of dextromethorphan and dextrorphan in urine, urine samples were collected periodically and the volume and pH-value of each period were measured. The urine sampling schedules were:

*Study (A)* immediately before administration and 0-2, 2-4, 4-6, 6-8, 8-12, 12-16 und 16-24 h after dosing;

*Study (B)* immediately before administration and, 0-6 und 6-12 h after dosing;

*Study (C)* immediately before administration and, 0-2, 2-4, 4-6, 6-8, 8-12 h after dosing.

Plasma and urine samples were analyzed at the Institute of Pharmacology, University of Cologne, according to a previously published validated LC-MS/MS method (Wyen et al. 2008). The lower limits of quantification were 0.103ng/mL for dextromethorphan and 0.101ng/mL for dextrorphan. Precision ranged from 3.2 to 7.8% for dextromethorphan, and from 4.7 to 9.2% for dextrorphan, while accuracy was 101.8–102.9%, and 97.4–99.5% for dextromethorphan and dextrorphan, respectively.

*Genotyping Assays:* All polymerase chain reaction amplifications were carried out in 50 µl reaction mixtures containing 100 ng of genomic DNA, 1x buffer, 2.3 mM MgCl<sub>2</sub>, 0.5 µM of each primer, 0.8 mM of dNTPs, and 2.5 U HotStarTaq DNA Polymerase (Qiagen). After purification, polymerase chain reaction products were sequenced using the BigDye Terminator Cycle Sequencing Ready Reaction Kit v2.0 (Applied Biosystems, Foster City, CA). Sequencing analysis was performed on a Genetic Analyzer 3100 capillary sequencer (Applied Biosystems) and pairwise sequence alignments were done with GenBank sequence NM\_000927 using MT Navigator PPC and Edit View software (Applied Biosystems).

## 2.4 Phenprocoumon Data

### 2.4.1 Clinical Studies and Ethical Conduct

A total of 278 Caucasian patients (173 male/105 female; mean age  $68.6 \pm 11$  (range: 26 -90) years; mean body weight  $81 \pm 15$  (range: 46 – 132) kg; mean body mass index  $27.9 \pm 4.6$  (range: 16.7 – 45.6)  $\text{kg/m}^2$ ) were enrolled in a multi-centre steady-state, clinical study that had been approved by the Ethics Committee of the University of Tübingen, University of Cologne and University of Mannheim. The study was conducted in accordance with the Declaration of Helsinki and the relevant European and international guidelines after obtaining written informed consent from all participants. All subjects were on stable dosing regimen (mean $\pm$ SD:  $13.62 \pm 5.75$  (range: 3.75 - 37.50) mg/week) of phenprocoumon (Marcumar<sup>®</sup>, Roche, Grenzach-Wyhlen, Germany; or Falithrom<sup>®</sup>, Hexal, Holzkirchen, Germany) for at least four weeks before inclusion date to ensure steady state achievement. Some minor modifications of the phenprocoumon dose during the last four weeks were present in many individuals. Information on phenprocoumon past dosage schedules and aim of the therapy was gathered from patients' anticoagulation documentations. Furthermore, information was documented regarding the presence of co-medication and other diseases, previous occurrence of bleeding in the last 30 days (if any), consumption of caffeine, alcohol, and cigarettes.

### 2.4.2 Measurements and Variables

A single blood sample was collected just before the next phenprocoumon (PPC) dose from each patient. An aliquot for genetic analysis was frozen immediately at  $-20\text{ °C}$ . The aliquot for quantification of PPC concentrations was centrifuged ( $1992 \times g$ , 15 min,  $4\text{ °C}$ ) and the obtained plasma samples were kept under  $-20\text{ °C}$  prior to LC-MS/MS analyses at the Institute of Pharmacology, University of Cologne.

Phenprocoumon was purchased from Hoffmann–La Roche, Grenzach-Wyhlen, Germany. The metabolites 4'-, 6-, and 7-OH phenprocoumon were synthesized in the Department of Chemistry, University of Konstanz, Germany. The internal standard warfarin was obtained from Sigma-Aldrich Chemie GmbH, Taufkirchen, Germany. Ammonium acetate ( $\geq 97\%$ ) and acetic acid (100%) were purchased from Carl Roth GmbH & Co, Karlsruhe, Germany. Acetonitrile was purchased from Merck KGaA, Darmstadt, Germany. All solvents used for LC-MS/MS were of chromatographic grade.

## MATERIALS AND METHODS

The liquid chromatography–tandem mass spectrometry system consisted of an Agilent 1200 LC Binary SL Pump (Agilent, Waldbronn, Germany), fitted with a tempered tray (5°C) of a CTC PAL Autosampler and an Agilent 1200 TCC SL column oven (30°C), coupled to a triple quadrupole mass spectrometer (API 5000 with QJet™ Ion Guide, Applied Biosystems, Foster City, CA) with an electrospray ionization source with positive polarity (ESI<sup>+</sup>). N<sub>2</sub> was used as sheath, auxiliary and as collision gas. The system was operated in the multiple reaction monitoring (MRM) mode. Analyst software (version 1.4.2, Applied Biosystems) was applied to control the instrument operation as well as the data acquisition and analysis. After thawing, 400 µl of acetonitrile (100%) and 20 µl of 1000 ng/ml warfarin (internal standard) was added to 200 µl plasma. Thereafter, the sample was vortex mixed and centrifugated at 14,000 x g for 10 min). Then, the supernatant was transferred into an LC-MS-vials and 40 µl were injected into the liquid chromatography-tandem mass spectrometry system. The parent and its metabolites were not analyzed enantiospecifically and thus measured concentrations represent the sum of both enantiomers. For chromatographic separation, an Aquasil C18 column (100 × 3 mm, 5 µm, Thermo Electron, Runcorn, UK) was used at a constant flow rate of 0.5 ml/min. The mobile phases were 10 mM ammonium acetate (pH 3.5) in 0.1% acetic acid (A), and 100% acetonitrile (B). The gradient of B was as follows: 10% (0–0.5 min), 10% (0.5–1 min), 50% (1–6 min), 50% (6–6.5 min) and 10% (6.5–7 min).

Calibration curves were developed by spiking 100 µL blank plasma with 100 µL of phenprocoumon and its metabolites using six different concentrations in the range of 200–12500 ng/ml phenprocoumon and 10–625 ng/ml (hydroxy metabolites), respectively. The following parent/product ions were monitored: phenprocoumon [M+H<sup>+</sup>] m/z 281 → 203, 4'-hydroxyphenprocoumon [M+H<sup>+</sup>] m/z 297 → 204, 6-hydroxyphenprocoumon [M+H<sup>+</sup>] m/z 297 → 220, 7-hydroxyphenprocoumon [M+H<sup>+</sup>] m/z 297 → 220, and warfarin [M+H<sup>+</sup>] m/z 309 → 163. Phenprocoumon, 4'-hydroxy-, 7-hydroxy-phenprocoumon and warfarin were eluted at 3.45, 2.35, 2.61, and 3.18 min, respectively. The metabolite 6-OH PPC could not be measured because it failed to meet stability criteria. Quantification of analytes was carried out using peak area ratios of the analyte and internal standard. The lower limits of quantification were 200 ng/mL for phenprocoumon, and 10 ng/mL for the 4'- and 7-hydroxy metabolites. The method was fully validated according to international guidelines. Precision ranged from 2 to 13% for phenprocoumon, and from 2 to 15% for 4'- and 7-OH PPC, while accuracy was 1 to 15%, and 1 to 20% for phenprocoumon and 4'- and 7-OH PPC, respectively.

## MATERIALS AND METHODS

The value of International Normalized Ratio (INR) of prothrombin time was determined by the respective routine methods of the Institute for Clinical Chemistry of the University Hospital of Cologne and the Clinical Chemistry Laboratory in Tübingen and Mannheim, and further external laboratories.

*Genotyping Assays:* Genotyping was done after isolation of genomic DNA from whole blood samples by the QIAamp DNA Blood Mini Kit (Qiagen, Hilden, Germany). CYP2C9 genotyping was carried out for CYP2C9 \*1, \*2, and \*3 alleles through specific hybridization probes using real-time polymerase chain reactions. Determination was done by the LightCycler-CYP2C9 Mutation Detection Kit (Roche Diagnostics GmbH, Mannheim, Germany) using a LightCycler Instrument (Roche Diagnostics GmbH, Mannheim, Germany).

The genotyping of the VKORC1 gene was carried out by direct sequencing of exons 1, 2 and 3 and their introns 1 and 2 and parts of the 5'- and 3'-untranslated regions. Appropriate primers for primary PCR were selected. After PCR the products were purified by vacuum filtration (MANU 3050, Millipore, Molsheim, France). Afterwards sequencing PCRs were carried out with the BigDye Terminator Cycle Sequencing Kit v1.1 (Applied Biosystems, Darmstadt, Germany) and appropriate oligonucleotides. After purification of the sequencing products using Sephadex G50 (Sigma Aldrich, Taufkirchen, Germany) the samples were analysed on a Genetic Analyzer Prism 3100 (Applied Biosystems, Darmstadt, Germany).

## 2.5 Data Analysis

### 2.5.1 Software

The noncompartmental evaluation was performed with the WinNonlin software (version 5.0.1, Professional Edition, Pharsight, Mountain View, CA, USA). Maximum drug concentration ( $C_{\max}$ ) and time of maximum concentration ( $t_{\max}$ ) were taken from the raw data, and the area under the curve from time 0 to the last sampling time  $AUC_0^t$  was calculated using the loglinear trapezoidal rule.

For the purpose of developing population models, all compartmental PK/PD analyses and simulations were performed using the software NONMEM version V, or VI (NONMEM software version 1.1, NONMEM Project Group, University of California at San Francisco,

1998). The first-order conditional estimation algorithm (FOCE INTER), assuming interaction between the residual error and the interindividual error, was used in all cases. Disposition kinetics of the developed models was parametrized in terms of the apparent clearance and apparent volume of distributions.

The software S-Plus (S-Plus version 8.0, Insightful Corporation, Seattle, WA, USA) was used for model diagnostic purposes and for exploration of possible covariate relationships (Mandema et al. 1992).

### 2.5.2 Model Justifications

Model derivation and justification was guided through the following criteria wherever applicable:

- A difference in the objective function value ( $\Delta\text{OFV}$ ) generated via NONMEM was used to carry out comparisons between any two models. A  $\Delta\text{OFV}$  of 3.84 (approximate  $\chi^2$ -distribution) for an additional parameter was used for determining statistical significance ( $P < 0.05$ ) of the difference between two models.
- Visual inspection of goodness-of-fit plots including individual and population predictions, residual plots, individual curve fitting.
- Physiological plausibility and statistical precision of parameter estimates and variability estimates.
- The 95% confidence intervals for the parameter estimates should not include zero or unity. Confidence intervals were estimated for each population parameter as  $\theta_p \pm \text{SE} \times Z$ , where  $\theta_p$  is the estimate population parameter, SE is its associated standard error, and Z is the interval coefficient for a standard normal distribution ( $Z=1.96$  for a 95% confidence interval).
- The final model performance was also justified by simulating concentration time profiles for 1000 subjects having different key parameters like different alleles or variants.
- The predictive performance was evaluated by visual predictive checks to assess, whether a model described the central tendency and variability of the observations adequately. The median, 5th and 95th percentiles of the concentration time curves were calculated by validated Perl scripts (Bulitta et al. 2007) (Active Perl, version 5.10.0; ActiveState, Vancouver, Canada).

### 2.5.3 Covariate Analyses

Multiple activities were performed to identify the kind of relationship between available covariates and individual pharmacokinetic parameter can produce the best description of the data. These relationships were first explored by visual inspection of plots of individual parameters versus covariates. Formal testing was then performed by inclusion of covariates, one by one, in the NONMEM model. A significance level of  $p \leq 0.05$  was used in the forward inclusion steps to generate the full model. This model was then reduced by eliminating covariate-parameter relationships, one by one, and only those covariate effects that were significant at the  $p \leq 0.001$  level were retained in the final model (Mandema et al. 1992).

### 2.5.4 Statistical Models

The interindividual variability was modelled with an exponential error model for all pharmacokinetic parameters, with stepwise cumulative inclusion of respective error terms according to the equation:

$$\theta_j = \theta_p \cdot \exp(\eta_{\theta_j})$$

where  $\theta_j$  is the estimate for a pharmacokinetic parameter in the  $j$ th individual as predicted by the regression model,  $\theta_p$  is the population mean of the pharmacokinetic parameter, and  $\eta_{\theta_j}$  represents the random variable with zero mean and variance  $\omega^2$  that distinguishes the  $j$ th individual pharmacokinetic parameter from the population mean value predicted by the regression model.

The intraindividual variability (Residual variability) was quantified by teasing out different models including:

- Additive model:  $C_{ij} = Cp_{ij} + \varepsilon_{1,ij}$
- Proportional model:  $C_{ij} = Cp_{ij} + \varepsilon_{1,ij} \cdot Cp_{ij}$
- Exponential model:  $C_{ij} = Cp_{ij} \cdot \exp(\varepsilon_{1,ij})$
- Combined model:  $C_{ij} = Cp_{ij} + \varepsilon_{1,ij} \cdot Cp_{ij} + \varepsilon_{2,ij}$

where  $C_{ij}$  is the observed concentration in individual  $i$  at time  $j$ ,  $Cp_{ij}$  is the model predicted concentrations in individual  $i$  at time  $j$ , and  $\varepsilon_{(x),ij}$  describes the independent, identically distributed statistical errors with mean 0 and variance  $\sigma^2$ .

### 2.5.5 Fluorescein Data Analysis

Raw data from the original studies have been published previously (Dinslage et al. 2002; Lux et al. 2003; Steinfeld et al. 2004), but no pharmacokinetic methods have been applied to these data. For all pharmacokinetic calculations, baseline correction of the original data was done to account for autofluorescence of ocular tissues by subtracting the observed fluorescence prior to administration from the values after administration.

A nonparametric evaluation of ocular pharmacokinetics parameters was performed with WinNonlin to obtain maximum fluorescein concentrations ( $C_{\max}$ ) in the cornea and anterior chamber, and the area under the time-concentration curve  $AUC_0^t$ . It was not possible to calculate the extrapolated area under the curve to infinity or the elimination rate constants for many subjects for both formulations due to the scatter of data around the corrected baseline and the fact that none of the studies covered the entire concentration vs. time profile of fluorescein. Point estimates of the ratios of lyophilisate over eye drops for  $AUC_0^t$  and  $C_{\max}$  including the respective 90% confidence intervals were calculated using standard bioavailability methods after log-transformation of the data.

**Population model building procedures:** Compartmental population pharmacokinetic parameters of fluorescein were estimated using NONMEM V. The ocular pharmacokinetic model of fluorescein was developed in two consecutive steps; the first step was to find a model for the eye-drop formulation only, and in the second step this was applied to estimate differences in pharmacokinetic parameters due to formulation effects. The model was parameterized in terms of clearances and distribution volumes using the PREDPP subroutine ADVAN 5 supplied in NONMEM. Covariate (e.g., sex, age, and body weight) data sets were not complete for all subjects and therefore they were not considered for the sake of model development; they are, however, not expected to have a major impact on ocular pharmacokinetics.

In the first step used to evaluate the eye-drop data, the absorption rate constant was fixed at a high value (i.e., 1,000/h). This assumption was made because the data indicated immediate drug absorption and did not support the estimation of an absorption process. The bioavailable fraction was assumed to be unity for this formulation. Initially an attempt was made to fit all fluorescein concentrations, for all subjects, in the cornea and anterior chamber to a previously described two-compartment open model (Coakes and Brubaker

1979; Mishima 1981). Because no adequate fit could be achieved with this model, a three-compartment model was chosen. In the second step, where lyophilisate data were to be evaluated, the apparent intercompartmental clearances, apparent volumes of distribution, and the apparent total clearances were fixed to the estimates obtained for the eye-drop data set, allowing only the relative bioavailability fraction and the absorption rate constant for the lyophilisate preparation to be estimated. This procedure is justified because these parameters are principally related to the physicochemical properties of fluorescein itself and not to the formulation.

**Statistical model:** Interindividual variability was modelled with an exponential error model. Residual variability was expressed using two separate error terms for the cornea and the anterior chamber. Each residual model was modelled using an additive model, a proportional model, or a combination of both.

### 2.5.6 Clarithromycin Data Analysis

A noncompartmental evaluation of clarithromycin pharmacokinetics was performed with WinNonlin to obtain maximum drug concentrations ( $C_{\max}$ ) in plasma, the  $C_{\max}$  time ( $t_{\max}$ ), apparent clearance and volumes of distributions parameters and the area under the time-concentration curve  $AUC_0^{\infty}$ .

**Population model building procedures:** A total of 624 samples of clarithromycin and 624 samples of its 14-(R) hydroxyl metabolite from 12 subjects were co-modelled using NONMEM V. The model was specified as a set of differential equations using the ADVAN6 subroutine.

A one-compartment open model with first-order absorption with or without a lag time was tested to describe clarithromycin plasma concentration profiles after the first dose with first-order elimination. A compartment for the hydroxyl metabolite was included. Absorption behaviour could not be described properly by first-order absorption; therefore a single phase Weibull function (Zhou et al.) was tested. This function was coded as:

$$WB = 1 - \exp(-(k_w * Tw)^\lambda)$$



## MATERIALS AND METHODS

where,  $k_w$  is the absorption rate constant,  $T_w$  is the time after the previous dose and  $\lambda$  is the shape parameter (Petricoul O 2007). This model appropriately described the absorption phase while using more complicated input models was not successful.

The distribution kinetics of the parent and metabolite was assumed to follow linear pharmacokinetics. This model was selected as a base structural model. Clarithromycin clearance was modelled with linear and/or nonlinear kinetics including a Michaelis-Menten model. Elimination of the metabolite was assumed to follow linear pharmacokinetics.

Individual body weights were related to a standard weight, i.e. 70 kg, and used as covariate for apparent volumes of distribution and total clearances parameters of clarithromycin and its metabolite as:

$$CL_i = \bar{CL} \cdot (BW / 70kg)^{0.75}$$

$$V_i = \bar{V} \cdot (BW / 70kg)$$

where  $CL_i$  and  $V_i$  stand for individual apparent total clearance and distribution volume respectively,  $BW$  is the individual body weight expressed in kg;  $\bar{CL}$  and  $\bar{V}$  represent mean clearance and mean volume of distribution, respectively, of typical subjects weighing 70 kg (Anderson et al. 1997).

**Statistical model:** An exponential-variability model was included to describe between subject variability for all pharmacokinetic parameters, with stepwise cumulative inclusion of respective error terms.

Two separate residual variability terms were included in the model: one for clarithromycin and the second for its hydroxyl metabolite. Each residual model was modelled using an additive model, a proportional model, or a combination of both.

**Simulation:** Based on the final parameter estimates of the selected population model, simulations were performed using NONMEM V to predict the concentration profiles for multiple doses of 250, 500, 750, or 1000 mg twice daily. The simulation was done for periods sufficient for achieving theoretical steady-state. For these doses, areas under the plasma curves of the free drug form ( $fAUC_{0-24}$ ), the  $fAUC_{0-24} / MIC$  ratio and the probability of attainment the pharmacodynamic target  $fAUC_{0-24} / MIC > 35$  h (Craig et al. 2002; Tessier et al. 2002) across various MIC values were calculated in steady-state, assuming no significant change in protein binding (Peters and Clissold 1992; Traunmuller et al. 2007).

### 2.5.7 Dextromethorphan Data Analysis

Among the participants of the study, there were two subjects carrying one \*9 allele each and one carrier of a \*10 s allele. Data from these three subjects were excluded from the evaluation as the low allele frequencies preclude estimation of population parameters.

Noncompartmental evaluations were performed using WinNonlin to derive model-independent pharmacokinetic parameters of dextromethorphan and dextrorphan in plasma.

**Population model building procedures:** All observed plasma and urine concentrations of dextromethorphan and dextrorphan from 47 volunteers were analysed simultaneously using NONMEM version VI. Models were specified in sets of differential equations using the ADVAN6 subroutine.

As a starting point, a four-compartment open model was tested to describe the whole data. Each compartment represents each site of measurement (i.e., two compartments each [plasma and urine] for dextromethorphan data and two compartments for dextrorphan data). The absorption process was assumed to follow first-order input kinetics. A first-order absorption rate constant with and without a lag time was explored. Disposition processes for both substances were assumed to follow linear kinetics. For the purpose of semimechanistic modeling, dextromethorphan was assumed to be converted totally to dextrorphan. This metabolic clearance was described as follows:

$$CL_m = CL_b + CL_{CYP2D6}$$

where  $CL_m$  is the total apparent clearance of dextromethorphan describing the biotransformation of dextromethorphan to dextrorphan,  $CL_b$  is the basic value for dextromethorphan metabolic clearance that is not subject to CYP2D6 allelic activity,  $CL_{CYP2D6}$  is the metabolic clearance due to CYP2D6 activity and was specified as follows:

$$CL_{CYP2D6} = n_{*1} * CL_{*1} + n_{*2} * CL_{*2} + n_{*42} * CL_{*41}$$

where  $n_{*x}$  and  $CL_{*x}$ , are the number of alleles observed and metabolic clearance values attributable to the respective allele. This model was selected as a basic structural model for further model building activities.

## MATERIALS AND METHODS

The activity of \*4, \*3 and \*6 alleles was set to zero as they are inactivating mutations (Marez et al. 1997). Clearance of dextromethorphan in individuals who are homozygous for these alleles was assumed to reflect the non-CYP2D6 mediated clearance. Hence, the study evaluated the activity of 2D6\*1, 2D6\*2 and 2D6\*41 alleles, which have recognized as true variants influencing dextromethorphan metabolism activity in vivo (Marez et al. 1997; Sachse et al. 1997; Cai et al. 2007; Sistonen et al. 2007). In addition to CYP2D6 polymorphisms, age, urine pH, and weight as covariates were considered during model building for their impact on pharmacokinetic parameters. An allometric model was used for weight, while exponential and combined models were used to centre the age effect to the mean or the median age values (Holford, N 2002).

**Statistical model:** An exponential interindividual variability model was included for all model parameters forward and backward step by step interchangeably. Four residual-error models were added, one for each data type (i.e., a separate residual-error model for plasma parent data, another for plasma metabolite data etc.). Each residual model was modelled using an additive model, a proportional model, or a combination of both.

### 2.5.8 Phenprocoumon Data Analysis

Data analysis was performed using the nonlinear mixed-effect software in NONMEM version VI using the PRED routine and the first-order conditional estimation method with interactions. Covariates were tested and forward included in the model in a stepwise manner starting with the covariate that resulted in the greatest reduction in the OFV. This procedure was repeated until no significant drop was obtained in the objective function value.

The CYP2C9 [VKORC1] polymorphisms, age, weight, and sex were considered during PK [PD] model building. In a sequential manner, final parameter estimates obtained from the pharmacokinetic model were used for pharmacodynamic model building. This approach has been shown to be computationally faster and can provide less biased PD estimates than the simultaneous analysis approach (Zhang et al. 2003a; Zhang et al. 2003b).

**Pharmacokinetic model building procedures:** All plasma concentrations of phenprocoumon and its 4'- and 7-hydroxy metabolites were analyzed simultaneously. Previous pharmacokinetic analysis of phenprocoumon in plasma after oral administration reported

## MATERIALS AND METHODS

the adequacy of an open one-compartment model (Masche et al. 1999). Thus, a three-compartment open model, one compartment for phenprocoumon concentrations and the other two compartments for 4'- and 7-hydroxy metabolite concentrations, was assumed to describe the whole data. Because only one sample was observed per subject, absorption process could not be evaluated. Furthermore, these observations were obtained at one sampling time at steady state and that was the same for everyone, therefore a meaningful apparent volume of distribution could not be obtained. Hence, the model was developed to describe the steady state concentration independent of volume of distribution of the parent and its metabolites. The input process was modelled as a constant infusion (dose/dosage interval) and just assumes all concentrations are at steady state. The model was parameterized in terms of clearance.

**Pharmacodynamic Model building procedures:** The calculated individual predictions of the parent from the final pharmacokinetic model were used to develop the pharmacodynamic model. A simple linear model was considered to describe the variability in INR values in this population. The VKORC1 polymorphisms, sex, body weight, age, and mass body index were evaluated as covariates on the parameters reflecting the patient's sensitivity to phenprocoumon.

**Statistical model:** Exponential interindividual variability terms were assumed and evaluated for PK and PD model parameters during model development processes. Because the model cannot separate the residual variability from interindividual variability based on one observation per subject (Ette et al. 1995), residual variability terms had to be fixed to small values. For the PK-model, three additive error terms were used to describe the residual variability for the parent and metabolites data and their values were fixed to the lower limits of the assay quantification. For the PD model, an additive residual error for INR was used and fixed to a priori information of 0.0325 (Hamberg et al. 2007). Plausibility of these fixed values was tested by replacing it with higher and lower values.

**Simulation:** Two simulations were executed with use of NONMEM to visualize the model performance using the final PK parameter estimates. The first simulation was run to simulate steady state plasma concentration profiles of the parent drug for male subjects having 70 kg body weight and being 45 years old but with different CYP2C9 features. The second

## MATERIALS AND METHODS

simulation was performed to show the effect of VKORC1 variants in determining the INR at steady state.

Finally and based on final model estimates, and assuming a target INR of 2.5 is clinically desirable, the required maintenance dose of phenprocoumon was calculated for 45 years old male subjects with 70 kg body weight, possessing different combinations of CYP2C9 and VKORC1 polymorphisms.

### 3 RESULTS

### 3.1 Fluorescein

All subjects were included in a noncompartmental and in a compartmental ocular pharmacokinetic analysis of fluorescein from eye drops and lyophilisate forms. The raw data are scattered, which can be attributed to methodological limitations of ocular fluorophotometry. Plots of fluorescein concentrations in the cornea and in the anterior chamber after baseline correction for both formulations are given in Figure 6.

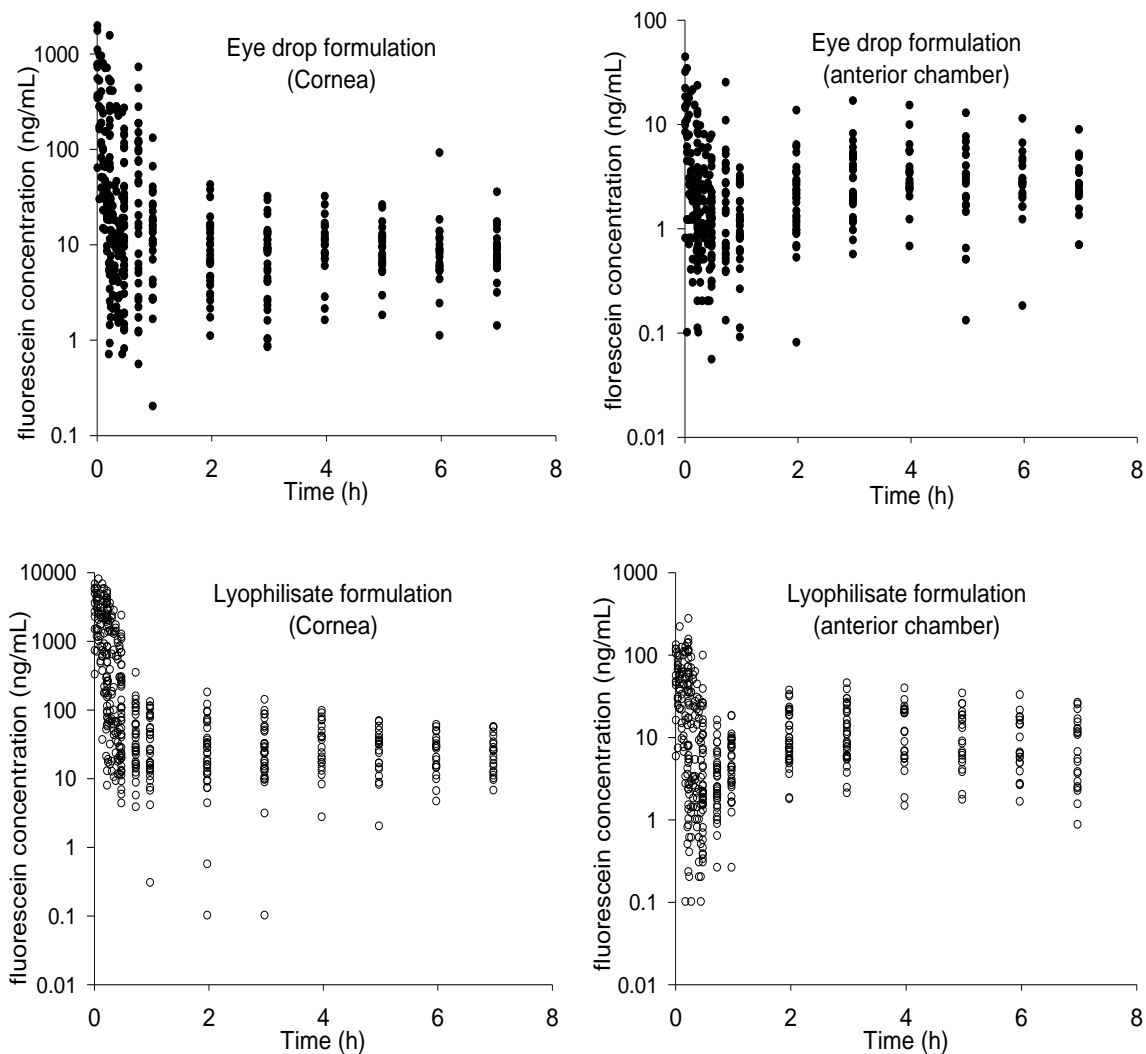


**Figure 6: Florescein concentrations (ng/mL) in the cornea and anterior chamber (raw data)**

These plots show that the original data are quite scattered. Despite this limitation, the noncompartmental pharmacokinetic parameters clearly show a higher extent of ocular

## RESULTS

bioavailability of fluorescein from lyophilisate relative to the eye-drop formulation. Values of  $AUC_0^t$  and  $C_{max}$  for both formulations and their ratios are given in Table 2.

**Table 2: Non-compartmental pharmacokinetics of fluorescein following administration of lyophilisate and eye drops**

Study	Dose (µg)	No. of subjects	Drops (mean ± SD) <sup>a</sup>	Lyophilisate (mean ± SD) <sup>a</sup>	Ratio (90% CI)
<b>Cornea</b>					
				$AUC_0^t$ (hr/ml/ng)	
1	68	10	48 ± 2.77	538 ± 2.11	11.3 (5.7 – 22.0)
2	204	22	90 ± 2.22	566 ± 3.78	6.3 (3.9 – 10.2)
3	68	12	9 ± 3.10	133 ± 3.04	14.6 (8.7 – 24.7)
				$C_{max}$ (ng/mL)	
1	68	10	601 ± 2.67	3514 ± 1.92	5.9 (2.9 – 11.8)
2	204	22	77 ± 3.23	968 ± 6.02	12.5 (6.6 – 23.8)
3	68	12	12 ± 3.04	243 ± 6.24	19.9 (10.2 – 38.9)
<b>Anterior chamber</b>					
				$AUC_0^t$ (hr/ml/ng)	
1	68	10	1.3 ± 2.84	11 ± 2.12	8.9 (4.9 – 16.4)
2	204	22	14 ± 1.98	66 ± 2.46	4.7 (3.10– 7.0)
3	68	12	3.0 ± 2.19	22 ± 1.70	6.9 (4.2– 11.23)
				$C_{max}$ (ng/mL)	
1	68	10	13 ± 2.17	80 ± 1.91	6.3 (3.3 – 12.1)
2	204	22	2.2 ± 3.20	30 ± 3.94	13.7 (8.0– 23.4)
3	68	12	4.1 ± 2.06	18 ± 2.59	4.3 (1.3 –14.1)

<sup>a</sup> Data given as geometric mean ± standard deviation

Sampling schedules were as follows: study 1: 0–30 min (15 observations); study 2: 0–420 min (10 observations) study 3: 0–180 min (6 observations).  $AUC_0^t$ : area under the concentration time curve up to the last observation time,  $C_{max}$ : maximum observed concentration, ratio point estimate for ratio of lyophilisate over eye drops, CI confidence interval, and a Geometric standard deviation.

Population kinetics indicated the superiority of the three-compartment model compared with two-compartment model based on individual and population predictions. This superiority was also confirmed by a marked drop in the objective function ( $\Delta$  OFV= 2106). Blue print of the final model is given in Figure 7.



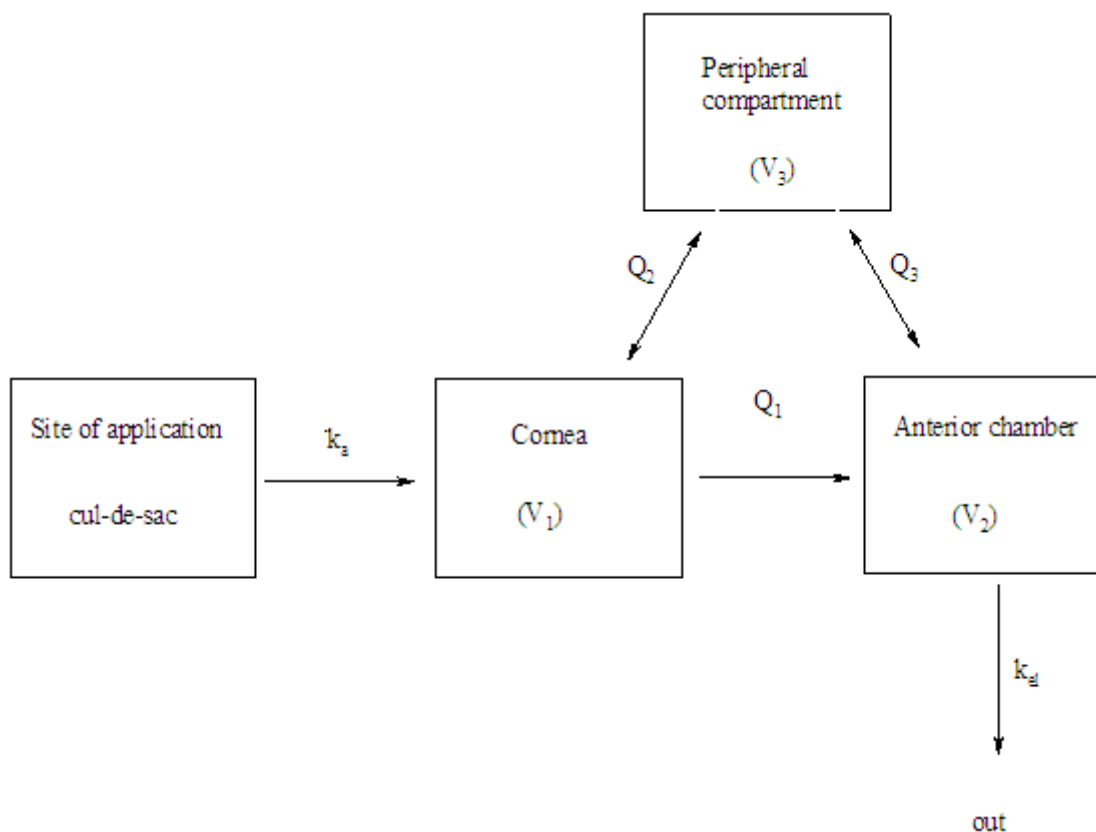


**Figure 7: Blueprint of the final fluorescein population pharmacokinetic model.**

A three-compartment model used to describe the transfer of fluorescein into and from the cornea and anterior chamber after topical administration of the drug as eye drops and lyophilisate.  $k_a$  is the absorption rate constant,  $V_1$ ,  $V_2$ , and  $V_3$  are the apparent volumes of distribution of fluorescein in the first, second and third compartments, respectively.  $Q_1$ ,  $Q_2$ , and  $Q_3$  are the intercompartmental clearances and  $k_{el}$  is the elimination rate constant.

This model was described by the following parameters:  $k_a$  is the apparent absorption rate constant,  $V_1$  is the apparent volume of distribution in the cornea,  $Q_1$  is the apparent intercompartmental clearance between cornea and anterior chamber,  $V_2$  is the apparent volume of distribution in the anterior chamber,  $CL_{tot}$  is the apparent total clearance,  $Q_2$  is the intercompartmental clearance between anterior chamber and the third compartment,  $V_3$  is the apparent volume of distribution in the third compartment, and  $Q_3$  is the intercompartmental clearance between the third compartment and the cornea. Elimination

## RESULTS

Fluorescein was assumed to be eliminated from the anterior chamber compartment with first order elimination rate constant,  $k_{el}$ .

Visualisation of the population data shows that this empirical model could adequately describe fluorescein data in the cornea and anterior chamber (Figure 8a and 8b). Examples of typical individual predictions are given in Figure 9. Diagnostic plots of the final model for both formulations are given in Figure 10 and 11. These plots of the observed concentrations vs. the population-predicted concentrations show the reasonable distribution of original data around the line of unity. Final model specifications are given in Figure 12. The effect of the formulation type on the absorption rate could not be assessed because there were not enough data points early after administration of fluorescein, but it was possible to estimate an apparent absorption rate following administration of the lyophilisate. The relative systemic bioavailability of fluorescein from lyophilisate was estimated to be about 3.7-fold higher (95% CI 2.9 – 4.5) than following administration of the eye drops. It should be noted that this estimate is based on ocular concentration vs. time profiles only, i.e., systemic availability via the ocular route was estimated; this does not take into account fluorescein lost by lacrimation and reaching the systemic circulation via conjunctival, nasal, or gastrointestinal routes. Population pharmacokinetic parameter estimates of fluorescein of the final models as well as the 95% confidence intervals are summarized in Table 3.

## RESULTS

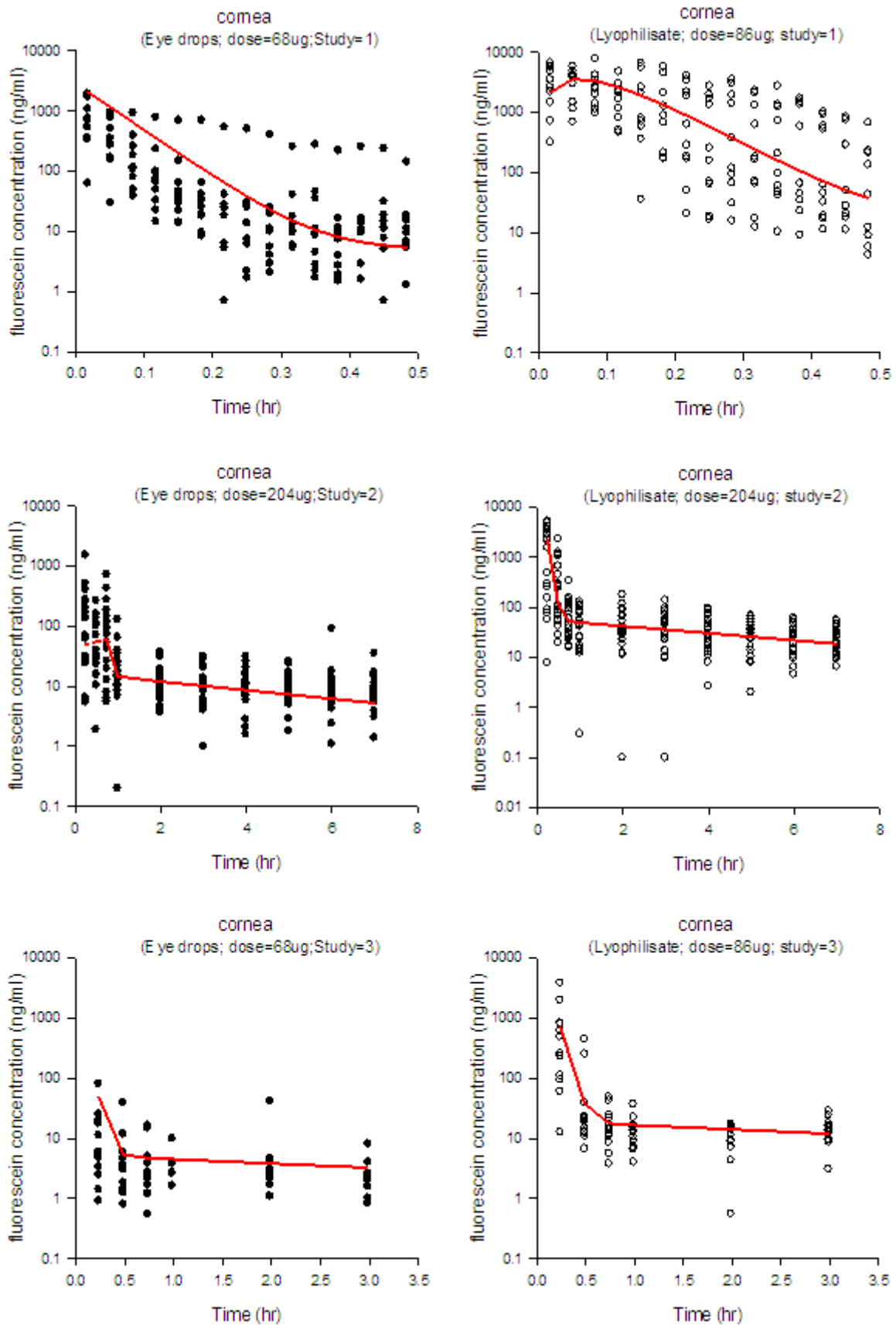


**Figure 8a: Fluorescein concentrations in the cornea with the population model (solid lines).** The eye drops in study #2 were administered at three different 68  $\mu\text{g}$  doses given 15 min apart

## RESULTS

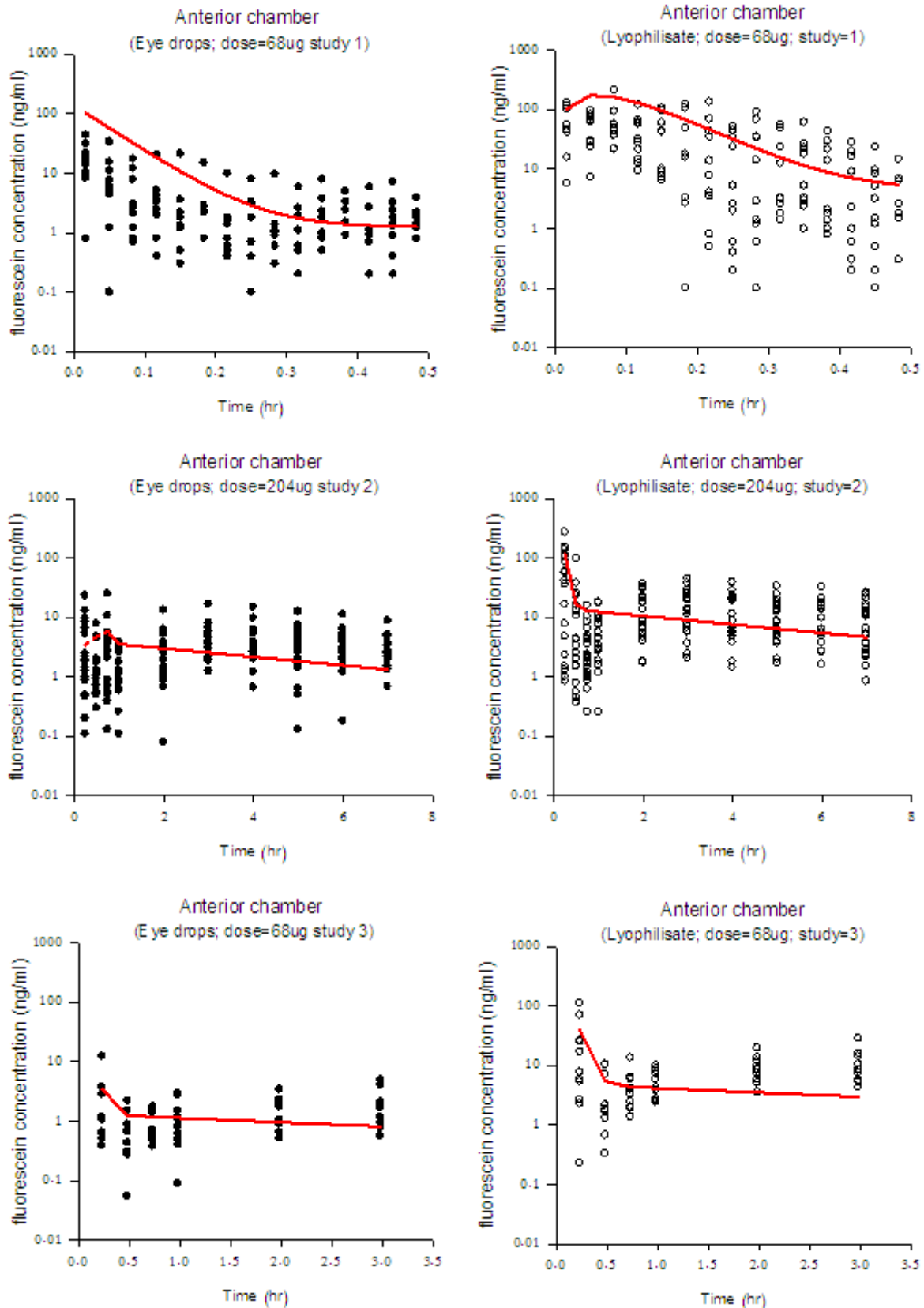


**Figure 8b: Fluorescein concentrations in the anterior chamber with the population model.**

The solid line is the population model. The eye drops in study #2 were administered at three different 68  $\mu$ g doses given 15 min apart.

## RESULTS

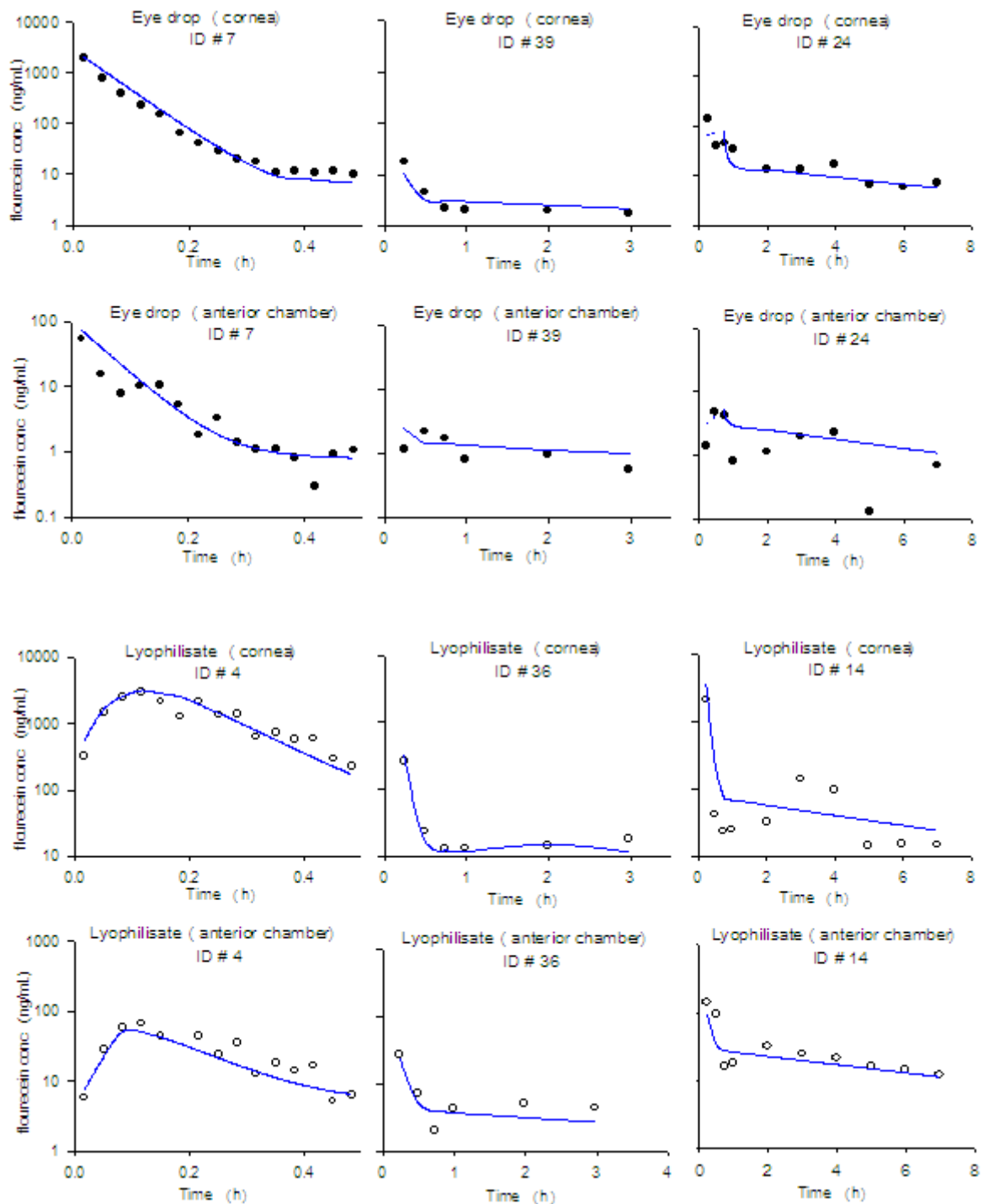


**Figure 9: Individual predictions of fluorescein level in the cornea and anterior chamber in three subjects**

Open and closed circles represent raw data for eye drop and lyophilisate formulation, respectively  
 Solid lines represent individual prediction model

## RESULTS

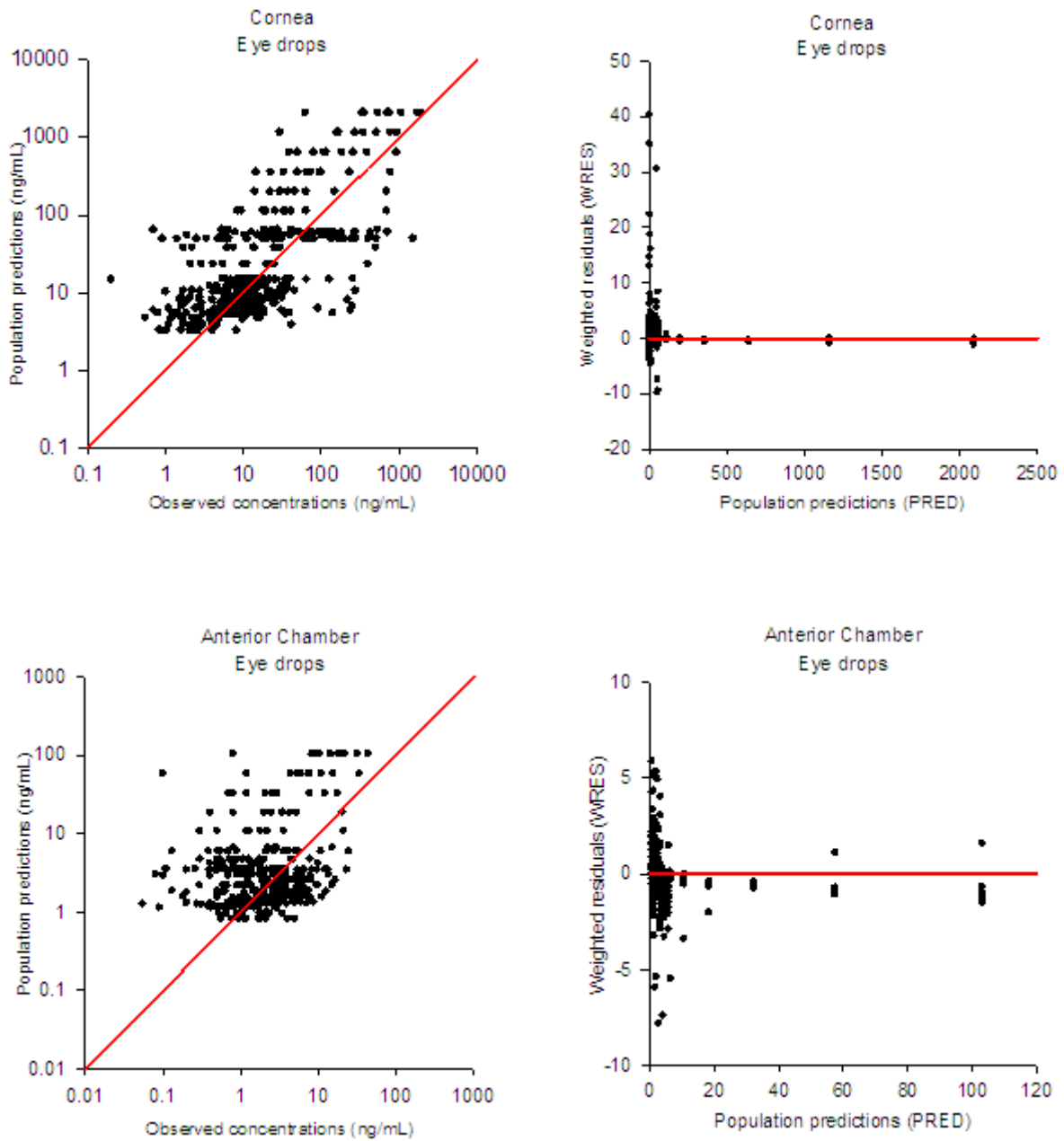


**Figure 10: Goodness-of-fit plots of the final model for the eye drop formulation.** Plots show unity and zero lines in the right and left panels respectively.

## RESULTS

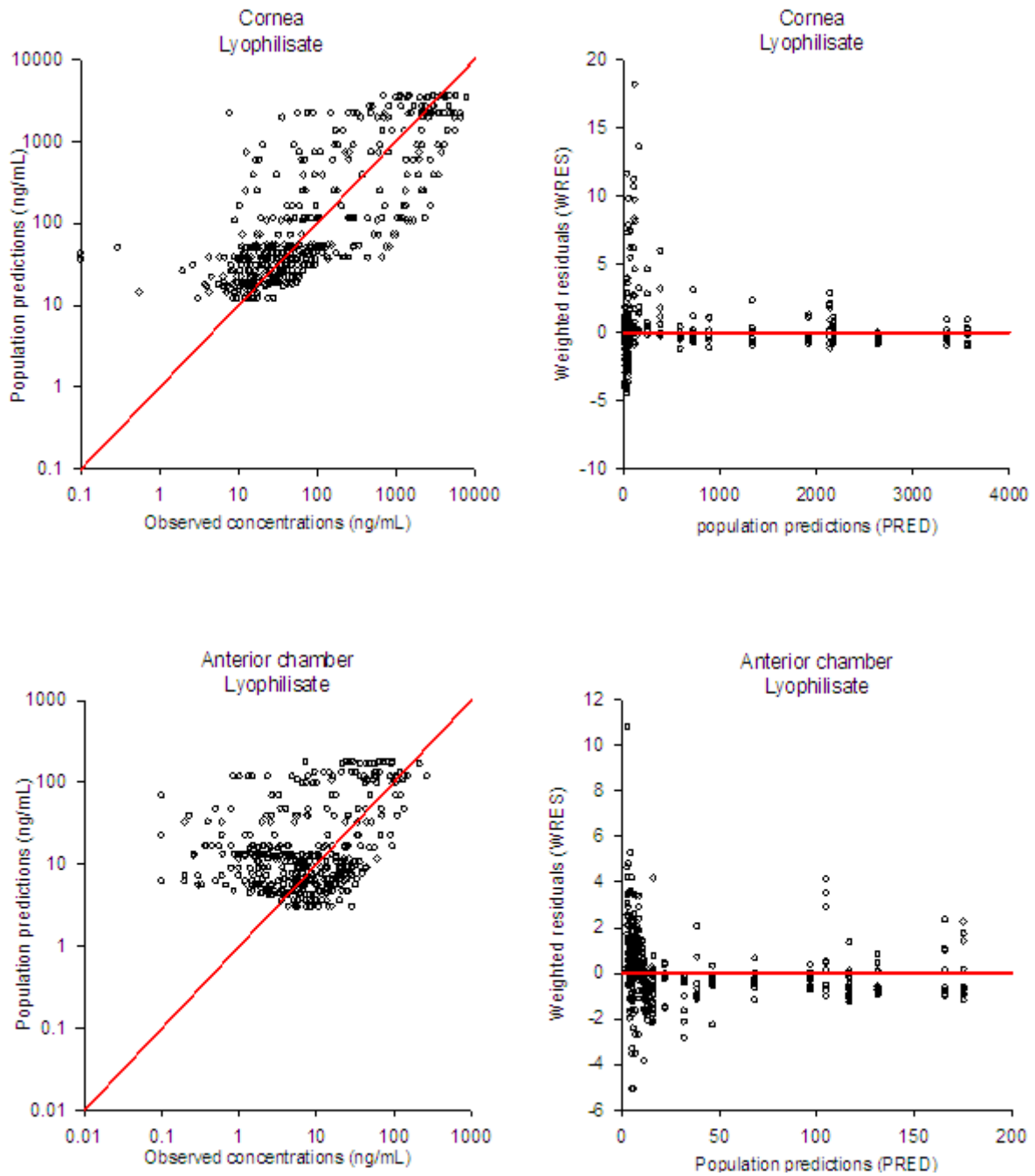


**Figure 11: Goodness-of-fit plots of the final model for the lyophilisate formulation**  
Plots show unity and zero lines in the right and left panels respectively.

**Table 3: Ocular population pharmacokinetics of fluorescein**

Parameter	Unit	Point estimate	95%CI
Absorption rate constant ( $k_a$ ) for lyophilisate <sup>a</sup>	1/hr	16.7	12.3 – 21.1
Apparent volumes of distribution of fluorescein in the first compartments $V_1$	$\mu$ L	24.6	3.6 – 45.6
Intercompartmental clearance $Q_1$	L/hr	0.25	0.08 – 0.42
Apparent volumes of distribution of fluorescein in the second compartments $V_2$	$\mu$ L	10.3	9.1 – 12.8
Apparent total clearance CL	L/hr	4.34	2.49 – 6.19
Intercompartmental clearance $Q_2$	L/hr	0.20	0.05 – 0.34
Apparent volumes of distribution of fluorescein in the third compartments $V_3$	L	3.42	1.99- 4.85
Intercompartmental clearance $Q_3$	L/hr	0.54	0.20 - 0.87
Relative bioavailability for lyophilisate (F)		3.7	2.9 – 4.5
Interindividual variability in ( $Q_1$ )		1.10	26.7 %*
Interindividual variability in (CL)		0.34	8.6 %*
Residual variability in cornea (CV %)		56.2	9.2%*
Residual variability in anterior chamber (CV %)		52.0	5.7%*

<sup>a</sup> =Immediate absorption and a relative bioavailability of 1 were assumed for eye drops,

\* = relative standard errors of the estimated variance.



## RESULTS

### Relevant part of the "Eye Drop" drop model

```
$SUBROUTINES ADVAN5
$MODEL
COMP=(DEPOT,INITIALOFF,DEFDOSE)
COMP=(CORNEA,NOOFF,DEF OBS)
COMP=(ANTCHAM,NOOFF)
COMP=(PERIPH,NOOFF)
```

```
$PK
V2=THETA(1)
Q1=THETA(2)*EXP(ETA(1))
V3=THETA(3)
CL=THETA(4)*EXP(ETA(2))
Q2=THETA(5)
V4=THETA(6)
Q3=THETA(7)
```

**KA= 1000**

```
K12=KA
K20=0
K23=Q1/V2
K32=Q1/V3
K30=CL/V3
K24=Q2/V2
K42=Q2/V4
K34=Q3/V3
K43=Q3/V4
```

```
S2=V2
S3=V3
```

```
$ERROR
DEL=0
IF(F.EQ.0) DEL=0.001
IF(CMT.EQ.2) THEN
Y=F*(1+EPS(1))
ELSE
Y=F*(1+EPS(2))
ENDIF
W=F
IPRED=F
```

```
$ESTIMATION METHOD=1 INTERACTION
```

### Relevant part of the "Lyophilisate" drop model

```
$SUBROUTINES ADVAN5
$MODEL
COMP=(DEPOT,INITIALOFF,DEFDOSE)
COMP=(CORNEA,NOOFF,DEF OBS)
COMP=(ANTCHAM,NOOFF)
COMP=(PERIPH,NOOFF)
```

```
$PK
V2=THETA(1)
Q1=THETA(2)*EXP(ETA(1))
V3=THETA(3)
CL=THETA(4)*EXP(ETA(2))
Q2=THETA(5)
V4=THETA(6)
Q3=THETA(7)
; All previous parameters were fixed to
estimates obtained from eye drop model
KA= THETA (8)
F1=THETA(9)
```

Other model specifications were similar to those of eye drop formulation

**Figure 12: Relevant NONMEM code of the final fluorescein model**

### 3.2 Clarithromycin

Data derived pharmacokinetic parameters estimated by non-compartmental analysis for clarithromycin and its hydroxymetabolite are given in Table 4.

**Table 4: Noncompartmental pharmacokinetic parameters of clarithromycin and its 14(R)-hydroxy metabolite**

	Parameter	1st dose	3rd dose	7th dose (Steady state)
Clarithromycin	$C_{max}$ ( $\mu\text{g}/\text{mL}$ )	$2.49 \pm 0.76$ (1.60 – 4.02)	$3.08 \pm 0.82$ (1.77 – 4.80)	$3.57 \pm 0.72$ (2.39 – 4.67)
	$t_{max}$ (h)	$3.54 \pm 0.99$ (1.50 – 5.00)	$3.54 \pm 0.86$ (2.50 – 4.50)	$3.92 \pm 0.87$ (2.00 – 5.50)
	$AUC_{12h}$ (h · $\mu\text{g}/\text{mL}$ )	$15.4 \pm 5.1$ (9.4 – 29.7)	$21.8 \pm 6.06$ (13.3 – 37.1)	$27.4 \pm 6.76$ (18.3 – 39.6)
	$t_{1/2}$ (h)	$3.58 \pm 0.71$ (2.83 – 5.47)	$4.26 \pm 0.82$ (3.24 – 5.18)	$4.65 \pm 1.04$ (3.34 – 7.75)
	$k_{el}$ (1/h)	$0.199 \pm 0.033$ (0.127 – 0.245)	$0.168 \pm 0.030$ (0.119 – 0.214)	$0.158 \pm 0.032$ (0.109 – 0.207)
	$C_{av}$ ( $\mu\text{g}/\text{mL}$ )	NA	NA	$2.29 \pm 0.563$ (1.52 – 3.30)
14-OH-Clarithromycin	$C_{max}$ ( $\mu\text{g}/\text{mL}$ )	$0.961 \pm 0.254$ (0.545 – 1.32)	$1.11 \pm 0.241$ (0.741 – 1.53)	$1.09 \pm 0.225$ (0.721 – 1.57)
	$t_{max}$ (h)	$4.33 \pm 1.29$ (2.00 – 6.00)	$3.96 \pm 1.03$ (2.50 – 5.50)	$4.71 \pm 0.88$ (2.50 – 6.00)
	$AUC_{12h}$ (h · $\mu\text{g}/\text{mL}$ )	$7.19 \pm 1.77$ (4.89 – 11.4)	$9.92 \pm 2.45$ (6.95 – 14.1)	$10 \pm 2.00$ (7 – 14.4)
	$t_{1/2}$ (h)	$38.07 \pm 9.56$ (20.09 – 57.32)	$9.13 \pm 2.96$ (5.67 – 14.81)	$8.89 \pm 2.69$ (4.61 – 15.56)
	$k_{el}$ (1/h)	$0.105 \pm 0.027$ (0.054 – 0.162)	$0.083 \pm 0.026$ (0.047 – 0.122)	$0.084 \pm 0.022$ (0.056 – 0.127)
	$C_{av}$ ( $\mu\text{g}/\text{mL}$ )	NA	NA	$0.838 \pm 0.166$ (0.584 – 1.20)

Clarithromycin was administered as repeated oral doses of 500mg b.i.d.;  $t_{max}$  is the time of maximum concentration ( $C_{max}$ );  $t_{1/2}$  is the elimination half life;  $k_{el}$  is the elimination rate constant;  $AUC_{12h}$  is the area under the plasma concentration-time curve up to 12 hours;  $C_{av}$  is the average concentration at steady state; NA: not applicable.

The absorption profiles of clarithromycin were best described by a Weibull absorption model that resulted in a marked improvement in the objective function value OFV ( $\Delta\text{OFV}$ , - 86) compared with a first order absorption model. A plot of four individual plasma concentrations of clarithromycin versus time after the first dose is shown in Figure 13. This

## RESULTS

figure shows how the Weibull model best described the absorption phase in comparison with a standard first-order absorption model.

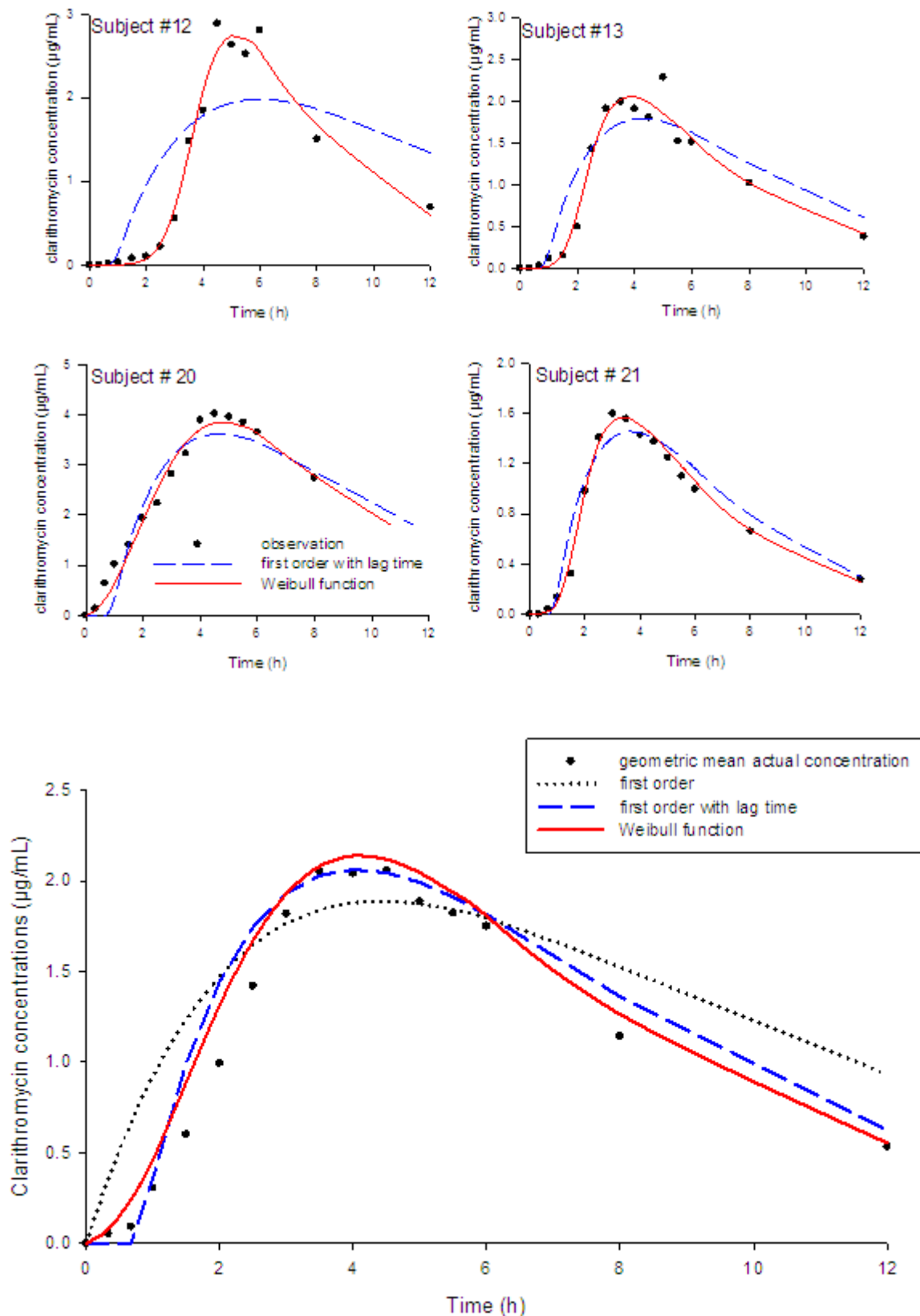


**Figure 13: Visualisation of different absorption models of clarithromycin.**

Clarithromycin plasma concentration-time profiles for four individuals (upper figures) and population mean, N=12 (lower figure) after the first dose assuming linear elimination pathway.

## RESULTS

Based on the multiple dose regimen of 500 mg, the apparent total drug clearance of clarithromycin (CLp) was found to decrease with time in a nonlinear fashion as shown by non-compartmental methods (Bulitta et al. 2003). As expected, a linear two-compartment model could not describe this nonlinearity. Addition of a nonlinear elimination pathway with Michaelis-Menten kinetics improved model fitting considerably ( $\Delta\text{OFV}$ , - 252), however the overall nonlinearity was still not properly explained as this model was not able to capture maximum plasma concentrations of clarithromycin (Figure 14).

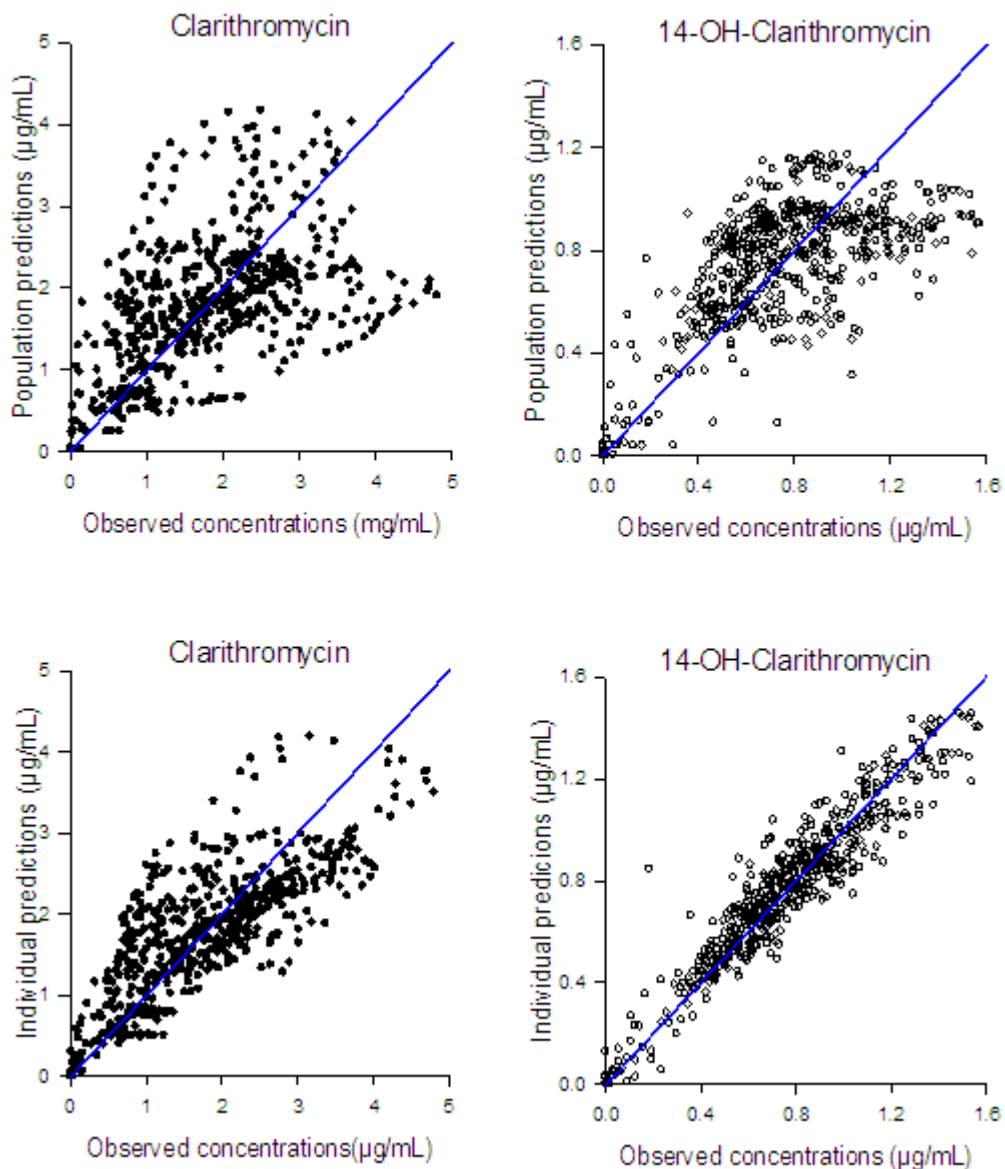


**Figure 14: Michaelis-Menten Model of clarithromycin.**

Clarithromycin fitting is on the left pane and its metabolite on the right with unity line.

## RESULTS

Finally, the inhibitory effect of clarithromycin on its apparent total clearance was modelled “mechanistically” by addition of a hypothetical inhibition compartment. The concentration of the parent drug was used to derive the extent of (reversible) inhibition in this compartment. Here, the total apparent clearance of clarithromycin (CLp) was split into two components. The first component was inhibited by the hypothetical clarithromycin concentration in the inhibition compartment ( $C_{inhibt}$ ), whereas the second component was not affected by  $C_{inhibt}$ . The fraction of CLp that was not inhibited by  $C_{inhibt}$  was described as FCLp and its estimate allowed to range from zero (i.e. 100% inhibition) to unity (i.e. no clearance inhibition) (Plock et al. 2007). A transfer rate constant between parent and inhibition compartments ( $k_i$ ) in addition to the concentration in this compartment yielding 50% inhibition of clarithromycin clearance ( $IC_{50}$ ) was included to explain the inhibition of clearance over time. This model is blueprinted in Figure 15 and its code specification is given in Figure 16. Inclusion of the inhibition compartment side by side to the drug model adequately described the nonlinear time-dependent auto-inhibition pharmacokinetics of clarithromycin. This model led to a significant improvement in the objective function compared to the Michaelis-Menten elimination model ( $\Delta OFV$ , - 752).

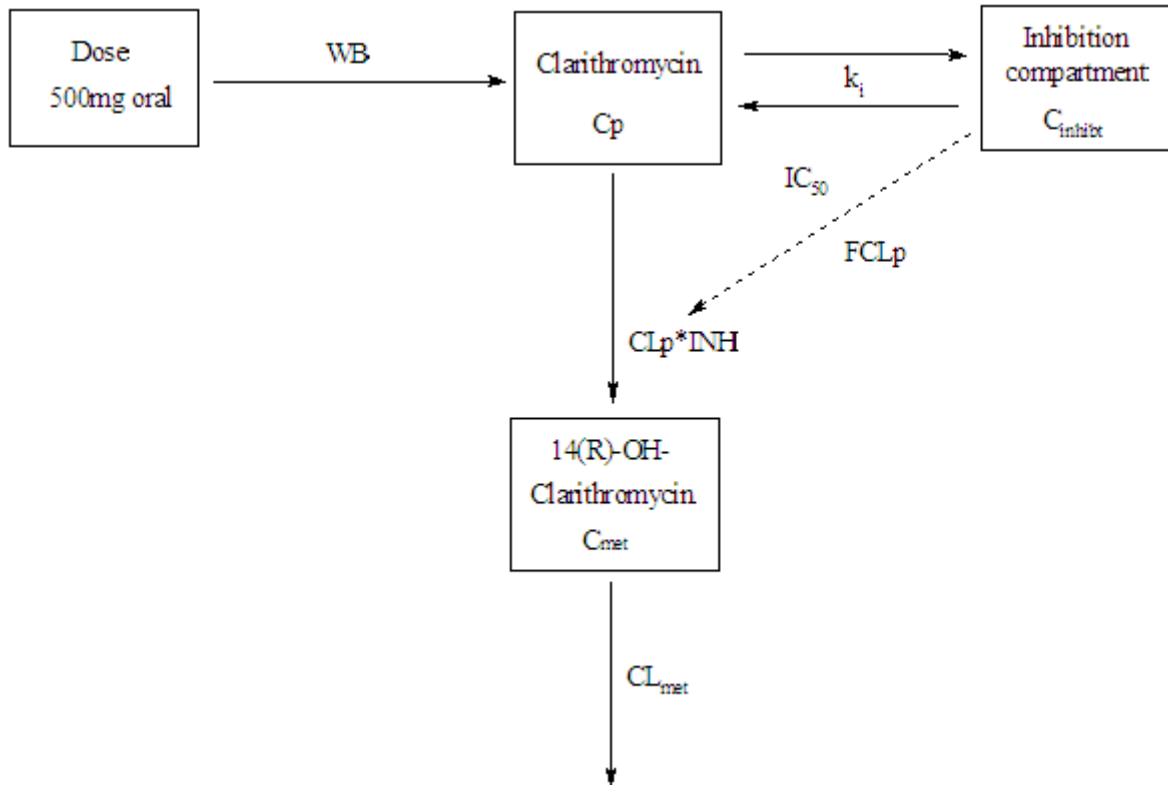
In the final model and for the available data, four between-subject variability terms were identified. In addition, residual additive error models resulted in the best model convergence compared with proportional and or combined error models. Pharmacokinetic parameter estimates of the final model are shown in Table 5. Standard goodness-of-fit plots of the final model of clarithromycin and its 14-(R) hydroxy metabolite are given in Figure 17. These plots suggested that the selected autoinhibition model adequately described both the plasma concentration time profiles of clarithromycin and its 14-(R) hydroxy metabolite simultaneously. The superiority of the inhibition model (final model) in comparison with the Michaelis-Menten model is given for three subjects in Figure 18. The visual predictive check of clarithromycin and its major metabolite indicated that the final model could predict the observations including the maximum plasma concentrations (Figure 19). The simulated 90% prediction interval closely reflected the observed plasma concentrations of clarithromycin and 14-(R) hydroxy clarithromycin.

Concentrations of clarithromycin in the theoretical inhibition compartment as well as the extent of time course inhibition are shown in Figure 20. The plot suggested that inhibition

## RESULTS

started rapidly and that the 500 mg b.i.d dose inhibited enzyme activity by approximately 50% to 70 % of initial values during steady state.

Based on the pharmacokinetic parameter estimates of the final model, the simulated medians for four dose levels, i.e., 250, 500, 750 and 1000 mg twice daily (Figure 21) suggested that the extent of auto-inhibition and the emerging changes in pharmacokinetics with time is much more pronounced for the higher doses. While for the 500 mg b.i.d standard dose no further increase of exposure occurs after the 2<sup>nd</sup> day of treatment, for a 1000 mg b.i.d dose reaching steady state it is expected to take several days. AUC values at steady state for the 1000 mg b.i.d dose would exceed those for the 500 mg b.i.d dose by 3.6-fold (Table 6). For the parent drug at steady state, the probability of achieving the target for pathogens having MIC value of 0.5 mg/L is 0 %, 43 %, 94 % and 100 % for the 250, 500, 750 and 1000 mg doses, respectively (Table 6 and Figure 22).



$$WB = [1 - \exp(-(k_w \cdot T_w)^\lambda)] h^{-1}$$

$$INH = FCLp + (1 - FCLp) \cdot (1 - C_{inhibt} / (IC_{50} - C_{inhibt}))$$

$$dA_{abs} / dt = -WB \cdot A_{abs}$$

$$dC_p / dt = (WB \cdot A_{abs} - C_p \cdot CLp \cdot INH) / V_p$$

$$dC_{inhibt} / dt = k_i \cdot C_p - k_i \cdot C_{inhibt}$$

$$dC_{met} / dt = (C_p \cdot CLp \cdot INH - C_{met} \cdot CL_{met}) / V_{met}$$

**Figure 15: Blueprint and differential equations of the final model**

WB is the Weibull absorption function from the gastrointestinal tract,  $A_{abs}$  is the amount of drug in the absorption compartment,  $k_w$  is the absorption rate constant,  $T_w$  is the time after the previous dose and  $\lambda$  is the shape parameter of the Weibull function.  $V_p$ ,  $V_{met}$ ,  $C_p$  and  $C_{met}$  are the apparent volumes of distribution and plasma concentrations of clarithromycin and its hydroxy metabolite respectively;  $k_i$  is the transfer rate constant between parent and inhibition compartments. Clarithromycin clearance ( $CLp$ ) is inhibited based on the concentration in the inhibition compartment  $C_{inhibt}$ ; and  $IC_{50}$  is the concentration in the inhibition compartment yielding 50% of maximum clearance inhibition of clarithromycin.  $INH$  is the overall inhibition parameter,  $FCLp$  is the fraction of the clearance not subject to inhibition and  $C_{inhibt}$  is the concentration of the clarithromycin effective in the inhibition compartment.  $CL_{met}$  is the apparent total clearance of 14(R)-hydroxy clarithromycin.

```

$ PROBLEM: Clarithromycin PK Model
$SUBROUTINES ADVAN6 TRANS1 TOL=4
$MODEL
COMP=(DEPOT,DEFDOSE)
COMP=(CENTRAL)
COMP=(INHIB)
COMP=(METAB)

$PK
KA1=THETA(1)*EXP(ETA(1))
GAMA1=THETA (2)
WB=1-EXP((-KA1*WBTM)**GAMA1))      ; Weibull function
  TVV2=THETA(3)*(WT/70)
V2=TVV2*EXP(ETA(2))
  TVCL=THETA(4)*((WT/70)**0.75)
CL=TVCL*EXP(ETA(3))
RCLF=THETA(5)
KIC=THETA(6)
IC50=THETA(7)
  TVCLM=THETA(8)*((WT/70)**0.75)
CLM=TVCLM*EXP(ETA(4))
V4=THETA(9)*(WT/70)

K24=CL/V2
K40=CLM/V4
S2=V2
S4=V4

$ERROR
DEL=0
IF(F.EQ.0) DEL=0.0001
IF(CMT.EQ.2) THEN
Y=F+EPS(1)
ELSE
Y=F+EPS(2)
END IF
W=F
IPRED=F
IRES=DV-IPRED
IWRES=IRES/(W+DEL)

$DES
C2=A(2) /V2
C4=A(4)/V4
INH=RCLF+(1-RCLF)*(1-A(3)/(IC50+A(3)))

DADT(1)=-WB*A(1)
DADT(2) =WB*A(1)-CL*INH*C2
DADT(3) =KIC*(C2-A(3))
DADT(4)=CL*INH*C2-CLM*C4

$ESTIMATION METHOD=1 INTERACTION

```

**Figure 16: Relevant NONMEM code of the final clarithromycin model**



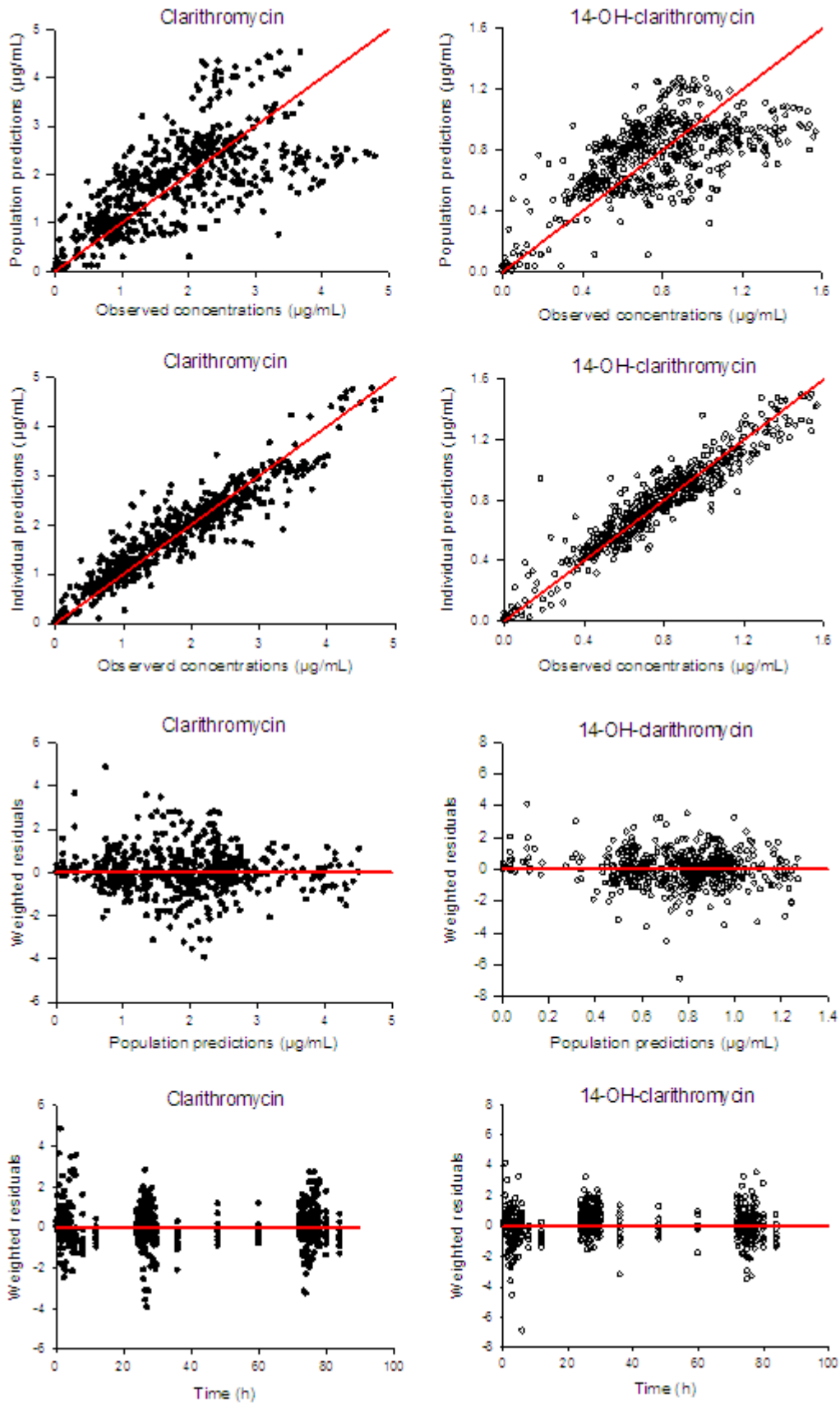


**Figure 17: Goodness-of-fit plots for the final model of clarithromycin.**

Plots include unity and zero lines for clarithromycin (left) and its hydroxyl metabolite (right)

## RESULTS

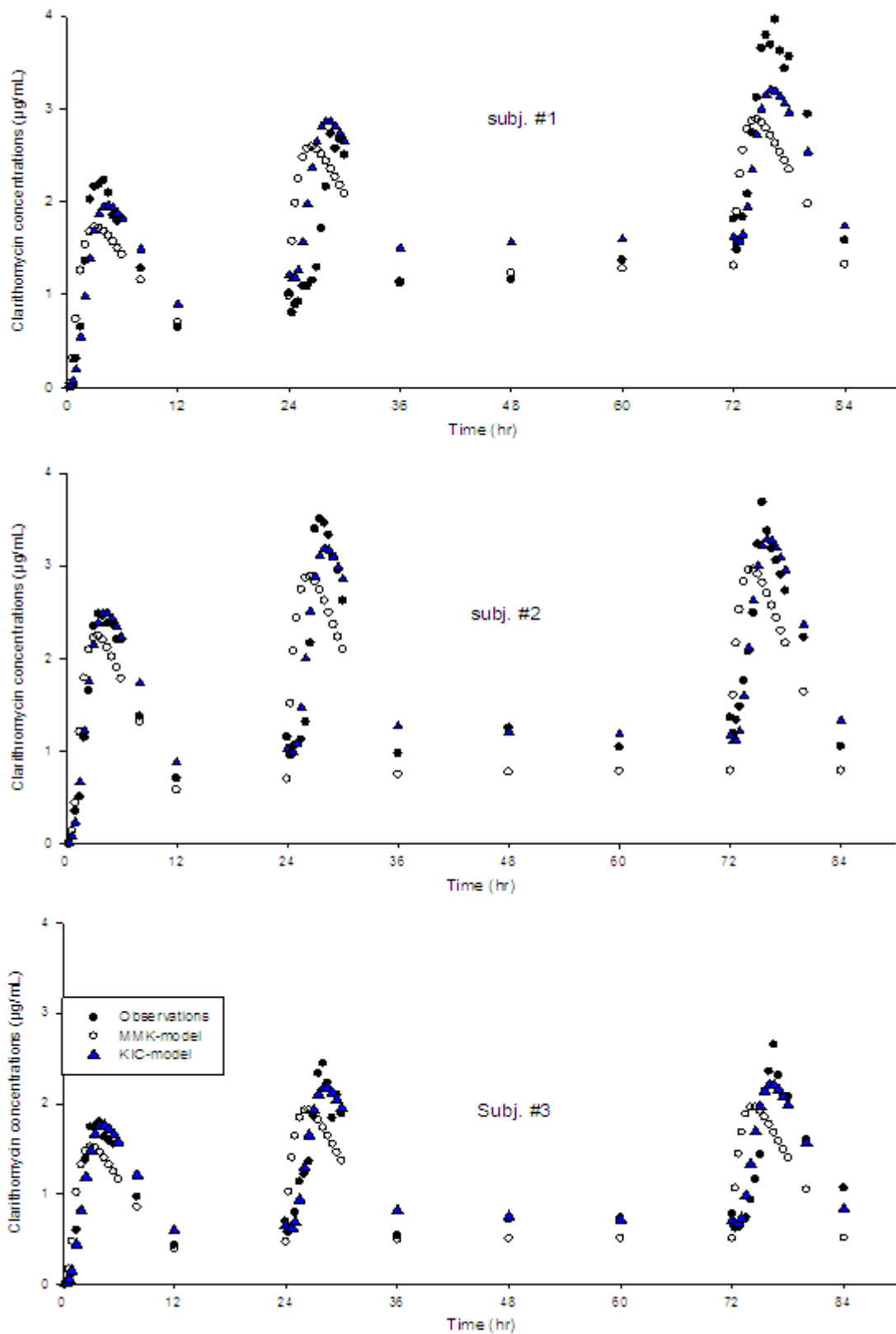


**Figure 18: Individual predictions of clarithromycin in 3 subjects.**  
KIC-model= inhibition-compartment model (final model),  
MMK-model =Michaelis-Menten model

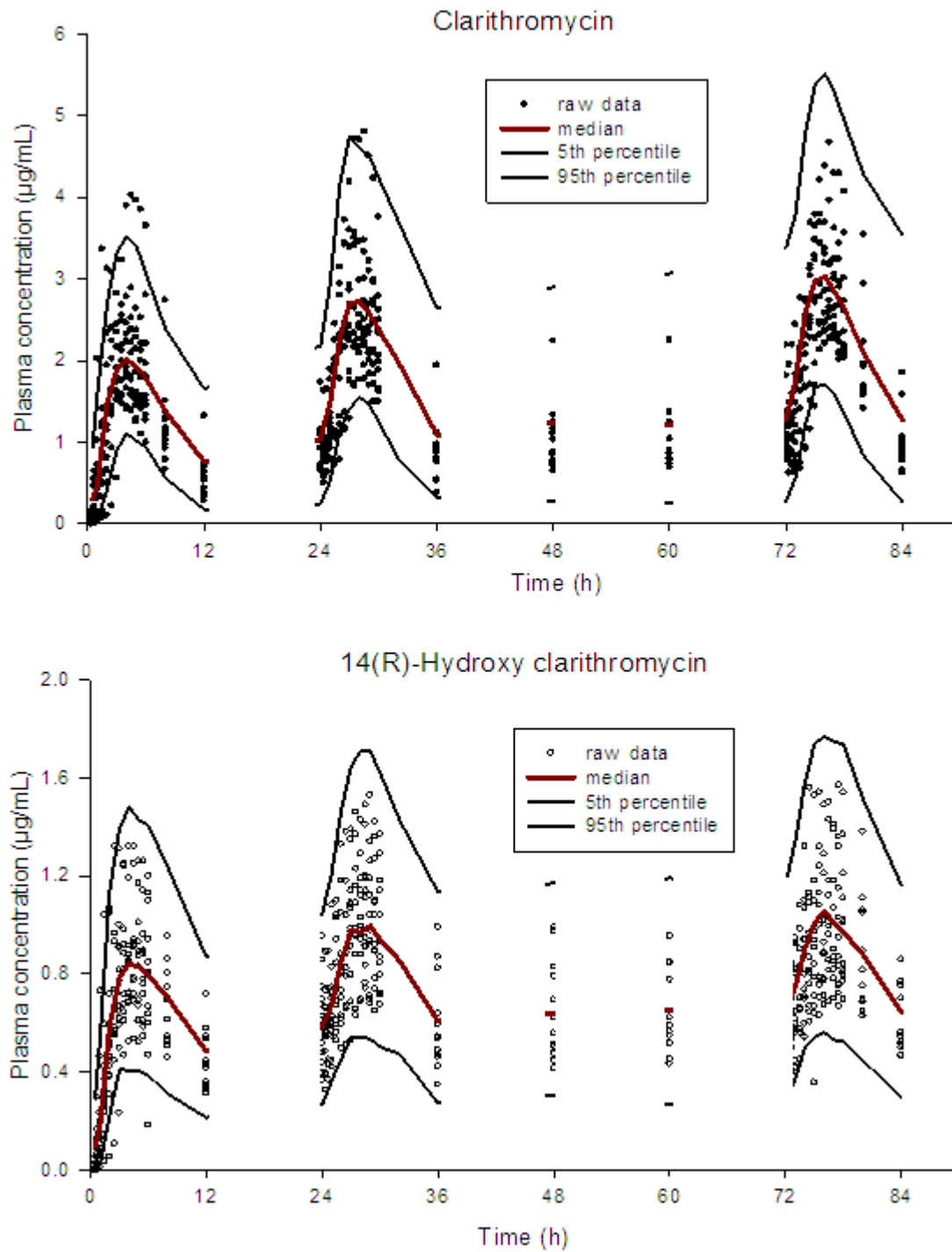
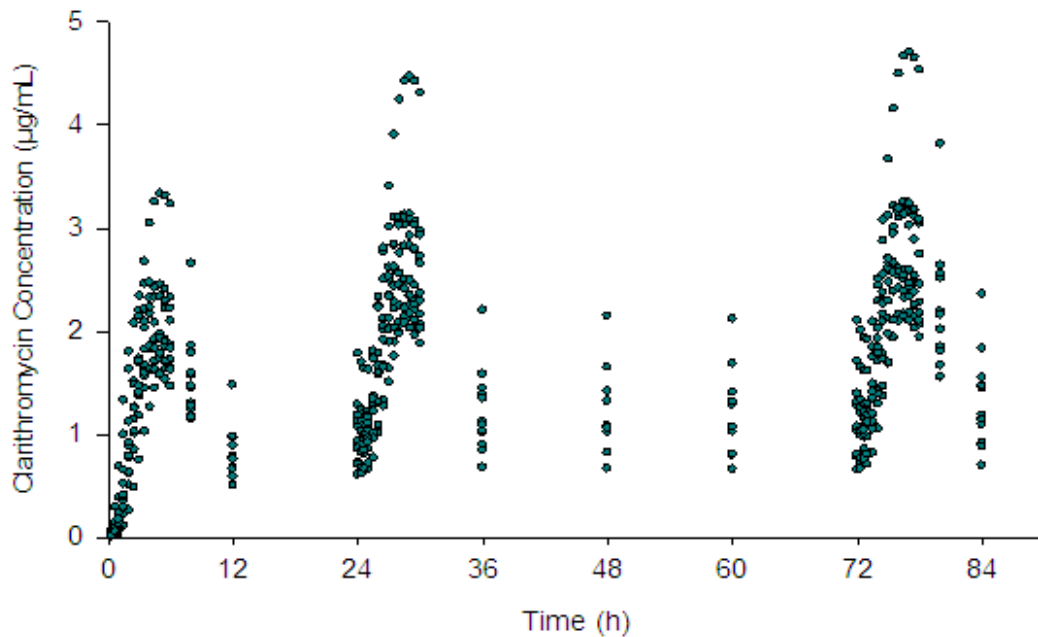


**Figure 19: Visual predictive check of clarithromycin model.**

Circles correspond to the actual plasma concentrations of clarithromycin (upper panel) and its metabolite (lower panel). Lines represent 5%, median and 95% percentiles

### Simulated clarithromycin concentration in the inhibition Compartment



### Clarithromycin inhibition profile

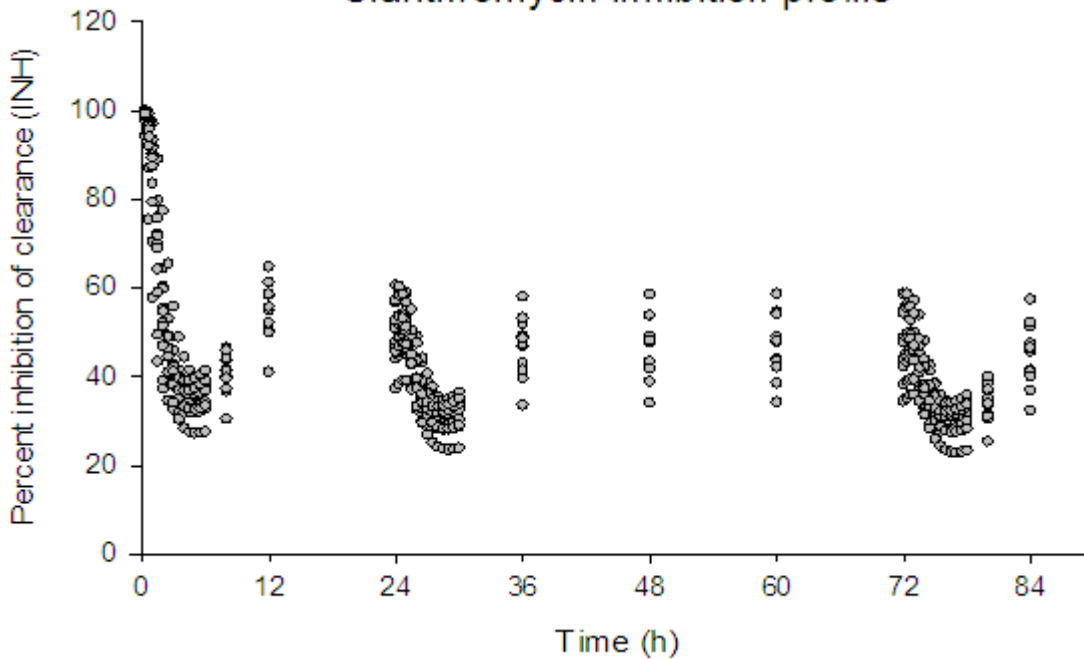


**Figure 20: Inhibition compartment profiles.**

Upper panel: simulated clarithromycin concentration in the inhibition compartment for the 500 mg bid dose.

Lower panel: autoinhibition of clarithromycin (%INH) INH is 100% if there is no inhibition, whereas maximal potential inhibition at high clarithromycin concentrations in the effect compartment would yield a value of 10% representing the non-inhibitable fraction of apparent clarithromycin clearance.

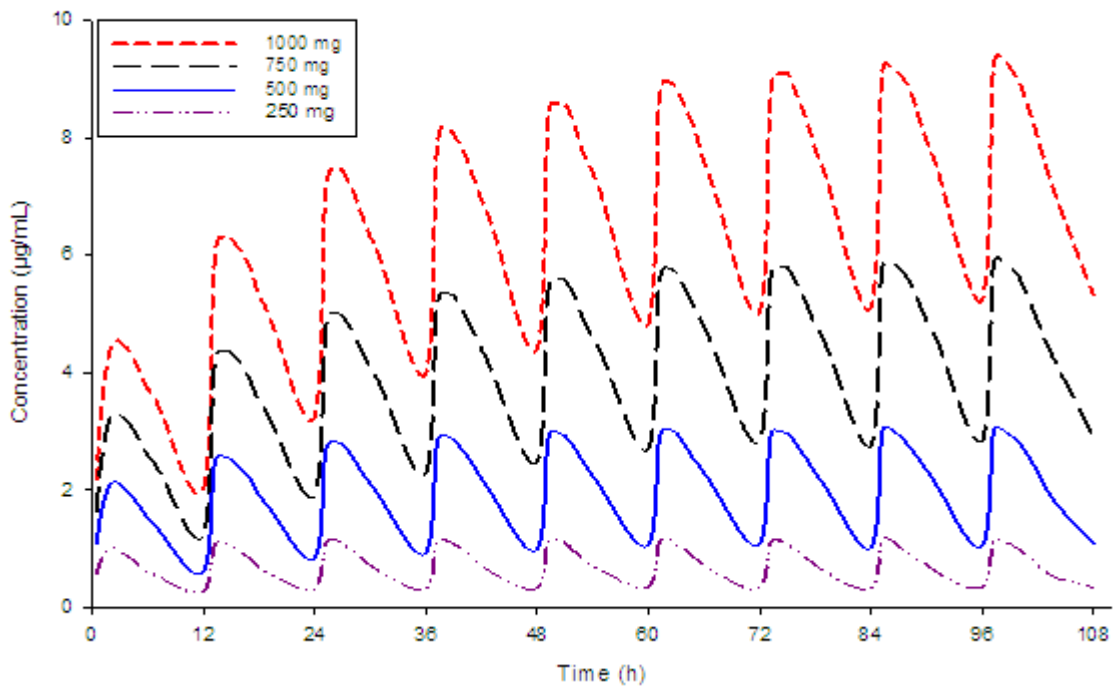


**Figure 21: Simulated median plasma concentrations of clarithromycin.**

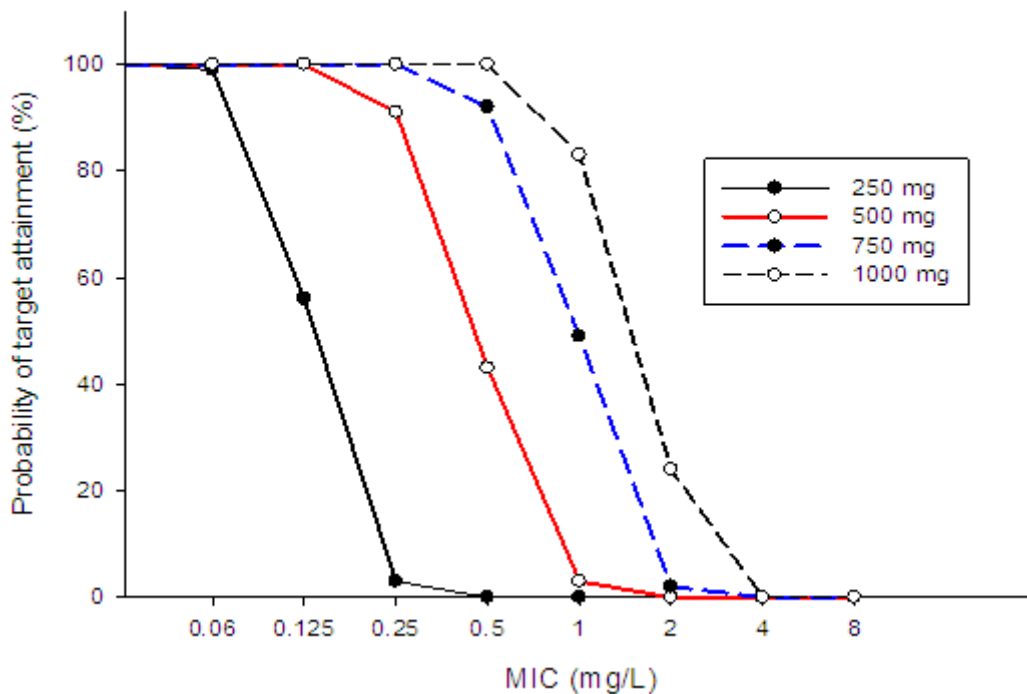


**Figure 22: Probability of target attainment of free clarithromycin.**

Probability of free clarithromycin to achieve a target (i.e.  $fAUC_{24h} / MIC > 35$  h) at steady state for various MIC values upon b.i.d. administration of the respective clarithromycin doses

## RESULTS

**Table 5: Population pharmacokinetic estimates of clarithromycin (500 mg b.i.d.) and its 14(R)-hydroxy metabolite**

	Model Parameter	Unit	Point estimate	95% CI
<b>Pharmacokinetic parameters</b>	Weibull absorption rate constant ( $k_w$ )	$\text{hr}^{-1}$	0.56	0.42 – 0.69
	Weibull shape parameter ( $\lambda$ )		2.23	1.67 – 2.77
	Apparent volume of distribution of clarithromycin ( $V_p$ )	L	172	145 – 198
	Apparent total clearance of clarithromycin ( $CL_p$ )	L/hr	60	40 – 80
	Non-inhibited fraction of clarithromycin clearance (FCL <sub>p</sub> )		0.10	0.02 – 0.17
	Transfer ate constant into and from inhibition compartment ( $k_i$ )	$\text{hr}^{-1}$	2.01	0.09 – 3.93
	Concentration in the inhibition compartment yielding 50% inhibition of maximum clearance ( $IC_{50}$ )	$\mu\text{g/mL}$	0.77	0.23 – 1.28
	Apparent total clearance of 14-OH-clarithromycin ( $CL_{\text{met}}$ )	L/hr	50.2	42.3 – 58.1
	Apparent volume of distribution of 14-OH-clarithromycin ( $V_{\text{met}}$ )	L	34	12 – 56
<b>Between subject variability*</b>	Between subject variability in $k_w$		45.3*	7.93% <sup>&amp;</sup>
	Between subject variability in $V_p$		25.3*	2.83% <sup>&amp;</sup>
	Between subject variability in $CL_p$		17.4*	1.15% <sup>&amp;</sup>
	Between subject variability in $CL_{\text{met}}$		27.9*	2.11% <sup>&amp;</sup>
<b>Residual variability</b>	Additive error of clarithromycin	$\mu\text{g/mL}$	0.12	2.40% <sup>&amp;</sup>
	Additive error of 14-OH-clarithromycin	$\mu\text{g/mL}$	0.01	0.18% <sup>&amp;</sup>

\* Coefficient of variation (%); <sup>&</sup>: These percentages are relative standard errors of the estimated variance.

RESULTS

**Table 6: Simulation of main PK/PD parameters of clarithromycin and 14-(R) hydroxyclearithromycin after multiple ascending doses using the population model estimates.**

	Dose (mg)	fAUC <sub>initial</sub> 0-24 h 90% PI (µg • h /mL)	fAUC <sub>ss</sub> , 24 h 90% PI (µg • h /mL)	Probability of target attainment (%) on steady state at different MIC values <sup>a</sup>							
				0.03	0.06	0.125	0.25	0.5	1	2	4
				mg/L	mg/L	mg/L	mg/L	mg/L	mg/L	mg/L	mg/L
clarithromycin	250	4.64 (1.06 – 9.20)	5.1 (1.19 – 10.18)	100	99	56	3	0	0	0	0
	500	11.11 (5.10 – 20.0)	15.10 (6.9 – 31.9)	100	100	100	91	43	3	0	0
	750	19.74 (10.9 – 34.7)	33.4 (17.4 – 62)	100	100	100	100	92	49	2	0
	1000	28.71 (18.2 – 51.2)	54.3 (30.4 – 95.0)	100	100	100	100	100	83	24	0
14-OH- clarithromycin	250	2.83 (1.16 – 5.07)	3.17 (1.29 – 5.57)					na			
	500	5.0 (2.45 – 8.39)	6.29 (3.29 – 10.25)					na			
	750	6.81 (3.75 – 11.14)	9.42 (5.34 – 15.10)					na			
	1000	8.29 (4.46 – 13.63)	12.48 (7.24 – 19.19)					na			

Values were calculated on a basis of twice daily oral dosing and represent median and 90% nonparametric prediction intervals. fAUC<sub>initial</sub> 0-24 h and fAUC<sub>ss</sub>, 24h are the areas under the free concentration-time curves over 24h on the first day and in steady-state. The fAUC was calculated by correcting the total AUC for the free fraction (f) which is 0.3 assuming non-significant change in protein binding (Peters and Clissold 1992; Traunmuller et al. 2007).

na: not applicable.

<sup>a</sup> assuming that a (fAUC<sub>ss</sub>, 24 h plasma) /MIC ratio target of at least 35 h is desirable in humans for pathogens eradication (Tessier et al. 2002)

### 3.3 Dextromethorphan

A total number of 1346 concentrations (537 plasma samples, 136 urine samples of dextromethorphan and a similar number of observations for dextroprphan) from 36 healthy Caucasian men obtained after oral administration of a 30 mg dextromethorphan-HBr dose were analysed in this study. The CYP2D6 genetic characteristics of these volunteers are given in Table 7.

**Table 7: CYP2D6 Genotypes of 36 individuals participated in dextromethorphan study.**

CYP2D6 variants	Study A	Study B	Study C	Total	
Observed alleles	*1	13	11	5	29
	*1x2	1	1	0	2
	*2	5	0	11	16
	*2x2	1	1	0	2
	*3	0	1	0	1
	*4	9	2	3	14
	*4x2	0	0	1	1
	*6	0	0	0	0
	*41	1	4	2	7
	*41x2	0	0	0	0
Observed genotypes	*1/*1	2	3	1	6
	*1/*2	2	0	2	4
	*1/*4	6	1	0	7
	*1/*41	1	3	1	5
	*4/*4	1	0	0	1
	*2/*4	1	0	3	4
	*2/*41	0	0	1	1
	*6/*41	0	0	0	0
	*4/*41	0	1	0	1
	*1x2/*2	1	0	0	1
	*1/*1x2	0	1	0	1
	*2/*2x2	1	0	0	1
	*2x2/*3	0	1	0	1
	*2/*2	0	0	2	2
	*2/*4x2	0	0	1	1

In general, there were large interindividual differences in the time-concentration profiles of the whole data, with the highest variability in case of dextromethorphan. Dextromethorphan initial plasma concentrations decreased rapidly in many but not all individuals (within the



## RESULTS

first 5 hours after dosing) indicating the known variability in drug clearance. Dextrophan plasma concentrations appeared in many individuals earlier than the parent supporting the importance of first-pass metabolism (Figure 23).

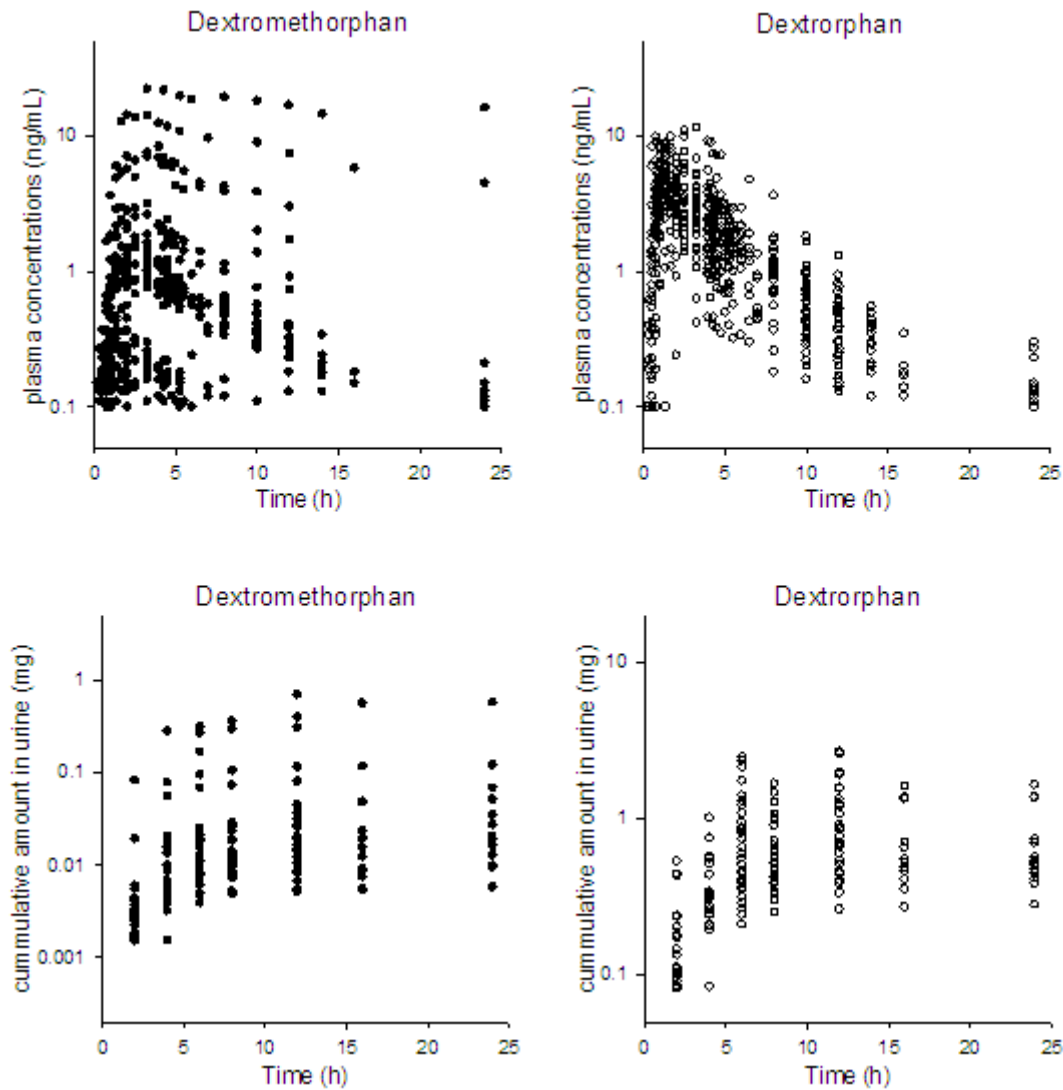


**Figure 23: Actual dextromethorphan and dextrophan observations in plasma and urine.**

Upper panel: plasma concentrations over time of dextromethorphan (filled circles) and dextrophan (unfilled circles). Lower panel: cumulative amount in urine over time of dextromethorphan (filled circles) and dextrophan (unfilled circles)

The values obtained from non-compartmental analysis for the area under the concentration-time curve (AUC), maximal observed plasma concentrations ( $C_{max}$ ), the corresponding times ( $t_{max}$ ), and the elimination rate constant for dextromethorphan and dextrophan are summarized in plasma are given in Table 8.

**Table 8: Non-compartmental pharmacokinetics of dextromethoephan and dextrorphan in plasma**

Parameters	Study arm			
	Study A	Study B	Study C	
<b>Dextromethorphan</b>	$t_{lag}$ (hr)	0.41 ± 0.33 ( 0.0 – 1.33)	0.41 ± 0.28 ( 0.0 – 1.0)	0.41 ± 0.11 ( 0 – 0.5)
	$t_{max}$ (hr)	1.95 ± 0.94 (0.50 - 3.25)	1.97 ± 0.68 (1.33 – 3.25)	2.67 ± 0.88 (0.75- 3.95)
	$C_{max}$ (µg/L)	2.36 ± 5.52 ( 0.18- 22.2)	1.92 ± 4.35 (0.16 – 14.24)	2.69 ± 2.75 (0.22-8.33)
	$AUC_t$ (µg/L/hr)	30 ± 95 (0.12 – 373)	21 ± 56 (0.26 -181)	15.44 ± 17.59 (0.47- 55.78)
	$AUC_{inf}$ (µg/L/hr)	94.7 ± 342 (0.35- 1330)	30.88 ± 83.53 (0.72- 268.36)	23.50 ± 25.95 (1.26 – 85.07)
	$Vz/F$ (L)	60117 ± 52521 (1338-190070)	76463 ± 53823 (2180-177310)	23887 ± 25782 (3425-93001)
	$CL/F$ (L/hr)	13251 ± 21297 (23 - 84795)	12555 ± 12220 (112-41619)	4306 ± 6965 (353- 23813)
	$k_{el}$ (1/hr)	0.159 ± 0.103 (0.017-0.446)	0.146 ± 0.082 (0.051-0.309)	0.143 ± 0.045 (0.102-0.256)
	$t_{1/2}$ (hr)	7.84 ± 9.73 ( 1.55 - 41.11)	6.45 ± 3.84 (2.25 – 13.52)	5.16 ± 1.20 ( 2.71- 6.78)
	<b>Dextrorphan</b>	$t_{lag}$ (h)	0.19 ± 0.18 ( 0.0 - 0.5)	0.33 ± 0.11 (0.17 - 0.50)
$t_{max}$ (hr)		1.58 ± 0.88 ( 0.75 – 3.25)	1.47 ± 0.69 (0.75 -3.25)	1.73 ± 0.85 ( 0.5 -3.25)
$C_{max}$ (µg/L)		5.33 ± 2.45 ( 0.42- 9.8)	4.70 ± 1.99 (1.46 – 8.86)	6.37 ± 2.92 (2.65 - 11.44)
$AUC_t$ (µg/L/hr)		22.4 ± 6.56 (5.18 - 34.4)	16.58 ± 6.45 (8.60 – 31.03)	22.94 ± 12.67 ( 5.06- 48.9)
$AUC_{inf}$ (µg/L/hr)		23.86 ± 6.56 (7.65- 35.54)	17.58 ± 6.68 ( 9.25- 32)	25.34 ± 13.95 ( 5.68- 54.24)
$Vz/F$ (L)		12087 ± 16032 ( 4164- 68793)	10221 ± 5017 (4443 - 17989)	7777 ± 5143 ( 2263-21002)
$CL/F$ (L/hr)		1422 ± 738 (844- 3922)	1929 ± 705 ( 938 - 3244)	1690 ± 1320 ( 553- 5286)
$k_{el}$ (1/hr)		0.163 ± 0.063 ( 0.057- 0.28)	0.206 ± 0.055 ( 0.078-0.272)	0.214 ± 0.032 (0.165-0.254)
$t_{1/2}$ (hr)		5.02 ± 2.48 ( 2.47- 12.16)	5.60 ± 3.25 ( 3.14-14.29)	3.31 ± 0.53 (2.73 – 4.21)

Dextromethorphan was administered as a single oral dose of 30 mg. The last plasma samples were obtained at 24 hr in study A, and B, and 12 hr in study C (see method section).  $t_{max}$  is the time of maximum concentration ( $C_{max}$ );  $t_{1/2}$  is the elimination half life;  $k_{el}$  is the elimination rate constant,  $AUC_t$  and  $AUC_{inf}$  are the area under the plasma concentration-time curve up to last observation and infinity;  $Vz/F$  is the apparent volume of distribution, and  $CL/F$  is the apparent total clearance.

## RESULTS

Modelling all data with the basic structure 4-compartment model (see Methods section) was not sufficient to describe the data, with misspecifications especially for parent concentrations in plasma. Addition of a peripheral compartment for dextromethorphan was associated with a significant drop in the objective function value ( $\Delta\text{OFV} = -114$ ). Based on individual and population predictions, this model was still unable to account for the early appearance of dextrorphan in plasma. Therefore, other models (Piotrovskij 1997; Moghadamnia et al. 2003; Levi et al. 2007) that take the first pass metabolism into account were tested. These models were stepwise simplified or extended for modelling the available data. A hypothetical metabolism compartment was added, which was assumed to be in rapid equilibrium with the central compartment of the parent drug, with all metabolic steps taking place in this compartment. After administration of the drug, it was assumed that the drug goes from the absorption site to the metabolism compartment before reaching the plasma. The model specifications are given in appendix A. This model was associated with a profound drop in the objective function value ( $\Delta\text{OFV} = -324$ ). Inclusion of a lag-time parameter led also to further significant drop in the objective function ( $\Delta\text{OFV} = -45$ ). Disposition kinetics revealed that dextromethorphan is widely distributed and rapidly metabolized to dextrorphan. As expected, CYP2D6 genotype had a major impact on the metabolic clearance ( $\Delta\text{OFV} = -532$ ). About 55% of the interindividual variability (CV %) in dextromethorphan metabolic clearance, CL<sub>23</sub>, was explained by addition of 2D6 genotypes. Inclusion of urine pH values as a covariate on renal clearance of dextromethorphan led to significant drop in objective function value ( $\Delta\text{OFV} = -105$ ). The best form of this relationship was that included in the final model and is described by the following empirical equation:

$$CL_r = TVCL \cdot \left( \frac{5.7}{pH} \right)^{\theta_s}$$

where, CL<sub>r</sub> is the individual value of renal clearance, TVCL is the population value of renal clearance, the value 5.7 represent a published mean of urine pH in humans (Florence, A T and Attwood, D 2006), pH is the measured individual urine pH at each collection period, and  $\theta_s$  is the shape parameter which explains the change in renal clearance in terms of change in urine pH on renal. Using the non-ionized fraction of dextromethorphan calculated according the Henderson-Hasselbalch equation as a covariate was not superior to this equation. Including an effect of urine pH on renal clearance of dextrorphan did neither improve model fitting nor led to a decrease in the OFV value.

## RESULTS

The model identified age as a recognizable covariate contributing to interindividual variability in apparent volume of distribution of dextrorphan ( $\Delta$  OFV = -21.9) and the clearance of dextrorphan to other species,  $CL_{30}$ , ( $\Delta$  OFV = -5.8). This covariate was modelled according to the relationship:

$$\theta_{PV} = \theta_{PV} \cdot \text{EXP} (\theta_{AGE} \cdot (\text{AGE} - 27))$$

$\theta_{PV}$  is the population value of the model parameter,  $\theta_{TV}$  is the typical value in an individual with age of 27 years (the median age in this study).  $\theta_{AGE}$  is the fractional change in  $\theta_{PV}$  per year different from 27 years of age. None of other apparent volumes of distribution, clearance, or intercompartmental clearance parameters has been found to be influenced by age in this study. Neither subject's body weight nor body height was found as significant covariates on model disposition parameters.

Plasma data were best fitted if a combination of an additive and proportional error terms were used, while urine data were best fitted with proportional error terms. The blueprint of the final model is shown in Figure 24 and its specifications are given in Figure 25. The descriptive equations used are explained in Figure 26.

The final pharmacokinetic parameter estimates with the corresponding 95% confidence intervals are shown in Table 9. The apparent metabolic clearance ( $CL_{23}$ ) estimate ranged from 10 to 10030 L/h in this population. In view of a hepatic blood flow of approximately 1.35 L/min in healthy young volunteers (Yzet et al. 2008) it implies largely extrahepatic metabolism. This is in accordance with the large apparent volume of distribution. The fraction of this clearance attributable to the presence of the \*1 allele was on an average of 2.5-fold greater than that mediated by allele\*2, whereas the \*41 allele showed the lowest activity: the point estimates per each \*1 allele is 5010 L/h versus 2020 L/h per the \*2 allele and 85 L/h per the \*41 allele.

Diagnostic plots of the final model are given in Figure 27 for plasma data and in Figure 28 for urine data showing the model adequacy. The simulated 5<sup>th</sup>, 50<sup>th</sup> and 95<sup>th</sup> percentiles from the simulated data, based on the final model estimates, are shown in Figure 29. Examples of individual fitting are shown in Figure 30. Simulated time courses of plasma concentrations and cumulative amounts excreted in urine for different genotypes with homozygosity for individual alleles are given in Figure 31. The expected values for the metabolic ratio of these genotype for standard CYP2D6 phenotypic metrics (i.e., at 3h in plasma and 0-8h in urine) are given in Table 10.

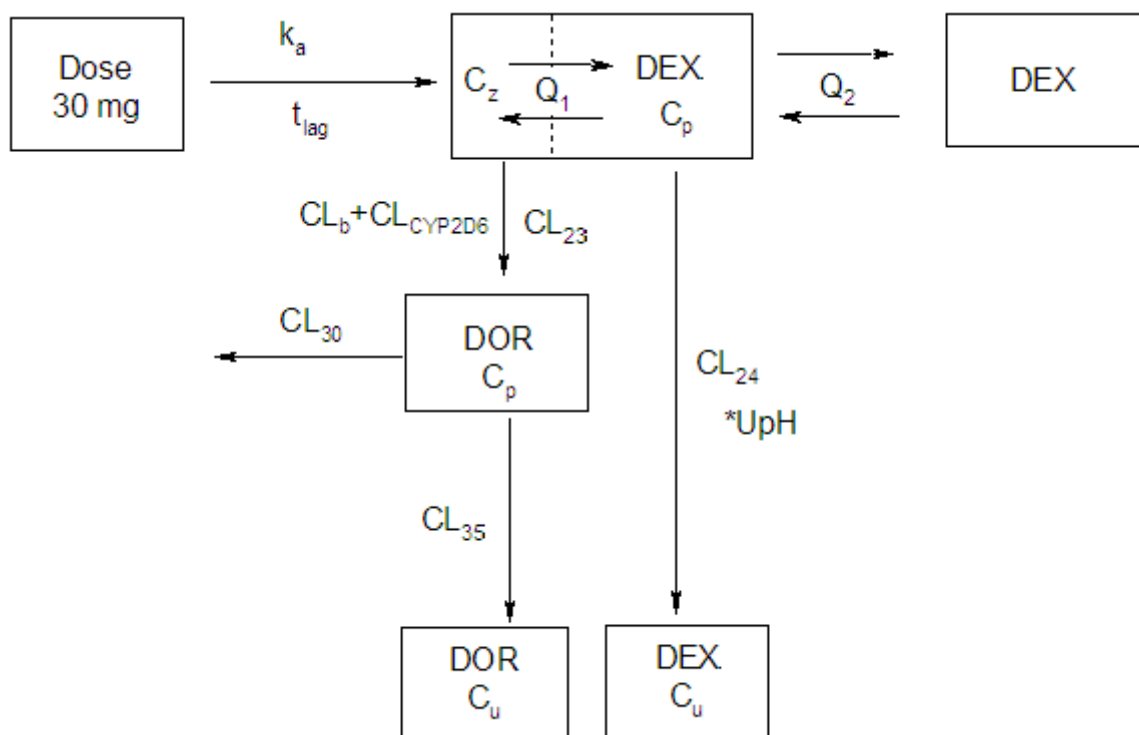


**Figure 24: Blueprint of the final population pharmacokinetic model of dextromethorphan.**

A semi-mechanistic population model was used to describe dextromethorphan (DEX) and dextrorphan (DOR) in plasma and urine after administration of single oral doses of 30 mg dextromethorphan hydrobromide. The absorption phase is described with a rate constant ( $k_a$ ) and lag time ( $t_{lag}$ ).  $C_z$  is the concentration of dextromethorphan in the hypothetical metabolizing enzyme compartment (METENZ), which is in rapid equilibrium with that in plasma.  $Q_1$  is the intercompartmental clearance between central compartment of DEX and METENZ.  $C_p$  and  $C_u$  are plasma and urine concentration of DEX or DOR in the corresponding compartment.  $CL_{23}$  is the apparent systemic metabolic clearance of DEX to DOR, which is the sum of CYP2D6-mediated clearance ( $CL_{CYP2D6}$ ) and non-CYP2D6 mediated clearance ( $CL_b$ ).  $Q_2$  is the intercompartmental clearance between central and peripheral compartments of dextromethorphan,  $CL_{24}$  is the renal clearance of DEX under the influence of urine pH (UpH),  $CL_{35}$  represents DOR renal clearance, and  $CL_{30}$  is the clearance of DOR to other species.

\$PROBLEM: Dextromethorphan PK Model

\$SUBROUTINES ADVAN6 TRANS1 TOL=4

**\$MODEL**

COMP=DEPOT

COMP=DEXPLASM

COMP=DORPLASM

COMP=DEXURIN

COMP=DORURIN

COMP=DEXPERIF

**\$PK**

PHEF=((5.7/UPH)\*\*THETA(15))

AGE1=1+(THETA(16)\*(AGE-31))

AGE2=1+(THETA(17)\*(AGE-31))

K12 = THETA(1)\*EXP(ETA(1))

ALAG1=THETA(2)

V2= THETA(3)

TCL24= THETA(4)\*PHEF

CL24=TCL24\*EXP(ETA(2))

Q = THETA(5)

CL2D6 = (G1 \* THETA(6) + G2 \* THETA(7) + G41 \* THETA(8))

CL B= THETA(9)

CL23=( CL2D6+CLB)\*EXP(ETA(3))

TVV3 = THETA(10)\*AGE1

V3=TVV3

TCL35= THETA(11)

CL35=TCL35\*EXP(ETA(4))

TCL30= THETA(12) \*AGE2

CL30=TCL30\*EXP(ETA(5))

Q2=THETA(13)

V6=THETA(14)

S2=V2/1000

S3=V3/1000

S4=UVOL/1000

S5=UVOL/1000

**\$ESTIMATION** METHOD=1 INTERACTION

**\$ERROR**

DEL=0

IF(F.EQ.0) DEL=0.01

IF(CMT.EQ.2) Y=F\*(1+EPS(1))+ EPS(2)

IF(CMT.EQ.3) Y=F\*(1+EPS(3))+ EPS(4)

IF(CMT.EQ.4) Y=F\*(1+EPS(5))

IF(CMT.EQ.5) Y=F\*(1+EPS(6))

W=F

IPRED=F

IRES=DV-IPRED

**\$DES**

C2=A(1) V2

C3=A(3) /V3

C6=A(6)/V6

CH=(K12\*A(1)+ Q\*C2) / (CL23+Q)

DADT(1)= -K12\*A(1)

DADT(2) = Q\*CH - (Q + CL24 +Q2) \*C2 +  
Q2\*C6

DADT(3)= CL23\*CH - (CL30+CL35)\*C3

DADT(4)= CL24\*C2

DADT(5)= CL35\*C3

**Figure 25: Relevant NONMEM code of the final dextromethorphan model**

Differential equations that specifying dextromethorphan model shown in Figure 24:

$$dA_1 / dt = - k_{12} A_1$$

$$C_z = k_{12} A_1 + Q_1 C_2 / (Q_1 + CL_{23})$$

$$dA_2 / dt = Q_1 C_z - Q_1 C_2 - Q_2 C_2 + Q_2 C_6 - CL_{24} C_2$$

$$dA_3 / dt = CL_{23} C_z - CL_{30} C_3 - CL_{35} C_3$$

$$dA_4 / dt = CL_{24} C_2$$

$$dA_5 / dt = CL_{24} C_2$$

$$dA_6 / dt = Q_2 C_2 - Q_2 C_6$$

The differential equation for the hypothetical enzyme compartment can be written as follows:

$$dC_z / dt = k_{12} A_1 + Q_1 C_2 - Q_1 C_z - CL_{23} C_z$$

where  $C_z$  is the concentration in the metabolizing compartment. The model assumes rapid equilibrium between this compartment and the dextromethorphan central compartment.

$$0 = k_{12} A_1 + Q_1 C_2 - (Q_1 + CL_{23}) C_z$$

This equation can be rearranged to get the following expression for  $C_z$

$$C_z = k_{12} A_1 + Q_1 C_2 / (Q_1 + CL_{23})$$

The differential expression for dextromethorphan in the central compartment ( $A_2$ ) is:

$$dA_2 / dt = Q_1 C_z - Q_1 C_2 - Q_2 C_2 + Q_2 C_6 - CL_{24} C_2$$

After substituting  $C_z$

$$dA_2 / dt = Q_1 (k_{12} A_1 + Q_1 C_2 / (Q_1 + CL_{23})) - Q_1 C_2 - Q_2 C_2 + Q_2 C_6 - CL_{24} C_2$$

Similarly for the dextromethorphan plasma compartment:

$$dA_3 / dt = CL_{23} C_z - CL_{30} C_3 - CL_{35} C_3$$

After substituting  $C_z$ :

$$dA_3 / dt = CL_{23} ((k_{12} A_1 + Q_1 C_2) / (Q_1 + CL_{23})) - CL_{30} C_3 - CL_{35} C_3$$

where  $A_i$  and  $C_i$  denote the amount and concentration of the species associated with the  $i^{\text{th}}$  compartment in Figure 24.

**Figure 26: Dextromethorphan model differential equations**

## RESULTS

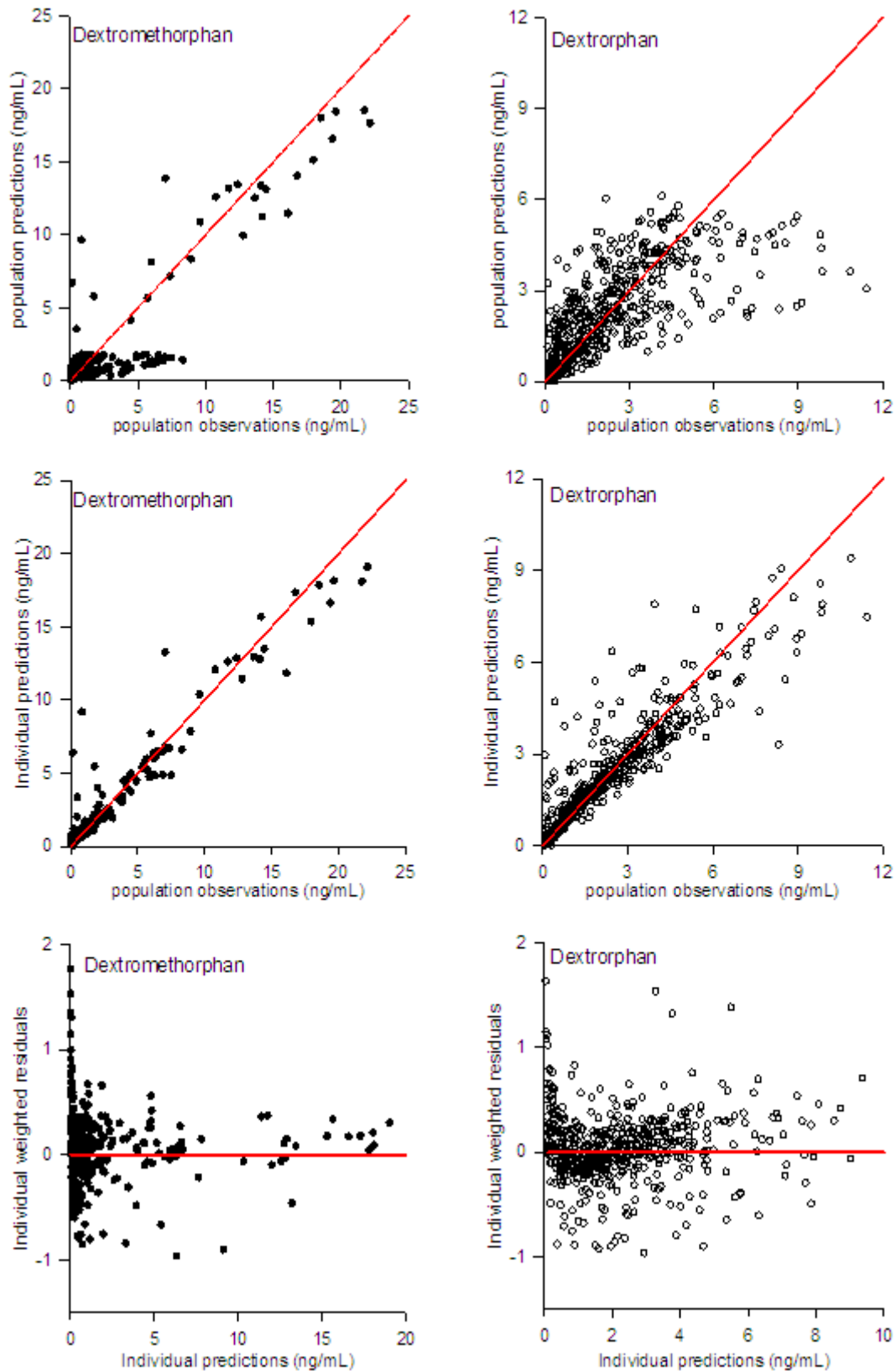


Figure 27: Goodness-of-fit plots for plasma concentrations of dextromethorphan (left) and dextrorphan (right)



## RESULTS

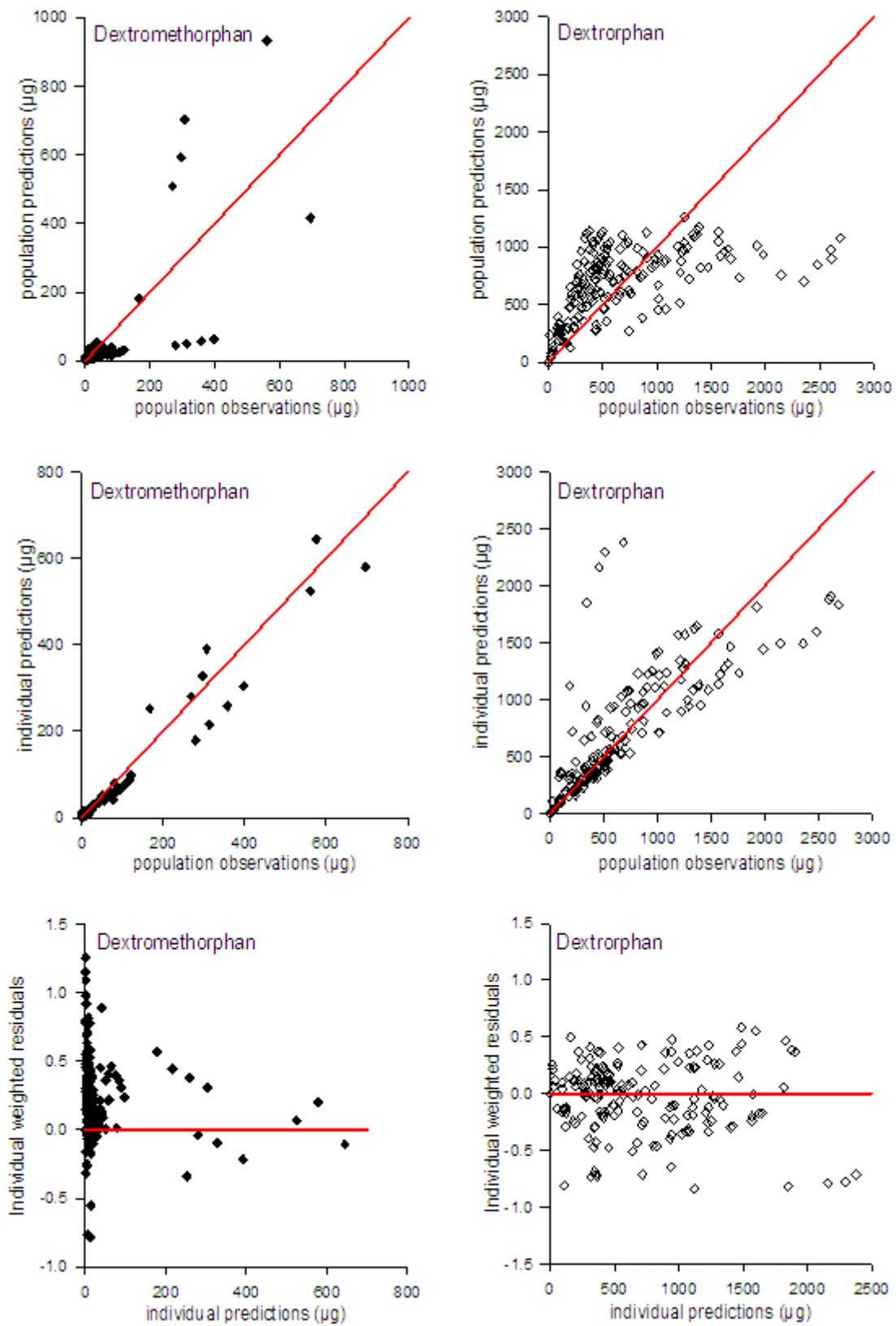
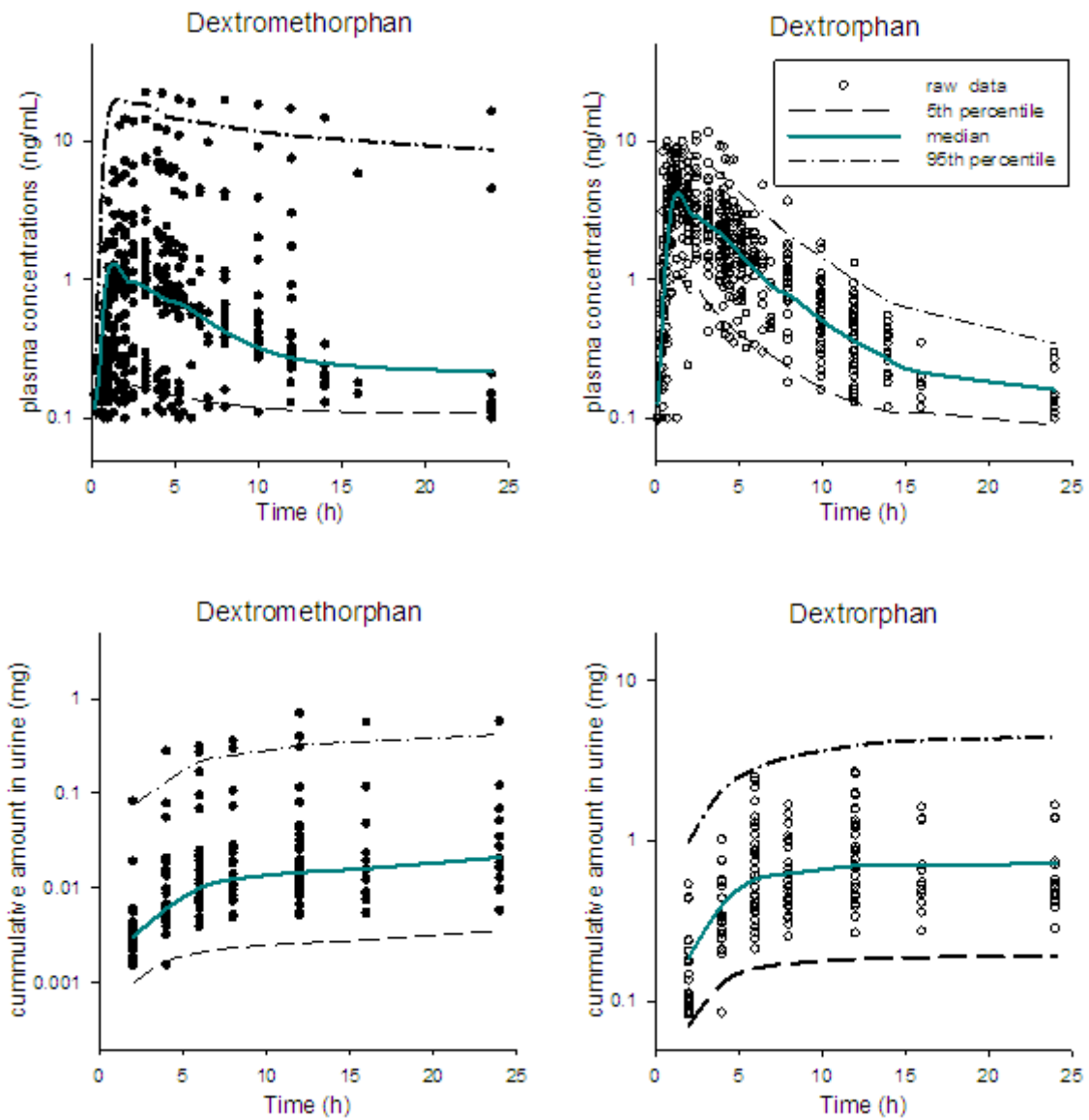


Figure 28: Goodness-of-fit plots for amounts excreted in urine of dextromethorphan (left) and dextrorphan (right)



**Figure 29: Visual predictive check plots of dextromethorphan population model.**

Actual data (filled black circles=dextromethorphan data, unfilled circles= dextrophan) are almost equally dispersed on the both side of simulated median (50<sup>th</sup> percentile). Plasma observations are shown on the upper panel.

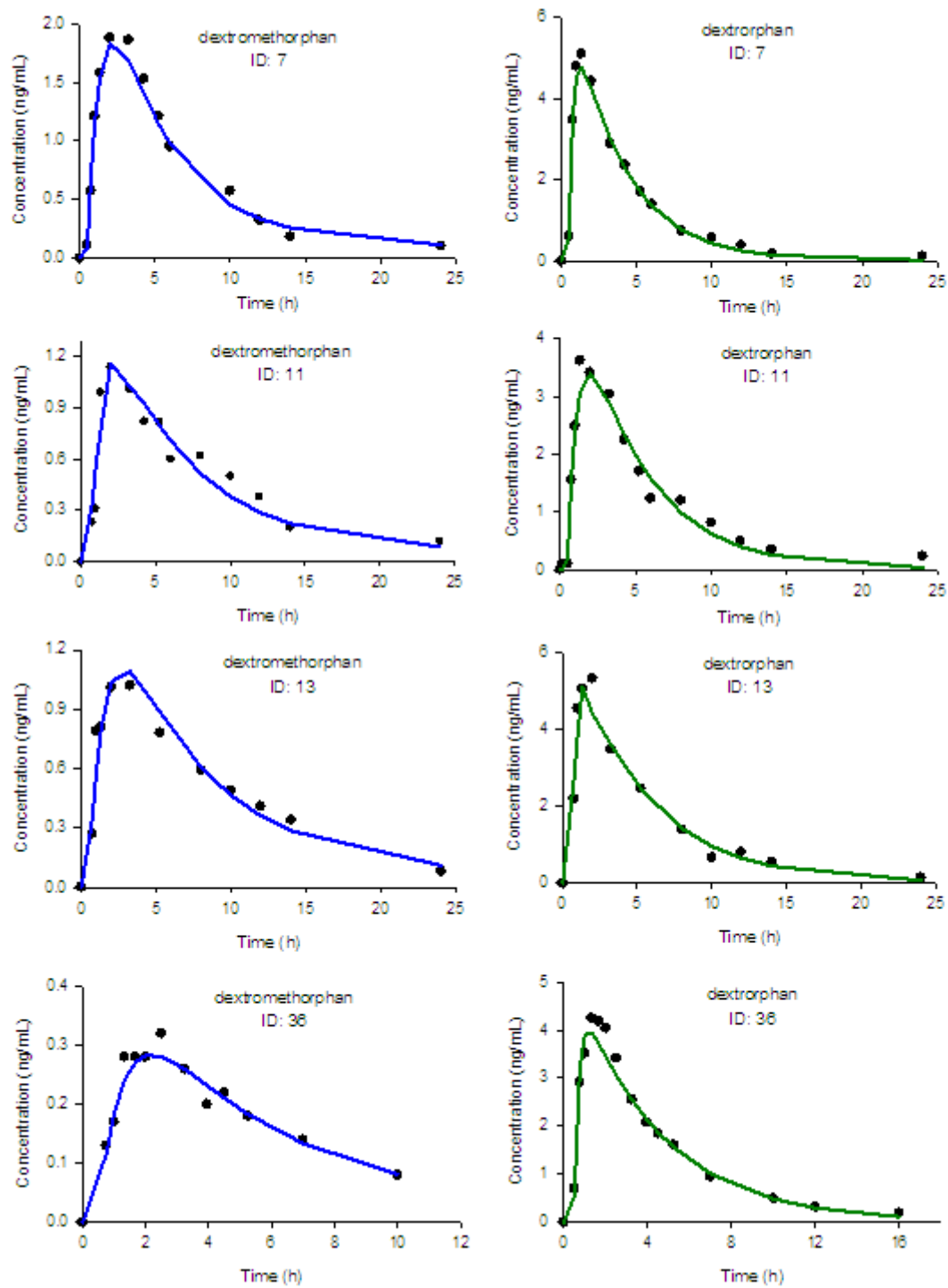


Figure 30: Examples of individual fitting of dextromethorphan (left) and dextrorphan (right) concentrations in plasma (circles = observations, line=individual predictions)

## RESULTS

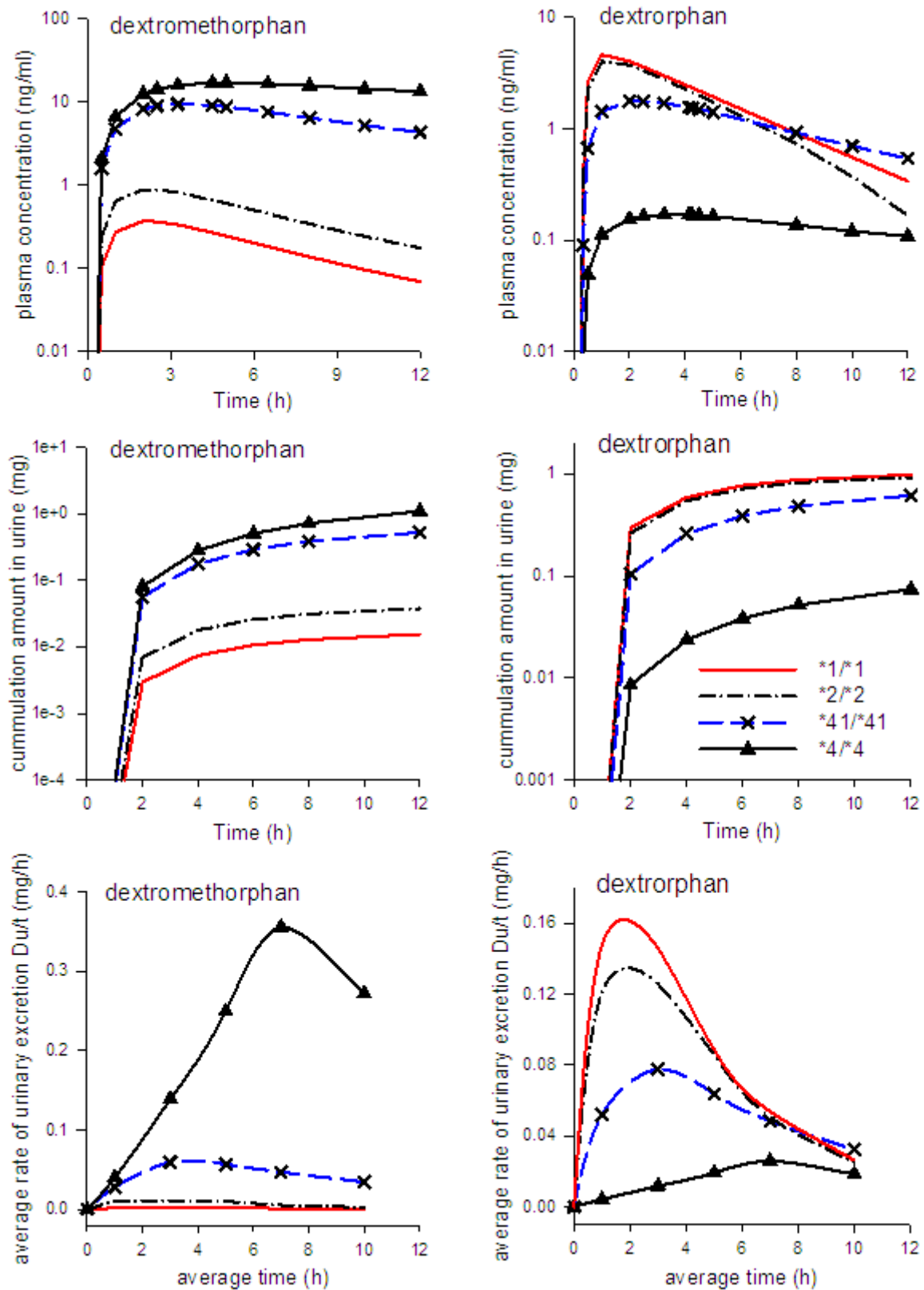


Figure 31: Simulated typical time courses in plasma and urine for individuals with different CYP2D6 genotypes

RESULTS

**Table 9a: Population pharmacokinetic estimates of dextromethorphan and dextrorphan**

Model parameter <sup>§</sup>			Point estimate	Standard error	
Basic Pharmacokinetic Parameters	Absorption rate constant , $k_a$		0.25	0.23 – 0.27	
	Lag time		0.31	0.30 – 0.32	
	Apparent volume of distribution of dextromethorphan in central compartment $V_{c,dex}$		648	493 - 803	
	Intercompartmental clearance $Q_1$		560	295 - 825	
	Apparent volume of distribution of dextromethorphan in peripheral compartment $V_{p,dex}$		1560	1092 - 2028	
	Intercompartmental clearance $Q_2$		173	129 - 217	
	Apparent renal clearance of dextromethorphan $CL_{24}$		6.52	4.84 – 8.20	
	Urine pH effect on dextromethorphan renal clearance in a man with a standard pH value of 5.7		3.93	2.74 – 5.12	
	Metabolic clearance	$BCL_{23}$	10.1	6.38 – 13.82	
		Allele *1	5010	3579 – 6441	
		Allele *2	2020	624 - 3416	
		$CL_{23}$ Allele *41	85.0	63.8 – 106.2	
	Apparent volume of distribution of dextrorphan $V_{m,dor}$		419	237 - 601	
	Age effect on $V_{m,dor}$ (% change/ year)**		0.042	0.016 – 0.068	
	Apparent renal clearance of dextrorphan $CL_{35}$		45.5	34.1 – 56.9	
	Apparent clearance of dextrorphan to other species $CL_{30}$		1260	1061 - 1460	
	Age effect on $CL_{30}$ (% change/ year)**		0.029	0.003 – 0.055	
Between subjects variability (BSV)	$BSV_{k_a}$ (%CV)		20.1	1.3*	
	$BSV_{CL_{24}}$ (%CV)		69.5	12.5*	
	$BSV_{CL_{23}}$ (%CV)		73.8	13.6*	
	$BSV_{CL_{35}}$ (%CV)		73.8	10.6*	
	$BSV_{CL_{30}}$ (%CV)		44.3	5.18*	
Residual variability	Plasma	DEX	Proportional error (CV %)	30.6	1.61*
		DOR	Additive error (ng/mL)	0.004	0.122*
			Proportional error (CV %)	32.6	1.06*
		Urine	DOR	Additive error (ng/mL)	0.006
	Proportional error (CV %)			56.2	3.82*
			DOR	Proportional error (CV %)	44.8

<sup>§</sup>see Figure 24 for individual parameters; \*= percentage of relative standard error

\*\* centered around 27 years

## RESULTS

**Table 10: Expected [dextrorphan/ dextromethorphan] metabolic ratios in plasma and urine for different genotype\***

Genotype	*1/*1	*2/*2	*41/*41	*4/*4
<b>Plasma metabolic ratio (3h)</b>	8.6	3.61	0.20	0.011
<b>Urinary metabolic ratio (0-8 h)</b>	68.2	26.6	1.26	0.07

\*27 years old male having urine pH of 5.7

### 3.4 Phenprocoumon

Relative frequency of CYP2C9 alleles was CYP2C9\*1, 79.3 %; CYP2C9\*2, 13.5 %; and CYP2C9\*3, 7.2 %). Details of CYP2C9 and VKORC1 alleles are presented below in Table 11. The weekly phenprocoumon dose ranged from 3.75 to 37.5 mg. There were large interindividual differences in plasma concentrations especially for the parent substance. Mean trough plasma concentration  $\pm$  SD (range) of phenprocoumon, 4'-OH phenprocoumon and 7-OH phenprocoumon were  $2744 \pm 1057$  (256 – 6510),  $56.1 \pm 27.3$  (11.5 – 137), and  $63.8 \pm 31.9$  (6.8 – 163) ng/mL, respectively. Measured INR values ranged from 1.10 to 5 (mean $\pm$ SD: 2.54 $\pm$ 0.57).

**Table 11: Observed CYP2C9 and VKORC1 genotypes of 278 patients participated in phenprocoumon study.**

		Characteristics	Value
CYP2C9 genotypes		*1/*1	172
		*1/*2	61
		*1/*3	36
		*2/*2	5
		*2/*3	4
		*3/*3	0
	VKORC1 genotypes	1173C > T	CC
CT			130
TT			51
36G > A		GG	271
		GA	7
		AA	0
85G > A		GG	277
		GA	1
		AA	0
106G > T (Asp36Tyr)		GG	276
		GT	2
		TT	0
129C > T		CC	275
		CT	3
		TT	0
358C > T	CC	275	
	CT	3	
	TT	0	

## RESULTS

Categorization of doses and INR measurements for the different combination of CYP2C9 and VKORC1 polymorphisms in this population are given in Table 12.

**Table 12: Empirically administered phenprocoumon dose and measured INR values of participants for each CYP2C9 and VKORC1 polymorphisms group.**

		<b>CYP2C9 *1/*1</b>	<b>CYP2C9 *1/*2</b>	<b>CYP2C9 *1/*3</b>	<b>CYP2C9 *2/*2</b>	<b>CYP2C9 *2/*3</b>
<b>VKORC1 CC</b>	<b>Dose</b> (mg /week)	17.89 ± 5.47 (7.5 – 28.5)	14.83 ± 6.97 (6 – 37.5)	14.08 ± 3.80 (7.5 – 21)	15	NA
	<b>INR</b>	2.48 ± 0.51 (1.4 – 3.71)	2.23 ± 0.50 (1.1 – 3.0)	2.77 ± 0.55 (2.0 – 3.62)	1.7	NA
	<b>n</b>	61	22	13	1	NA
<b>VKORC1 CT</b>	<b>Dose</b> (mg /week)	14.50 ± 5.42 (4.5 - 36)	12.88 ± 4.23 (5.25 – 22.5)	10.78 ± 2.97 (5.25 – 19.5)	9.58 ± 0.80 (9 – 10.5)	9.0 ± 5.41 (4.5 – 15)
	<b>INR</b>	2.60 ± 0.63 (1.58 – 5.0)	2.63 ± 0.66 (1.2 – 3.8)	2.59 ± 0.50 (1.47 – 3.8)	2.90 ± 0.26 (2.6 – 3.1)	2.51 ± 0.41 (2.07 – 2.89)
	<b>n</b>	78	26	20	3	3
<b>VKORC1 TT</b>	<b>Dose</b> (mg /week)	9.47 ± 5.41 (3.75 – 15.0)	6.84 ± 2.89 (3.75 – 10.5)	8.00 ± 2.27 (6.0 – 9.0)	6.00	5.25
	<b>INR</b>	2.55 ± 0.41 (1.5 – 3.6)	2.62 ± 0.56 (1.7 – 3.48)	2.66 ± 0.52 (2.42 – 2.9)	NA	1.50
	<b>n</b>	33	13	3	1	1

Data given as mean ± SD (range); n= number of patients in each group

### Empirical dose requirements:

There was no obvious effect of CYP2C9 and/or VKORC1 genotype on the INR reached, with mean values for the individual groups randomly distributed in the 2.23-2.90 range (Table 12). In contrast, the effect of CYP2C9 polymorphism in this population is reflected by a higher dose requirement for CYP \*1/\*1 carriers compared to carriers of mutant alleles. The difference is approximately 1.25-fold relative to heterozygote carriers of one mutant allele and 1.5-fold compare to \*2/\*2 individuals. VKORC1 CC carriers required a 2-fold higher dose than TT carriers, with heterozygous individuals in between.

### PK model:

All plasma concentrations of the parent and its metabolites were evaluated simultaneously. A three compartment model was found appropriate to describe the data of the parent at its 4'- and 7-hydroxy metabolites.



## RESULTS

The total apparent clearance of phenprocoumon ( $CL_t$ ) was defined as the sum of metabolic clearance mediated by CYP2C9 enzyme ( $CL_{CYP2C9}$ ) and other pathways ( $CL_{N2C9}$ ) as follows:

$$CL_t = CL_{CYP2C9} + CL_{N2C9}$$

where  $CL_{CYP2C9}$  was coded as:

$$CL_{CYP2C9} = n_{*1} \cdot CL_{*1} + n_{*2} \cdot CL_{*2} + n_{*3} \cdot CL_{*3}$$

The  $CL_{*1}$ ,  $CL_{*2}$  and  $CL_{*3}$  stand for the activity of each \*1, \*2 and 3 individual allele, and  $n_{*1}$ ,  $n_{*2}$ , and  $n_{*3}$  for the number of these alleles, respectively.

The formation clearance of PPC to 4-hydroxy ( $CL_{4'-OH}$ ) and 7-hydroxy ( $CL_{7-OH}$ ) metabolites were assumed to be mediated by CYP2C9 as

$$CL_{4'-OH} = f_{4'-OH} \cdot CL_{CYP2C9}$$

$$CL_{7-OH} = f_{7-OH} \cdot CL_{CYP2C9}$$

where  $f_{4'-OH}$  and  $f_{7-OH}$  are the fraction of total  $CL_{CYP2C9}$  resulting in 4'-OH and 7-OH metabolites formation. To maintain the mass balance, the clearance of phenprocoumon to non-[4'- and 7-]-hydroxymetabolites,  $CL_{other}$ , was modelled according to the following equations:

$$CL_{other} = CL_t - (CL_{4'-OH} + CL_{7-OH})$$

Identified covariates contributing significantly to the interindividual variability and model fitting were CYP2C9 variants, age, and body weight. Inclusion of patients alleles in the model led to marked drop in the objective function value compared with a model without CYP2C9 information ( $\Delta OFV = -38$ ). An age dependent decrease of clearance modeled via an apparent proportional decrease function was associated with significant drop in the OFV ( $\Delta OFV = -35$ ). Centering the age model to a 50 years old patient or to the data median (70 years old) did not improve the model ( $\Delta OFV = -0.3$ ). Body mass index did not result in model improvement ( $\Delta OFV = -0$ ), while inclusion of body weight led to additional drop in the objective function value ( $\Delta OFV = -28$ ). Finally, inclusion of sex as a covariate led to significant drop in objective function ( $\Delta OFV = -5$ ), but the 95% confidence interval included unity. Therefore, the impact of this covariate was excluded in the final model.

Inclusion of individual habits, alcohol, coffee, tea, and cola drinking did not lead to a significant drop in the objective function. Accordingly, the final PK model included individual

## RESULTS

CYP2C9 alleles, age, and total body weight as important covariates on the total clearance of phenprocoumon. They were best described according to the following relationship:

$$CL_t = \begin{cases} (CL_{CYP2C9} + CL_{N2C9}) \cdot \left(\frac{WT}{70}\right)^{0.75} & \text{If } age \leq 50 \text{ years} \\ (CL_{CYP2C9} + CL_{N2C9}) \cdot \left(\frac{WT}{70}\right)^{0.75} \cdot e^{-(\theta \cdot AGE)} & \text{If } age > 50 \text{ years} \end{cases}$$

An interindividual variability term was quantified on the total apparent clearance of phenprocoumon. A blueprint of the assumed PK population model is given in Figure 32. The control stream of the final PK model is given in Figure 33.

The model identified notable differences in the metabolic activity between CYP2C9 alleles. The estimated metabolic activity value were about 12.3, 6.5, and 2.9 mL/h for \*1, \*2, and \*3 alleles (per allele), respectively. The resulting pronounced differences for the respective genotypes however were dampened by a clearance fraction not mediated by CYP2C9 of 15.1 mL/h. A summary of population pharmacokinetic parameters estimates of the final model is shown in Table 13. The Goodness-of-fit plots of the pharmacokinetic model are given in Figure 34.

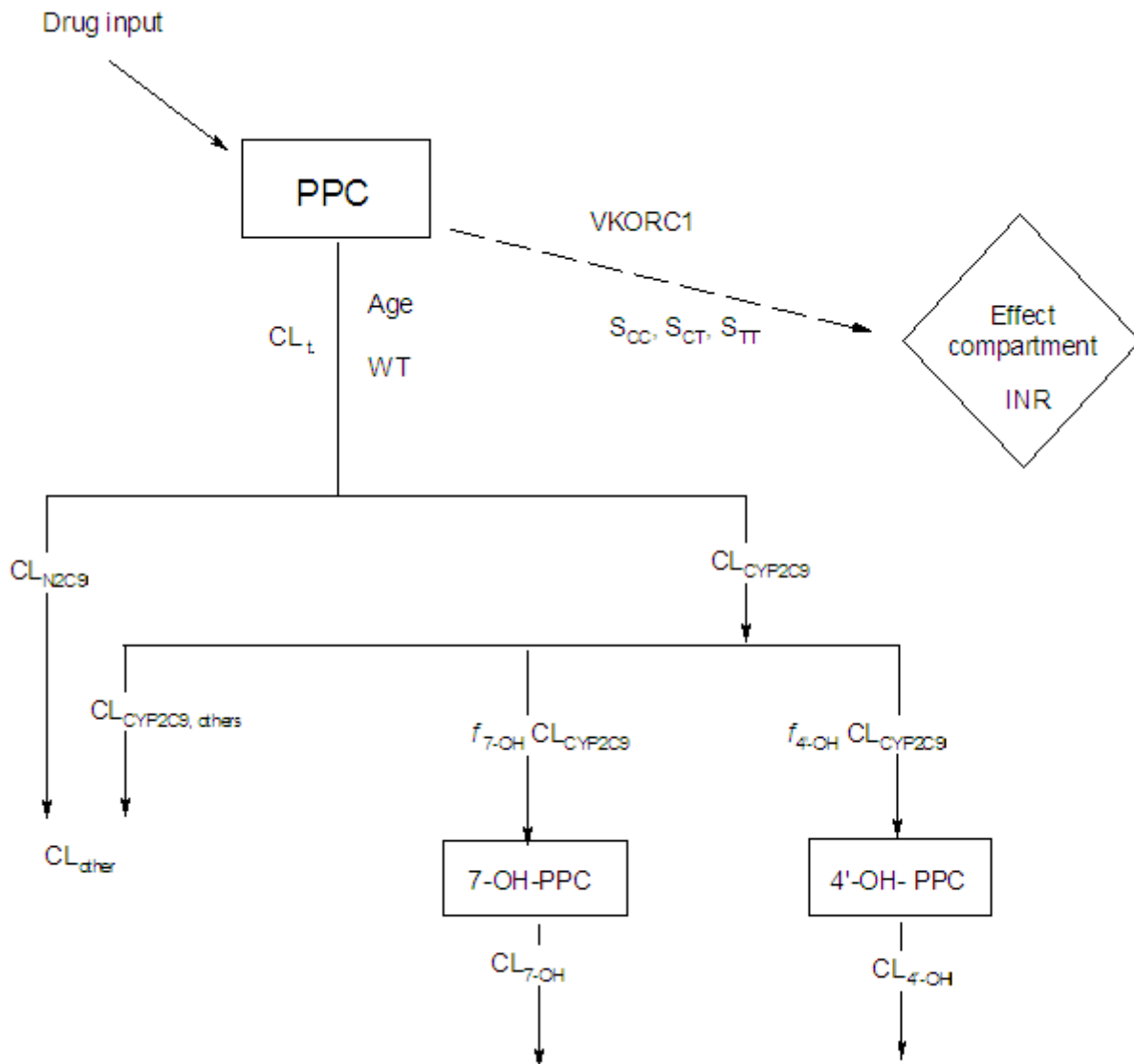


**Figure 32: Blueprint of the final population PK-PD model of phenprocoumon (PPC) and its 4'- and 7-hydroxy metabolites.**

Drug input was modelled as a constant infusion of administered dose per week, CL<sub>T</sub> is the total clearance of PPC, CL<sub>N2C9</sub> is the non-CYP2C9 mediated clearance of PPC, CL<sub>CYP2C9</sub> is the CYP2C9-mediated clearance of PPC,  $f_{4'-OH}$  and  $f_{7-OH}$  are the respective fractions of CL<sub>CYP2C9</sub> resulting in 4'-OH and 7-OH metabolites formation, CL<sub>CYP2C9, other</sub> is the CYP2C9-mediated clearance of PPC not resulting in formation of 4'-OH or 7-OH metabolites, INR is the international normalized ratio,  $S_{CC}$ ,  $S_{CT}$ , and  $S_{TT}$  control the rate increase in PPC response according to vitamin K epoxy reductase complex 1 (VKORC1) variants.

The NONMEM code used for phenprocoumon pharmacokinetic model

\$PROB Phenprocoumon Pharmacokinetics at steady state  
\$PRED

; for parent drug

AGEEF=EXP(-(THETA(9)\*AGE))

WTEF=(WT/70)\*\*0.75

CL2C9= (GN1\*THETA(1)+GN2\*THETA(3) +GN3\*THETA(4))

N2C9=THETA(4)

TCLPP=(CL2C9+N2C9)\*WTEF

IF(AGE.GT.50) TCLPP=(CL2C9+N2C9)\*WTEF\*AGEEF

CLT=TCLPP\*EXP(ETA(1))

DRAT=DOSE/168

CP=DRAT/CLT

; for 4-hydroxy metabolite

CL12=THETA(5)\*A2C9

CL20=THETA(6)

C4HO=CP\*CL12/CL20

; for 7-hydroxy metabolite

CL13=THETA(7)\*A2C9

CL30=THETA(8)

C7HO=CP\*CL13/CL30

; for others

CL10=CLT - (CL12+CL13)

IF (CMT.EQ.1) Y=CP + EPS(1) ; for parent

IF (CMT.EQ.2) Y=C4HO+ EPS(2) ; for 4-hydroxy metabolite

IF (CMT.EQ.3) Y=C7HO + EPS(3) ; for 7-hydroxy metabolite

\$ ESTIMATION METHOD=1 INTERACTION

**Figure 33: Relevant NONMEM code of the final phenprocoumon PK-model**

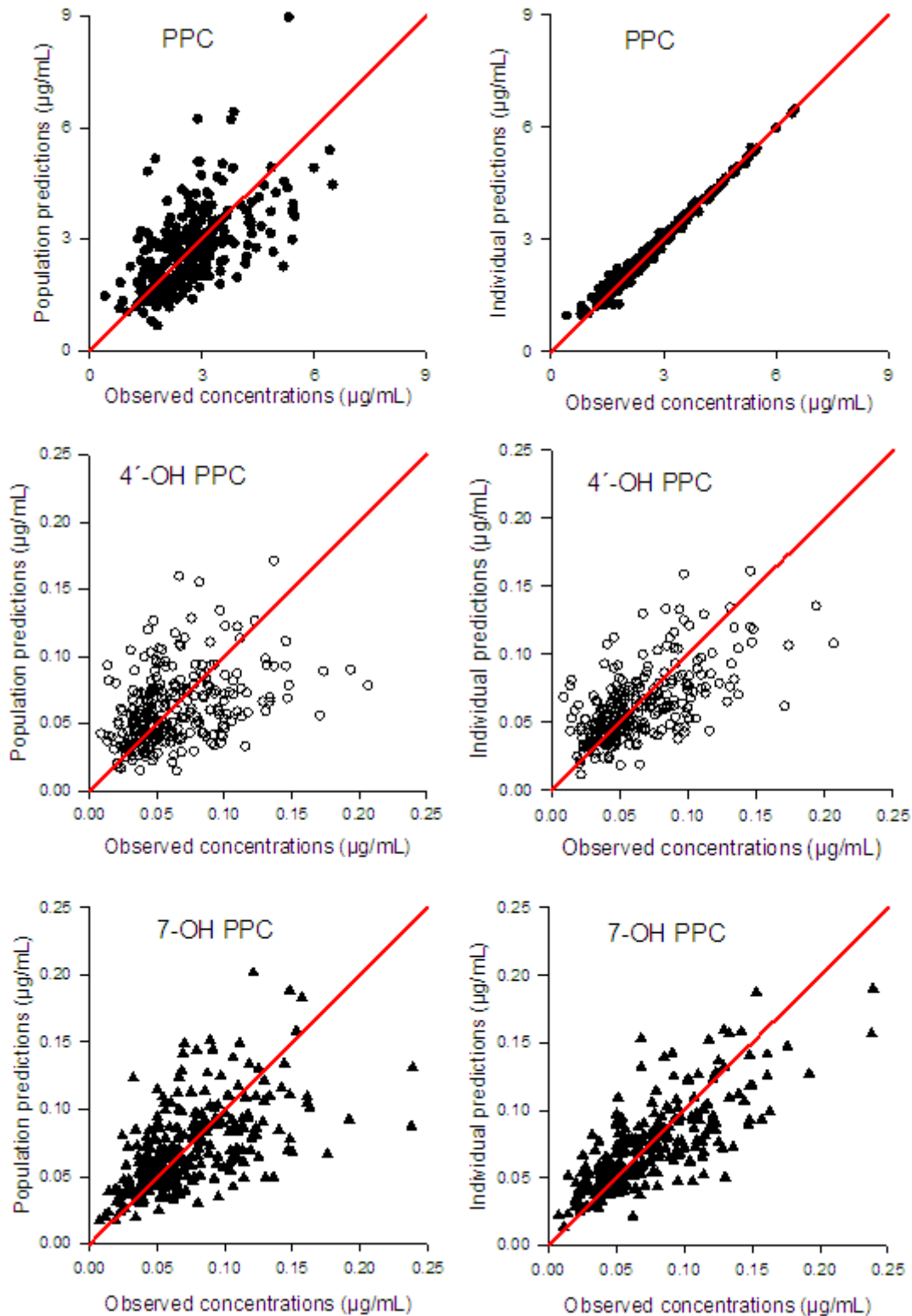


**Figure 34: Goodness-of-fit plots for the final pharmacokinetic model of phenprocoumon**  
Phenprocoumon (filled circles), 4'-hydroxy phenprocoumon (open circles) and 7-hydroxy phenprocoumon (triangles)

**Table 13: Population pharmacodynamic parameter estimates of phenprocoumon (PPC)**

Parameters		Point estimates	95% CI
Clearance of PPC ( $CL_{CYP2C9}$ ) per individual CYP2C9 allele	CYP 2C9 *1 (mL/h)	12.3	7.62 – 16.98
	CYP 2C9 *2 (mL/h)	6.53	3.20 – 9.86
	CYP 2C9 *3 (mL/h)	2.85	0.10 – 5.61
$CL_{Non-2C9}$ ; clearance of PPC by non-CYP2C9 pathway (mL/h)		15.1	7.24 – 22.96
Between subject variability in the apparent PPC total CL (% CV)		30	9.7*
$f_{4'-OH}$ ; fraction of $CL_{CYP2C9}$ responsible for 4'-OH-PPC formation		0.15	0.09 – 0.21
Apparent clearance of 4'-OH-PPC (mL/h)		144	114 - 174
$f_{7-OH}$ ; proportion of total CYP2C9 mediated clearance responsible for 7-OH-PPC formation		0.49	0.45 – 0.53
Exponential decline rate of total PPC clearance after 50 years (ml/hr/year)		5.48	3.59 – 7.37
Apparent clearance of 7-OH-PPC (mL/h)		543	436 - 650
Additive residual error for PPC concentrations ( $\mu\text{g/mL}$ )		0.1 fixed	n.a
Additive residual error for 4'-OH-PPC concentrations (ng/mL)		8 fixed	n.a
Additive residual error for 7-OH-PPC concentrations (ng/mL)		8 fixed	n.a

n.a.= not applicable.

\*= percentage of standard error

#### PD model:

The following linear model was assumed to predict INR:

$$INR = E_0 + C_{PPC} \cdot SF$$

where  $E_0$  is the basal level corresponding to the dose=0. This parameter was assumed to be one in these evaluations,  $C_{PPC}$  is the predicted concentration of phenprocoumon at steady state, and SF (sensitivity factor) is a parameter governing the patient's sensitivity to phenprocoumon. The variability in VKORC1 gene was assumed to be the major determinant factor of pharmacodynamics variability of phenprocoumon (Reitsma et al. 2005; Schalekamp et al. 2007; Stehle et al. 2008). The VKORC1 polymorphisms were coded as

$$INR = \begin{cases} E_0 + [C_{PPC} \cdot SF_{CC}] \cdot \exp(\eta_{INR_i}) & \text{if } CC \text{ genotype} \\ E_0 + [C_{PPC} \cdot SF_{CT}] \cdot \exp(\eta_{INR_i}) & \text{if } CT \text{ genotype} \\ E_0 + [C_{PPC} \cdot SF_{TT}] \cdot \exp(\eta_{INR_i}) & \text{if } TT \text{ genotype} \end{cases}$$

The contribution of VKORC1 genotypes was identified as an important covariate. Subdividing the population into three groups CC, CT and TT was associated with a profound drop in the objective function value ( $\Delta OFV = -106$ ). Inclusion of other covariates did not improve the model fitting and none of them led to a significant decrease in the objective function. Accordingly, the final PD model includes only VKORC1 variants as covariates (Figure 32). The control stream of the final PD model is given in Figure 35. The goodness-of-fit plots of the pharmacodynamic model are given in Figure 36.

```
; Problem: Phenprocoumon PD model for INR
$PRED

IF(VKR2.EQ,0) TSENS=THETA(1); TT (defective allele)
IF(VKR2.EQ,1) TSENS=THETA(2); CC (wild allele)
IF(VKR2.EQ,2) TSENS=THETA(3); CT (heterozygous allele)

SENS=TSENS*EXP(ETA(1))
IPRE=1+CONC*SENS

Y=IPRE+ERR(1)

$ESTIMATION METHOD=1 INTERACTION
```

**Figure 35: Relevant NONMEM code of the final phenprocoumon PD-model**

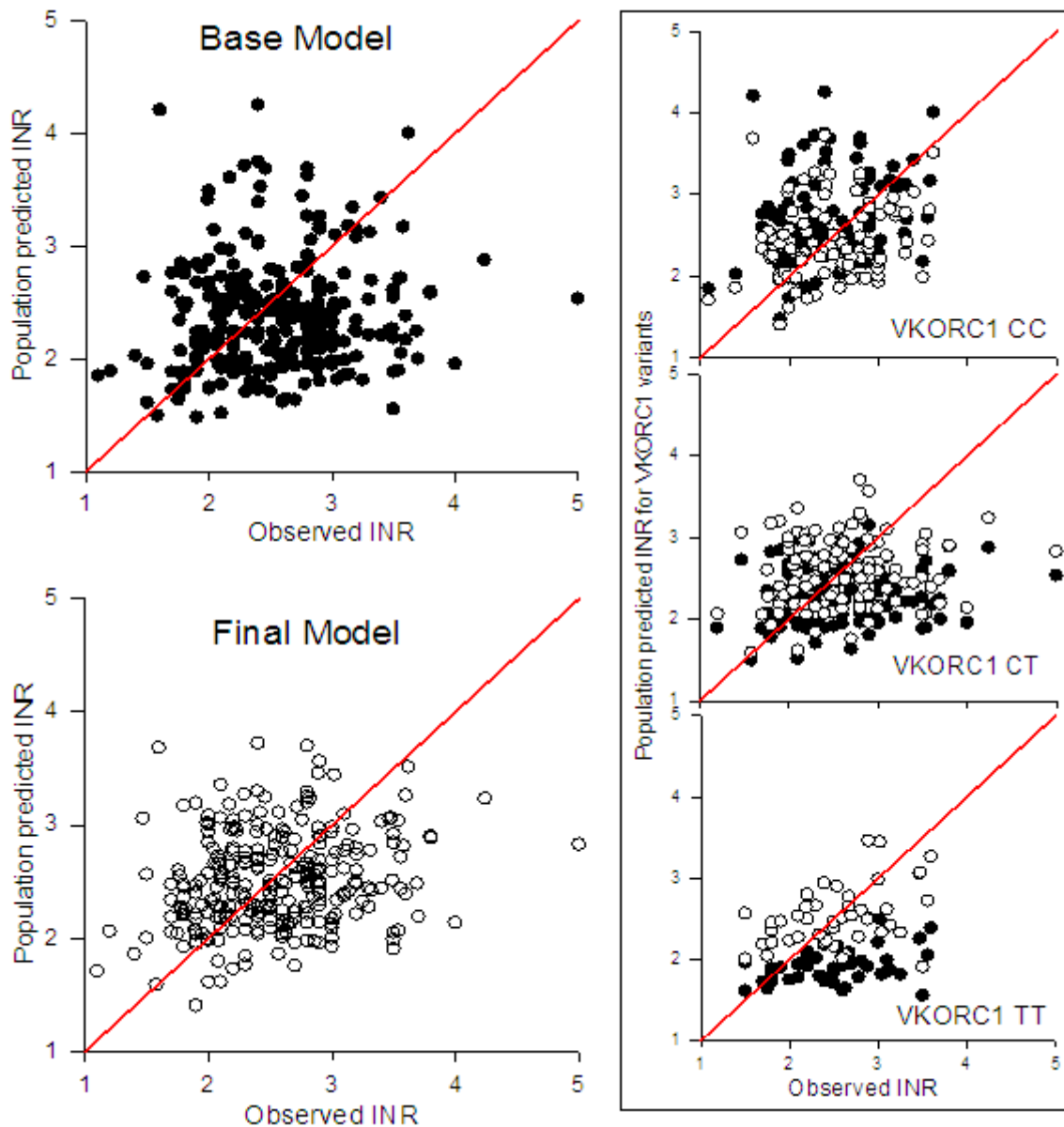


**Figure 36: Goodness-of-fit plots for the final pharmacodynamic model of phenprocoumon**

Population predictions of INR represented as filled circles (base model) and open circles (final model) without and with VKORC1 polymorphisms, respectively.

Summary of population pharmacodynamic parameters estimates from the final model are shown in Table 14. From this table, the highest values of the sensitivity factor (SF) was observed for the VKORC1 TT variant, while the wild type CC shows lower sensitivity. Based on these estimates, the trough phenprocoumon plasma concentrations required to reach a target INR value of 2.5 for individuals with CC, CT and TT variants of VKORC1 is 3.57, 2.5, and 1.82  $\mu\text{g}/\text{mL}$ , respectively.



**Table 14: Population pharmacodynamic parameter estimates of phenprocoumon**

Parameters	Point estimates	95%CI
Basal INR value ( $E_0$ )	1 Fixed	n.a.
SF VKORC1 CC genotype	0.42	0.38 – 0.46
SF for VKORC1 CT genotype	0.60	0.55 – 0.64
SF for VKORC1 TT genotype	0.83	0.74 – 0.91
Interindividual variability in SF (CV %)	39.6	12.2*
Residual (additive) error for INR	0.033 Fixed	n.a.

$E_0$  is the basal INR level corresponding to dose=0, SF is a parameter governing the patient's sensitivity to phenprocoumon, n.a.=not applicable.

\*= percentage of standard error

#### Simulation of phenprocoumon PK/PD profiles:

Simulation of Based of steady state phenprocoumon plasma concentration profiles displays different scenarios according to CYP2C9 genotypes (Figure 37).

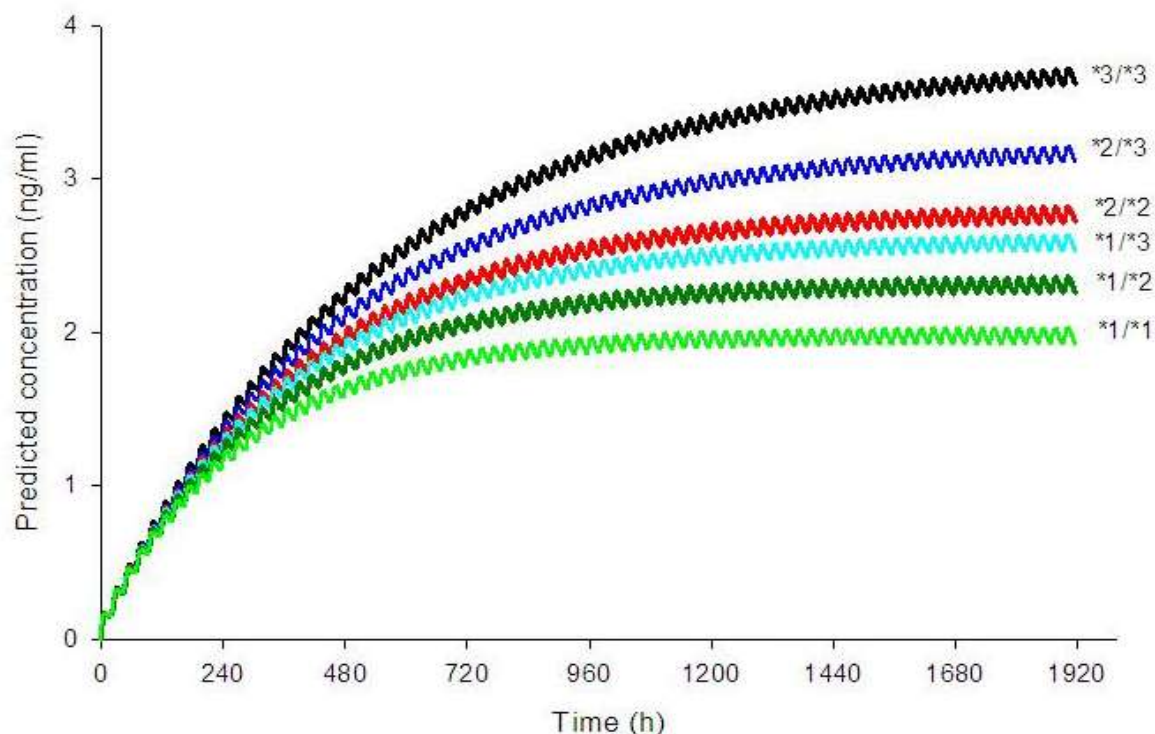


**Figure 37: Simulated mean phenprocoumon plasma concentrations for the different CYP2C9 genotypes based on final model parameters.**

(dose=2 mg/day, age=45 years, total body weight =70 kg). A volume of distribution of 12 L and absorption rate constant of  $2 \text{ h}^{-1}$  were assumed (Kitteringham et al. 1984; Kitteringham et al. 1985; Hausteiner and Huller 1994; Masche et al. 1999).

## RESULTS

The simulation results for the effect of VKORC1 polymorphisms on determining the INR level, for the wild-type CYP2C9 \*1/\*1 genotype, is given in Figure 38.

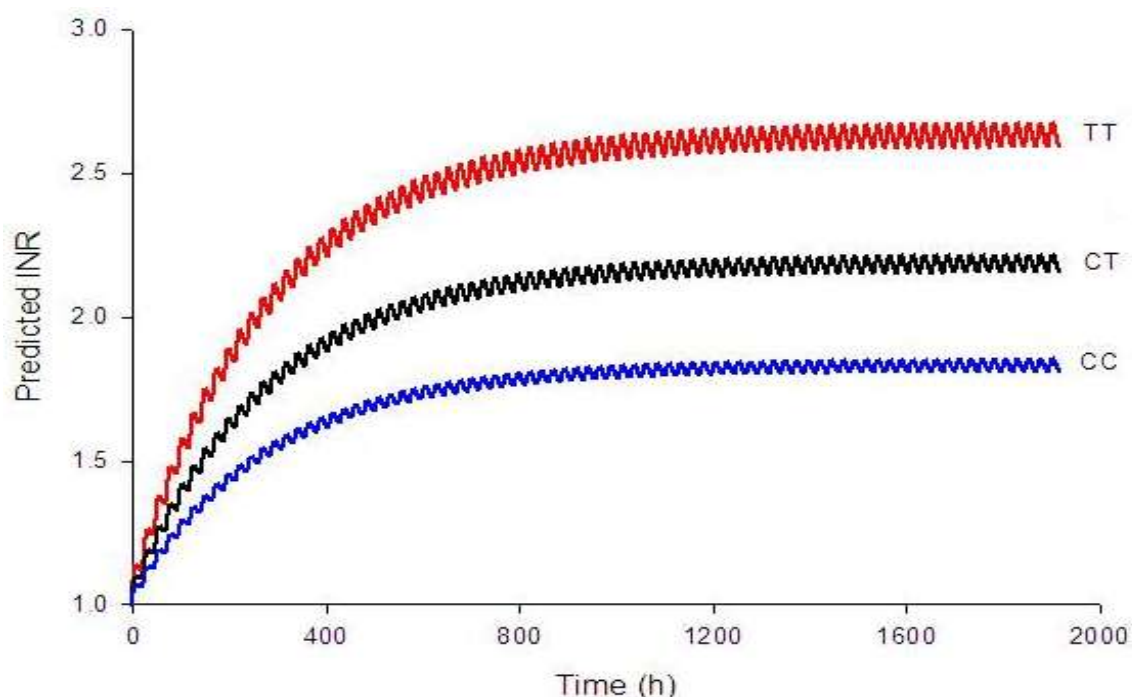


**Figure 38: Simulated INR levels for different VKORC1 variants in individuals carrying CYP2C9 \*1/\*1 genotype.**

Simulated plasma concentration for CYP2C9\*1/\*1 carriers given in Figure 38 were used to drive INR prediction in PD-model.

### Maintenance dose calculations:

Based on final PK/PD parameter estimates, the maintenance daily dose for phenprocoumon required to achieve a steady state INR of 2.5 in 18 different genetic combinations of CYP2C9 and VKORC1 polymorphism are given in Table 15.

**Table 15: Predicted daily dose (mg) to achieve a steady state INR value of 2.5 in typical individuals having different combination of CYP2C9 and VKORC1 genotypes\***

Genotypes		CYP2C9					
		*1/*1	*1/*2	*1/*3	*2/*2	*2/*3	*3/*3
VKORC1	CC	3.61	3.08	2.75	2.56	2.22	1.89
	CT	2.52	2.16	1.92	1.79	1.56	1.32
	TT	1.84	1.57	1.40	1.30	1.13	0.96

\*assuming a typical individual of 45 years old and 70 kg body weight

General algorithm to calculate the maintenance daily doses of phenprocoumon:

The daily maintenance doses (Table 15) were calculated according to the following equations:

$$Dose = F \cdot C_{av} \cdot CL_t$$

Where *Dose* is the required dose, *F* is the bioavailable fraction of drug (this evaluation assumed 100% bioavailability i.e., *F*=1), *C<sub>av</sub>* is the average plasma concentration at steady state required to achieve a presumed target INR, and *CL<sub>t</sub>* is the total drug clearance. Based on VKORC1 variant *C<sub>av</sub>* can be determined according to the following equation

$$C_{av} = \begin{cases} (INR - E_0)/0.42 & \text{for } CC \text{ } VKORC1 \text{ gene} \\ (INR - E_0)/0.42 & \text{for } CT \text{ } VKORC1 \text{ gene} \\ (INR - E_0)/0.42 & \text{for } TT \text{ } VKORC1 \text{ gene} \end{cases}$$

*E<sub>0</sub>* is the basic INR level in the absence of drug (*E<sub>0</sub>* was assumed to be one in this evaluations). The total clearance of phenprocoumon (*CL<sub>t</sub>*) can be determined by the derived total clearance equation

$$CL_t = \begin{cases} (0.0123 \cdot n_{*1} + 0.0065 \cdot n_{*2} + 0.0029 \cdot n_{*3} + 0.015) \cdot \left(\frac{WT}{70}\right)^{0.75} \\ \quad \text{if } \text{age} \leq 50\text{yrs} \\ (0.0123 \cdot n_{*1} + 0.0065 \cdot n_{*2} + 0.0029 \cdot n_{*3} + 0.015) \cdot \left(\frac{WT}{70}\right)^{0.75} \cdot e^{-0.005 \cdot \text{Age}} \\ \quad \text{if } \text{age} > 50\text{yrs} \end{cases}$$

Where *n\*1*, *n\*2*, and *n\*3* are the number of \*1,\*2,\*3 alleles in individual CYP2C9 genotypes.

## 4 DISCUSSION

## 4.1 Fluorescein

An ocular population model has been presented that adequately describes fluorescein pharmacokinetics in the anterior eye segment and estimates ocular and resulting systemic bioavailability of fluorescein from a lyophilisate relative to an eye-drop formulation in humans. These results confirm the original results (Dinslage et al. 2002; Lux et al. 2003; Steinfeld et al. 2004) of rapid release of the drug from lyophilisate and the higher bioavailability achieved from this formulation and provides a quantitative estimate for the difference.

Fluorescein sodium is a water-soluble ophthalmologic diagnostic substance with a negligible binding affinity to any vital tissue, which accounts for its low toxicity. It is freely and widely distributed into ocular structures by diffusion; however, active transport is needed to reach the retina (Maurice 1967). After topical instillation of fluorescein as a solution, like any other aqueous preparation, the drug is rapidly washed out by tear secretion depending on the degree of lacrimation. The massive pre-corneal loss of fluorescein significantly limits its ocular bioavailability and presents unique challenges for achieving high concentration in the internal structures of the eye (Maurice 1967; Adler et al. 1971; Mishima 1981; Linden and Alm 1997).

Different efforts have been made to enhance fluorescein bioavailability from conventional eye drops, all of which are based on prolonging the contact time on the ocular surface by way of increasing vehicle viscosity or topical instillation of large volume. Increasing vehicle viscosity in conventional eye drops may enhance fluorescein retention and decrease fluorescein loss via lacrimation (Adler et al. 1971; Ludwig et al. 1992; Linden and Alm 1997), but increasing viscosity is clinically limited by the corresponding increase in irritation and blurred vision that occur with some gel forming agents resulting in lacrimation and a higher blink frequency (Ludwig et al. 1992). Actually, the observed increase in the pre-corneal tear film retention was found to be mainly due to an increase in the tear reservoir volume of the delivery vehicle and not to be viscosity dependent (Benedetto et al. 1975). On the other hand, administration of five consecutive 10- $\mu$ L fluorescein drops at only 1-min intervals resulted only in twofold higher concentration in the cornea and anterior chamber for 8 h (Linden and Alm 1997). In contrast, noncompartmental results show that the lyophilisate

## DISCUSSION

significantly increased ocular fluorescein concentrations and the ocular bioavailability at least fivefold without the need to increase the dose. The probable mechanism is that the freeze-dried lyophilisate formulation resides for a longer period in the lower conjunctival fornix, resulting in higher tear film saturation before being washed out by tear secretion (Dinslage et al. 2002; Lux et al. 2003).

NONMEM evaluation shows a rapid absorption phase for the lyophilisate formulation. The absorption rate constant ( $k_a$ ) was estimated at  $16.7 \text{ h}^{-1}$  (95% CI 12.3–21.1), which corresponds to an absorption half-life of about 2.5 min (calculated as  $t_{1/2} = \ln 2/k_a$ ). The absorption process is slower and longer than that after administration of eye drops, where absorption appeared to be completed at the time of the first measurement in study 1, i.e., after not more than 2 min. The shortness of the absorption phase from eye drops could be ascribed to the rapid loss of the drug from the conjunctival fornix. The prolonged absorption observed with the lyophilisate confirms the assumption of a longer pre-corneal/formulation contact time as the reason for effective absorption of fluorescein from lyophilisate (Dinslage et al. 2002). Furthermore, lyophilisate probably decreases its pre-corneal loss by reducing tear turnover because of its preservative-free properties.

As soon as the fluorescein enters the cornea, it is rapidly distributed, mainly into the anterior chamber and then to other ocular tissues and the blood stream (Maurice 1967; McLaren et al. 1993). Alternatively, part of the absorbed fraction of the dose may be eliminated by the tears after which it enters the gastrointestinal tract via the nasolacrimal ducts and is reabsorbed into the circulation. The compartmental model indicates that the systemic bioavailability of fluorescein from lyophilisates via the ocular route is approximately four times that from eye drops. This can be attributed to the improvement in the absorption profile of fluorescein from lyophilisate. The advantage of compartmental analysis using NONMEM over noncompartmental analysis is that the noncompartmental analysis directly compares the ocular concentrations for both formulations, while the compartmental analysis also compares the systemic bioavailability of fluorescein via the ocular route from both formulations and is also able to jointly evaluate different data sets. In this study, the systemic fluorescein concentration in plasma was not measured, thus, the systemic bioavailability of fluorescein originating from intestinal absorption of the dose fraction lost

by lacrimation can not be judged, but probably this would be higher for the eye-drop formulation.

## 4.2 Clarithromycin

This study proposes a population pharmacokinetic model in which the nonlinearity in clarithromycin pharmacokinetic profile was quantitatively described in term of an inhibitable fraction of the total clearance. This was modelled by addition of an inhibition compartment to the model, where the change of clarithromycin clearance over time in the drug compartment is dependent on the concentration in the inhibition compartment. This study supports the idea of explaining the auto-inhibition effect of a drug on its metabolizing enzyme by inclusion of the inhibition compartment side by side to the drug compartment. This model was successively used to describe the inhibitory effect of linezolid on its own metabolizing enzyme and the nonlinear increase in the extent of bioavailability, which leads to the appearance of the side effects with time (Plock et al. 2007). The new features of the presented clarithromycin model were the incorporation of a Weibull function input, the allometric scaling approach for the covariate “body weight” on clearance and volumes of distributions, the ability to describe parent and metabolite plasma concentration profiles, as well as the auto-inhibition process of the parent elimination over time.

A single Weibull function successfully described the absorption process of clarithromycin. The adequacy of the Weibull function emerges in its ability to reflect the change in the absorption process from linearity with time, most probably as a consequence of intestinal CYP inactivation. Thus, an adequate empirical description of the absorption phase greatly contributed to the successful modelling of the non-linear elimination.

In the final model, distribution of clarithromycin throughout the body was assumed to follow linear kinetics and a one-compartment model was sufficient. This is in accordance with a previous study (Chu, S et al. 1993) and with data on tissue pharmacokinetics obtained by microdialysis showing that elimination rather than distribution processes govern the concentration vs. time profiles (Traunmuller et al. 2007). The observed peak concentrations shown in individual predictions versus observations plot for clarithromycin (see clarithromycin result Figure 17) were slightly higher than the fitted concentrations. This might have been caused by the presence of a second disposition compartment. Attempts to

## DISCUSSION

estimate a model with two disposition compartments for clarithromycin however were unsuccessful.

The active metabolite 14-(R) hydroxyclearithromycin may be formed in part in the enterocytes as a result of first pass metabolism. This process could not be modelled separately here because the metabolite was not administered separately neither were clarithromycin i.v. data available in this study. Thus, the final model assumption was that all clarithromycin molecules are converted to the metabolite. Modelling additional elimination pathways was not possible because neither metabolite formation fraction was known nor the metabolite was administered intravenously. This assumption should not affect the quality of the model fits or its predictive performance. Modelling the elimination process of the hydroxyl metabolite with a saturable kinetic model did not improve the model fitting, however circumstantial evidence for nonlinearity has been reported (Ferrero et al. 1990b; Chu, S et al. 1993) as this metabolite undergoes further biotransformation (Ferrero et al. 1990b; Yamamoto et al. 2004).

For the final model, apparent volume of distribution of clarithromycin was 172 litres (95%CI 145–198), which is in agreement with the previously reported range 126-306 litres (Chu, S et al. 1993; Traunmuller et al. 2007). The apparent total clearance of clarithromycin was 60 L/h and it could be inhibited to 10% of its original value (Table 5). This point estimate of oral clearance is the basic clearance value and decreases over time with the subsequent doses until steady state is achieved. Hence, it should not be compared directly with the previously reported range for apparent total clearances at steady state 19-105 L/h with similar regimens (Chu, S et al. 1993; Gorski et al. 1998; Traunmuller et al. 2007). This decrease in the clarithromycin clearance reflects the increasing inhibition of the metabolizing enzyme CYP3A during long-term clarithromycin intake, which is important to optimize dosage regimens of co-administered CYP3A substrates. However, while more complex inhibition models are probably required if other compounds that modify CYP3A4 activities or expression are present, the model may still be considered as long as no specific data for these substrates are available. Furthermore, an approximate 60 % decrease in CYP3A activity was observed for 500 mg clarithromycin b.i.d at the steady state (see clarithromycin results Figure 20, lower panel). Therefore, concentrations of co-administered CYP3A-substrates may be more than doubled which may reach clinical relevance (Fuhr 2008). For higher doses, a further pronounced decrease of CYP3A activity is to be expected.



## DISCUSSION

The application of the fAUC/MIC concept for the current study assumes that the model adequately describes the pharmacokinetics of clarithromycin including its metabolism and that clarithromycin mediates the main part of the antimicrobial activity while the metabolite makes only a minor contribution. The appropriateness of the former assumption was confirmed via visual predictive checks. Given that the AUC of clarithromycin is approximately 3-times as high as for its metabolite, the latter assumption seems reasonable (Jones et al. 1990; Martin et al. 2001). The calculated fAUC<sub>24, plasma</sub> values at steady state after different doses indicated that the normal adult dose of 500 mg b.i.d is sufficient to produce effective antibacterial activity (fAUC/MIC >35 h (Traunmuller et al. 2007)) as long as the desired MIC of the pathogens is approximately 0.25 mg/L or lower (see clarithromycin results Table 6) with a probability for target attainment of 91% (see clarithromycin results Figure 22). The presented model suggests that increasing the dose two-fold from 500 mg b.i.d. to 1000 mg b.i.d. would increase steady state exposure of clarithromycin by almost 4-fold, suggesting that infections with pathogens with MIC values of up to 1 mg/L could be treated successfully. However, further clinical studies are required to support this conclusion.

Because of both a rapid elimination and a rapid exchange with tissues including the inhibition compartment defined here, in subjects without hepatic and/or renal failure no further increase of exposure upon chronic administration of the 500 mg standard dose is expected after the 2<sup>nd</sup> day of treatment (see clarithromycin results Figure 21). Accordingly, both therapeutic action and inhibitory effects on co-administered drugs should have reached its maximum on the 2<sup>nd</sup> day. This provides some re-assurance that no late augmentation of any drug interactions would occur, although depending on the co-administered drug it may take longer than 2 days to subsequently reach its new steady-state. Also, the hope for subsequently increasing concentrations to support continuation of an unsuccessful antimicrobial therapy beyond a few days of treatment seems not justified for the 500 mg dose. In contrast, it may take several days until steady state is reached with the 1000 mg b.i.d dose, thus changes in the extent of inhibition and in the bacterial susceptibility e.g. due to emergence of resistance need to be taken into account during this period. The theoretical benefit of the high increase in plasma concentrations with increasing the dose to obtain better clinical outcomes remains to be assessed in clinical trials. Because it will take some time for the auto-inhibition of clearance to result in notably higher AUCs and the clinical

success probably depends on antimicrobial exposure during the first day(s) of therapy, the clinical benefit of the auto-inhibition might be less pronounced than predicted by the steady-state AUCs. For the same reasons, it might be reasonable considering a clarithromycin loading dose.

Thus, the developed semi-mechanistic population PK model has the advantage of the ability to describe both the concentration-time course of clarithromycin concentrations and of the inhibitory action on CYP3A, and especially the change of its clearance over time. The model does not incorporate “all” underlying mechanisms, such as clarithromycin first pass metabolism and a separate time course for inhibition of intestinal and hepatic CYP3A enzymes. However, the model was still useful for the assessment of a possible dose adjustment, as well as for the purpose of further pharmacokinetic/pharmacodynamic considerations and model development activities.

### 4.3 Dextromethorphan

The main objective of this study was to quantify the metabolic activity of attributable to individual CYP2D6 alleles using dextromethorphan as a probe drug.

Based on the final model estimates, the activity of the \*1 allele is about two-fold higher than \*2 allele. This result supports previous in vitro results obtained for the substrate dextromethorphan where the same ratio was found (Bapiro et al. 2002). Furthermore, this study shows that the metabolic clearance of \*41 allele is markedly less than that of the CYP2D6 \*1 allele. While it is well-known that the activity for the \*41 allele is lower than that for \*1 and \*2 alleles, this is the first quantitative estimate for the respective in vivo activity. The mean CYP2D6 mediated clearance  $CL_{CYP2D6}$  is about 15030 L/h in subjects who carry the CYP2D6 \*1/\*1x2 genotype, whereas it is about 170 L/h in subjects who carry two CYP2D6\*41/\*41 alleles, and obviously zero in the subpopulation carrying two dysfunctional alleles such as CYP2D6 \*4/\*4 genotype. This wide range of reflects the interindividual difference in the metabolic activity of CYP2D6 enzyme.

The obtained results that \*1 allele is related to an about 2-fold higher activity than the \*2 alleles is in contradiction to the assumption of equal activity as was made for the activity

## DISCUSSION

score (Gaedigk et al. 2008) and semi-quantitative scoring (Steimer et al. 2004) systems. Similarly, in the previous systems (Steimer et al. 2004; Gaedigk et al. 2008) the presumed value for \*41 allele was about half of the wild-type \*1 allele, which is in contrast with the estimated difference in this study (~ 60 fold). Dextromethorphan pharmacokinetics for these different scenarios were simulated based on final parameter estimates (see dextromethorphan results Figure 31). The new results warrant further evaluation for other CYP2D6 substrates since previous studies suggested that the allelic activity of CYP2D6 is substrate dependent (Kirchheiner et al. 2004b; Shen et al. 2007; Kusama et al. 2009).

The final model is able to describe the pharmacokinetic profiles of dextromethorphan and its major metabolite adequately. In this model, inclusion of the hypothetical metabolism compartment was able to explain the appearance of dextrorphan in plasma before dextromethorphan. The presented model shares some features with previously reported models that have been successfully applied to describe first-pass metabolism (Moghadamnia et al. 2003; Levi et al. 2007). The specific features in the presented model for dextromethorphan are that, (i) activity of active alleles of CYP2D6 were estimated separately, (ii) urinary data of both parent and metabolite were included in the model and simultaneously evaluated with plasma data; (iii) it can be extended to estimate the activity of other additional alleles such as \*9, \*10, and \*17 alleles. These features increase applicability of the model. Clinical implications of these features remain to be ascertained.

The presented results are in line with published data assuming a two-compartment model for dextromethorphan (Moghadamnia et al. 2003; Duedahl et al. 2005) and one-compartment models for dextrorphan (Moghadamnia et al. 2003). The absorption rate constant estimate is about  $0.25 \text{ h}^{-1}$ , which is in the range of previously reported values of  $2.6 \text{ h}^{-1}$  (Moghadamnia et al. 2003) and  $0.1 \text{ h}^{-1}$  (Silvasti et al. 1987). The lag time was estimated to be 0.31 h, which is also within the range of previous studies with 0.8 h (Moghadamnia et al. 2003) and 0.087 h (Duedahl et al. 2005). The model estimates for the apparent central and peripheral volumes of distribution of dextromethorphan in this study are smaller 648 L and 1560 L compared with the previous ones 961 L and 1951 L (Moghadamnia et al. 2003). The volume of distribution of dextrorphan with 419 L is smaller than the previously reported value 650 L (Albers et al. 1995) and 3776 L (Moghadamnia et al. 2003), but higher than other reported value 109 L (Demirbas et al. 1998). The significant role of urine pH as a covariate to

explaining the variability of dextromethorphan between individuals is in agreement with a previous study, where urinary pH led to about 20-fold variation in the urinary metabolic ratio (Labbe et al. 2000). Taken together, these comparisons suggest that the developed model is valid.

The goodness-of-fit plots (see dextromethorphan results Figure 27) show a possible overestimation of some dextromethorphan and dextrorphan concentrations due to model misspecification which is a semimechanistic rather than a fully mechanistic model. This may be explained by the existence of other sources of variability that could not be taken in to account in the final model. Possible sources could be the interindividual variability in CYP3A4/5, incomplete description of the first pass metabolism like the formation of methoxymorphinan from dextromethorphan, the lack of modeling the metabolic fate of dextrorphan, the possible contribution of glucuronidation, and inter-study variability. The interaction between the final model and the study design can be seen from the simulated predictive check plots (see dextromethorphan results Figure 29). The noticed overestimation may be also explained in part by the fact that many samples as in the terminal phase of plasma dextrorphan profiles had concentrations below the lower limit of quantification. However, generally these inadequately fitted concentrations form only a negligible fraction of the whole data set.

#### 4.4 Phenprocoumon

In the present study, phenprocoumon PK and PD parameters were estimated by a semi-mechanistic model in patient population and found that exposure depends on the metabolic activity of CYP2C9 variants, individuals' age, and weight, while the response depends on VKORC1 variants. The parameter estimates which were obtained also taking metabolite concentrations into account enable a genotype-based dose adjustment.

The mean apparent total clearance of phenprocoumon in this population was 0.037 L/h and ranged from 0.012 to 0.077 L/h depending on the CYP2C9 polymorphisms, age, and weight. Previous studies showed an apparent clearance of 0.04-0.06 L/h (Kitteringham et al. 1984; Russmann et al. 2001; Kirchheiner et al. 2004c), which is in agreement with this evaluation. The estimated fraction of CYP2C9-mediated clearances leading to 7-OH-PPC formation (49%)

## DISCUSSION

was more than 3-fold compared with that resulting in 4'-OH-PPC formation (14%). This is in agreement with previous findings that demonstrated the higher affinity of CYP2C9 to form the 7-hydroxy metabolite (Ufer et al. 2004c). The model underestimates the higher concentrations of metabolites (see phenprocoumon results Figure 35). This is most probably caused by model mis-specifications since the formation of these metabolites, mainly the 4'-OH metabolite, is also mediated by other CYP enzymes (Ufer et al. 2004b; Ufer et al. 2004c; Kammerer et al. 2005). However, based on the available data, modelling such additional pathway was unsuccessful.

The proposed linear PD model is quite simple and approximates the biological process of increasing INR values after phenprocoumon treatment. Its performance at the observed concentrations in this study is reasonably well. The limited INR range did not enable to use a more complex model, which therefore cannot be extrapolated to higher concentrations. This type of pharmacodynamic models has also been applied to describe warfarin concentration-effect relationship (Sheiner 1969; Holford 1986). In the absence of drug, the model mimics normal INR value through the assumed basic value of unity (Harrington et al. 2008).

In previous clinical pharmacokinetic studies on phenprocoumon, a higher metabolic capacity for the CYP2C9\*1 allele compared with the \*3 allele after single doses in healthy population was reported (Kirchheiner et al. 2004c). In the present study, the activity of \*2 and \*3 variants of CYP2C9 was found to be 47% and 77% lower than that of \*1 allele (see phenprocoumon results Table 13). The apparent total clearance in carriers of CYP2C9\*1/\*1 genotypes was clearly higher than that in CYP2C9\*3 homozygous individuals (0.042 L/h vs. 0.022 L/h). In general, these results are in concordance with previous phenprocoumon studies that have reported the important role of CYP2C9 genotypes (Hummers-Pradier et al. 2003; Schalekamp et al. 2004; Qazim et al. 2008; Stehle et al. 2008; Werner et al. 2009). The slightly more pronounced differences in clearance estimates (2-fold) compared to reported differences in empirical doses (1.5-fold) suggests that doctors are reluctant to prescribe required doses at the extremes of the dose range. A simulation of the impact of different CYP2C9 genotypes on steady state phenprocoumon concentrations is shown in Figure 40 (see phenprocoumon results). This figure also shows the longer time elapsed until

## DISCUSSION

phenprocoumon reaches its steady state in  $*3/*3$  carriers compared with wild type  $*1/*1$  genotype carriers.

Among tested covariates, VKORC1 polymorphisms variation was the only covariate that showed an impact on the pharmacodynamic model by modifying the sensitivity to phenprocoumon concentration reflecting different level of INR (see phenprocoumon results Table 14). These scenarios can be clearly observed in Figure 41 (see phenprocoumon results). The estimated difference in the INR for VKORC1 polymorphism suggests a significant increase in the anticoagulation sensitivity in VKORC1 TT carriers, indicated by notable higher estimates of the sensitivity factor compared with wild-type CC carriers (0.83 vs. 0.42). Correspondingly, the concentrations required to achieve an INR value of 2.5 for carriers of the VKORC1 TT variant was calculated to be 2-fold smaller compared with a homozygous VKORC1 CC carrier (1.82 vs. 3.57  $\mu\text{g/ml}$ ). The magnitude of these differences is very similar to empirical dose differences reported for patients under phenprocoumon therapy (Schalekamp et al. 2007; Stehle et al. 2008; Werner et al. 2009).

It has been demonstrated that carriers of a combination of a low activity CYP2C9 variant and a high sensitivity VKORC1 polymorphism need more accurate dose adjustment to avoid increased risk of severe over-anticoagulation (Ufer 2005b; Schalekamp et al. 2007; Stehle et al. 2008). While the present study was not aimed to study the risk of bleeding, the consistency of results across studies suggests that INR is an appropriate surrogate parameter also for the comparison between genotypes. The required daily dose needed to maintain an INR value of 2.5 at steady state for subjects with  $2C9*1/*1$  - VKORC1 CC genotypes was calculated to be approximately 2-fold higher than that required for  $2C9*3/*3$  - VKORC1 CC genotype carrier and 4-fold higher than that required for  $2C9*3/*3$  - VKORC1 TT carrier (see phenprocoumon results Table 14). The magnitude of differences supports that prospective dose adjustments based on both CYP2C9 and VKORC1 genotypes may be beneficial for patient under phenprocoumon therapy (Hummers-Pradier et al. 2003; Schalekamp et al. 2004; Qazim et al. 2008; Stehle et al. 2008; Werner et al. 2009).

The additional information such as the severity of the patient's disease, liver and renal functions, CYP3A5 genotypes, CYP3A phenotypes, plasma concentration of further hydroxyl

## DISCUSSION

metabolites, enantioselective concentrations of phenprocoumon and its metabolites were not available.

The presented study has several limitations; the sampling was limited to a single observation per patient, data were obtained from a heterogeneous population and the small (therapeutic) range in observed INR values did not allow for assessment of a full PD model. The structure of the presented semi-mechanistic PK model is not only a way to evaluate the role of CYP polymorphisms but it makes use of all available information with the following additional features beyond mere estimation of PK parameters: (i) it provides a tool to evaluate the individual clearance attributable to each allele involved in the total metabolic clearance; (ii) it increases the model applicability to incorporate other metabolic pathways; (iii) it may be used to predict drug profiles of genotypes not observed in this population (such as CYP2C9 \*3/\*3); and (iv) it may provide a dosage scheme for transition from one drug to another (e.g. warfarin to phenprocoumon).

Due to sampling limitation to one sample of parent drug and its metabolites as well as the residual error of INR per subject, it was not possible to estimate residual errors of these vectors. Fixing these error terms to values like assay limits or prior information gave a chance to assess the interindividual variability and influencing covariates on the PK and PD parameter estimates, however these estimates may be biased with respect to the point estimates. Changing the fixed values within a factor of ten up and down the limits of quantifications was associated with different point estimates of model parameters. Higher and lower residual error values led to significant deterioration in both accuracy and precision of the model, however varying the error around assay limitations resulted in greater precision of parameter estimates. The deterioration effect of very high residual error values has been observed in previous study on animals (Ette et al. 1995). The number of individuals under the study (278 patients) was large enough to ensure precise parameter estimates. Because metabolite data were evaluated simultaneously with parent concentration, bias in model estimates is expected to be reduced. Since the “true” parameter estimates are unknown, neither the precision of estimates nor the degree of bias relative to true values could be quantified. The PK model was more sensitive than the PD model to initial estimates as the former contains more parameters to be estimated compared with PD model, but data would allow a prospective dose adjustment for phenprocoumon, with subsequent check of INR.

## 5 CONCLUSIONS



## 5.1 Fluorescein

The fluorescein study demonstrated that the bioavailability of fluorescein is superior when given as lyophilisate in comparison to eye drops in the anterior eye segment. A less pronounced increase in systemic bioavailability was seen via the ocular route, which is probably the result of a lower early loss of fluorescein for ocular absorption from the lyophilisate formulation. Depending on the physicochemical properties of a drug, this may be essential for achieving effective drug concentrations in the eye for a sufficient period of time. These advantages of the lyophilisate formulation over conventional eye drops suggest that lyophilisate is the formulation of choice to fulfill such needs in ophthalmology. Studies with other drugs, including direct quantification of ocular and systemic concentrations, are needed to assess whether this is general property of ocular lyophilisate preparations.

## 5.2 Clarithromycin

The clarithromycin study identified and quantified a time-dependent decrease of clarithromycin clearance in a non-linear fashion, which was completed on the 2<sup>nd</sup> day of treatment for the 500 mg bid doses. Reaching steady state was predicted to take several days for a 1000 mg bid dose. A semi-mechanistic population pharmacokinetic model for clarithromycin and its 14-(R) hydroxy metabolite was developed, which provides an adequate description of the time course of clearance inhibition within the used regimen. The seemingly atypical absorption process could be the result of saturable / inhibited first pass metabolism and may contribute to the overall nonlinear profiles of clarithromycin. The presented model serves as a useful tool to predict clarithromycin plasma concentrations and provides a rationale to improve its safety with regard to drug-drug interactions and its efficacy based on PK/PD consideration. The applicability of the model in the presence of additional CYP3A ligands (inhibitors or substrates) and the potential clinical benefit of the pronounced increase in plasma concentrations with increasing the clarithromycin dose remain to be assessed in further clinical trials.

### 5.3 Dextromethorphan

Dextromethorphan data evaluation ended up with a final population model that adequately described dextromethorphan and dextrorphan pharmacokinetics in healthy Caucasian men. The results confirmed that individual CYP2D6 genotype and to a lesser degree urine pH contribute to the variability in pharmacokinetic profiles of dextromethorphan. The estimated quantitative differences in the metabolic capacity of individual CYP2D6 alleles, including \*1, \*2 and \*41, suggest that existing scoring systems to predict CYP2D6 activity from CYP2D6 genotype need to be refined. Whether the observed activity differences between functional alleles for dextromethorphan as a substrate are the same for other substrates remains to be assessed (Fuhr 2009).

### 5.4 Phenprocoumon

The phenprocoumon study presented a semi-mechanistic model that provided quantitative estimates for the impact of subject genotype, i.e. CYP2C9 and VKORC1 polymorphisms and of other covariates of phenprocoumon PK/PD profiles. An algorithm was derived from the results in order to predict individual weekly doses required to achieve a given INR. While this procedure makes use of existing knowledge, it would be desirable to study its clinical utility in prospective clinical trials.

## 6 SUMMARY

The major message from these analyses is that modelling pharmacokinetics and pharmacodynamics, based on previous knowledge and by utilizing the benefits of readily available techniques, are best interpreted in term of how much they change our view regarding these complex processes rather than expecting them to tell us what we should end up believing.

The ophthalmic lyophilisate formulation has been known for its safety, tolerability, and ability to achieve higher concentrations of a drug in the internal tissue of the eye compared with the conventional eye drop. Based on this prior information, population pharmacokinetic modelling was executed and quantified an improvement in the absorption phase. These outcomes will generate novel concept to improve ocular drug delivery straightforward with patient care improvement.

Modelling clarithromycin auto-inhibition started from the previous knowledge that clarithromycin decreases its own clearance with repeated dosing. A significant quantitative description of the size of inhibition boosts the faith in it to something approaching clinical impacts in efficacy of the administered doses, drug interaction and/or dose adjustment.

The final model provides parameters for dose adjustment depending on patient body weight and MICs required for susceptible pathogen eradication. Combining available information about the MIC of a pathogen with the model parameter estimates provided a useful means to develop ideas toward optimization of therapy.

The dextromethorphan study aimed to provide a clear picture of the metabolic activity of individual CYP2D6 alleles frequently observed in a healthy Caucasian population. Evaluations were based on prior knowledge of highly variable metabolism of CYP2D6 substrates, that is heavily dependent on CYP2D6 genotype, and the problem that phenotypic prediction is still pawned by the variability of metabolic activity of different alleles. Once the impact of individual alleles is quantitatively and significantly estimated, confidence in this approach is improved. These observations call for further evaluation of ethnic, substrate and disease impact, but for now it can be stated that these information are “highly” clinical relevant and significant towards therapeutic optimization.

## SUMMARY

The phenprocoumon study aimed to identify genetic and demographic covariates for dose-exposure response in a Caucasian population. Applications of previous knowledge of the role of evaluated covariates, led to confidence in the differential impact of both CYP2C9 polymorphisms on the exposure profiles and the contribution of VKORC1 polymorphisms to the overall phenprocoumon response. In addition to these findings, the differential activity of CYP2C9 alleles provided understanding of the importance of individualised drug dosing (based on genetic and demographic information) to phenprocoumon PK-PD profiles. This is not only of clinical importance in order to avoid overanticoagulation or therapy failure, but it will also decrease therapy expenses.

**7 REFERENCES:**

- Aarons, L (1999). Software for population pharmacokinetics and pharmacodynamics. *Clin Pharmacokinet* 36(4): 255-64.
- Abdul Manap, R, Wright, CE, Gregory, A, Rostami-Hodjegan, A, Meller, ST, Kelm, GR, Lennard, MS, Tucker, GT and Morice, AH (1999). The antitussive effect of dextromethorphan in relation to CYP2D6 activity. *Br J Clin Pharmacol* 48(3): 382-7.
- Adler, CA, Maurice, DM and Paterson, ME (1971). The effect of viscosity of the vehicle on the penetration of fluorescein into the human eye. *Exp Eye Res* 11(1): 34-42.
- Agoram, B, Woltosz, WS and Bolger, MB (2001). Predicting the impact of physiological and biochemical processes on oral drug bioavailability. *Adv Drug Deliv Rev* 50 Suppl 1: S41-67.
- Ahmed, I (2003). The noncorneal route in ocular drug delivery. In: Mitra AK (ed) *Ophthalmic drug delivery system; drugs and the pharmaceutical sciences*, 2nd edn. Marcel Dekker, New York, pp 335–363.
- Ahmed, I and Patton, TF (1985). Importance of the noncorneal absorption route in topical ophthalmic drug delivery. *Invest Ophthalmol Vis Sci* 26(4): 584-7.
- Alberio, L (2003). Oral anticoagulation with vitamin K antagonists [in German]. *Ther Umsch* 60(1): 5-9.
- Albers, GW, Atkinson, RP, Kelley, RE and Rosenbaum, DM (1995). Safety, tolerability, and pharmacokinetics of the N-methyl-D-aspartate antagonist dextrorphan in patients with acute stroke. Dextrorphan Study Group. *Stroke* 26(2): 254-8.
- Anderson, BJ, McKee, AD and Holford, NH (1997). Size, myths and the clinical pharmacokinetics of analgesia in paediatric patients. *Clin Pharmacokinet* 33(5): 313-27.
- Ansell, JE (2003). Optimizing the efficacy and safety of oral anticoagulant therapy: high-quality dose management, anticoagulation clinics, and patient self-management. *Semin Vasc Med* 3(3): 261-70.
- Bagli, M, Suverkrup, R, Quadflieg, R, Hoflich, G, Kasper, S, Moller, HJ, Langer, M, Barlage, U and Rao, ML (1999). Pharmacokinetic-pharmacodynamic modeling of tolerance to the prolactin-secreting effect of chlorprothixene after different modes of drug administration. *J Pharmacol Exp Ther* 291(2): 547-54.
- Bagli, M, Suverkrup, R, Rao, ML and Bode, H (1996). Mean input times of three oral chlorprothixene formulations assessed by an enhanced least-squares deconvolution method. *J Pharm Sci* 85(4): 434-9.
- Banh, HL, Burton, ME and Sperling, MR (2002). Interpatient and inpatient variability in phenytoin protein binding. *Ther Drug Monit* 24(3): 379-85.
- Bapiro, TE, Hasler, JA, Ridderstrom, M and Masimirembwa, CM (2002). The molecular and enzyme kinetic basis for the diminished activity of the cytochrome P450 2D6.17 (CYP2D6.17) variant. Potential implications for CYP2D6 phenotyping studies and the clinical use of CYP2D6 substrate drugs in some African populations. *Biochem Pharmacol* 64(9): 1387-98.
- Barnhart, JW (1980). The urinary excretion of dextromethorphan and three metabolites in dogs and humans. *Toxicol Appl Pharmacol* 55(1): 43-8.
- Bauer, RJ, Guzy, S and Ng, C (2007). A survey of population analysis methods and software for complex pharmacokinetic and pharmacodynamic models with examples. *Aaps J* 9(1): E60-83.
- Beal, SL and Sheiner, LB (1980). The NONMEM system. *American Statistician* 34(2):118-119.

## REFERENCES:

- Benedetto, DA, Shah, DO and Kaufman, HE (1975). The instilled fluid dynamics and surface chemistry of polymers in the precocular tear film. *Invest Ophthalmol* 14(12): 887-902.
- Bjorkman, S, Wada, DR, Berling, BM and Benoni, G (2001). Prediction of the disposition of midazolam in surgical patients by a physiologically based pharmacokinetic model. *J Pharm Sci* 90(9): 1226-41.
- Black, RE, Gertler, R, Wright, PM, Cancemi, MT, Hein, HA and Ramsay, MA (2003). Pharmacokinetic analysis of rapacuronium and its metabolite during liver transplantation: an assessment of its potential as a pharmacodynamic probe. *Proc (Bayl Univ Med Cent)* 16(3): 275-9.
- Bock, KW, Schrenk, D, Forster, A, Griese, EU, Morike, K, Brockmeier, D and Eichelbaum, M (1994). The influence of environmental and genetic factors on CYP2D6, CYP1A2 and UDP-glucuronosyltransferases in man using sparteine, caffeine, and paracetamol as probes. *Pharmacogenetics* 4(4): 209-18.
- Bois, FY (2001). Applications of population approaches in toxicology. *Toxicol Lett* 120(1-3): 385-94.
- Bonate, PL (2006). Pharmacokinetic-pharmacodynamic modeling and simulation. Springer, Medeia, Inc. USA.
- Bonnacker, I, Berdel, D, Suverkrup, R and von Berg, A (1989). Renal clearance of theophylline and its major metabolites: age and urine flow dependency in paediatric patients. *Eur J Clin Pharmacol* 36(2): 145-50.
- Booth, BP and Gobburu, JV (2003). Considerations in analyzing single-trough concentrations using mixed-effects modeling. *J Clin Pharmacol* 43(12): 1307-15.
- Borges, S, Li, L, Hamman, MA, Jones, DR, Hall, SD and Gorski, JC (2005). Dextromethorphan to dextrorphan urinary metabolic ratio does not reflect dextromethorphan oral clearance. *Drug Metab Dispos* 33(7): 1052-5.
- Bosch, TM (2008). Pharmacogenomics of drug-metabolizing enzymes and drug transporters in chemotherapy. *Methods Mol Biol* 448: 63-76.
- Bourgain, R and Wright, IS (1955). Marcumar, a new anticoagulant. *Rev Hematol* 10(2): 387-9; discussion, 412-22.
- Breimer, DD (1983). Interindividual variations in drug disposition. Clinical implications and methods of investigation. *Clin Pharmacokinet* 8(5): 371-7.
- Brightman, FA, Leahy, DE, Searle, GE and Thomas, S (2006). Application of a generic physiologically based pharmacokinetic model to the estimation of xenobiotic levels in human plasma. *Drug Metab Dispos* 34(1): 94-101.
- Bruce, MA, Hall, SD, Haehner-Daniels, BD and Gorski, JC (2001). In vivo effect of clarithromycin on multiple cytochrome P450s. *Drug Metab Dispos* 29(7): 1023-8.
- Bulitta, JB, Horkovics-Kovats, S, Borek, M, Skott, A, Illauer, M, Rodamer, M, Kinzig-Schippers, M and Sorgel, F (2003). Self-Inhibition of Clarithromycin's (CLA) Metabolism in Humans at Steady-State. Poster A-1625, 43rd Interscience Conference on Antimicrobial Agents and Chemotherapy; Chicago, Illinois/USA; September 14 - 17.
- Bulitta, JB, Duffull, SB, Kinzig-Schippers, M, Holzgrabe, U, Stephan, U, Drusano, GL and Sorgel, F (2007). Systematic comparison of the population pharmacokinetics and pharmacodynamics of piperacillin in cystic fibrosis patients and healthy volunteers. *Antimicrob Agents Chemother* 51(7): 2497-507.
- Cai, H, Stoner, C, Reddy, A, Freiwald, S, Smith, D, Winters, R, Stankovic, C and Surendran, N (2006). Evaluation of an integrated in vitro-in silico PBPK (physiologically based pharmacokinetic) model to provide estimates of human bioavailability. *Int J Pharm* 308(1-2): 133-9.

## REFERENCES:

- Cai, WM, Chen, B and Zhang, WX (2007). Frequency of CYP2D6\*10 and \*14 alleles and their influence on the metabolic activity of CYP2D6 in a healthy Chinese population. *Clin Pharmacol Ther* 81(1): 95-8.
- Caldwell, MD, Awad, T, Johnson, JA, Gage, BF, Falkowski, M, Gardina, P, Hubbard, J, Turpaz, Y, Langae, TY, Eby, C, King, CR, Brower, A, Schmelzer, JR, Glurich, I, Vidaillet, HJ, Yale, SH, Qi Zhang, K, Berg, RL and Burmester, JK (2008). CYP4F2 genetic variant alters required warfarin dose. *Blood* 111(8): 4106-12.
- Carlsson, KC, Hoem, NO, Glauser, T and Vinks, AA (2005). Development of a population pharmacokinetic model for carbamazepine based on sparse therapeutic monitoring data from pediatric patients with epilepsy. *Clin Ther* 27(5): 618-26.
- Chang, SC and Lee, VH (1987). Nasal and conjunctival contributions to the systemic absorption of topical timolol in the pigmented rabbit: implications in the design of strategies to maximize the ratio of ocular to systemic absorption. *J Ocul Pharmacol* 3(2): 159-69.
- Chastain, JE (2003). General considerations in ocular drug delivery. In: Mitra AK (ed) *Ophthalmic drug delivery system; drugs and the pharmaceutical sciences*, 2nd edn. Marcel Dekker, New York, pp 59–107.
- Chiou, WL (1986). A new simple approach to study the effect of changes in urine flow and/or urine pH on renal clearance and its applications. *Int J Clin Pharmacol Ther Toxicol* 24(10): 519-27.
- Choi, MK and Song, IS (2008). Organic cation transporters and their pharmacokinetic and pharmacodynamic consequences. *Drug Metab Pharmacokinet* 23(4): 243-53.
- Chrai, SS, Makoid, MC, Eriksen, SP and Robinson, JR (1974). Drop size and initial dosing frequency problems of topically applied ophthalmic drugs. *J Pharm Sci* 63(3): 333-8.
- Chrzanowska, M, Kurzawski, M, Drozdziak, M, Mazik, M, Oko, A and Czekalski, S (2006). Thiopurine S-methyltransferase phenotype-genotype correlation in hemodialyzed patients. *Pharmacol Rep* 58(6): 973-8.
- Chu, S, Wilson, DS, Deaton, RL, Mackenthun, AV, Eason, CN and Cavanaugh, JH (1993). Single- and multiple-dose pharmacokinetics of clarithromycin, a new macrolide antimicrobial. *J Clin Pharmacol* 33(8): 719-26.
- Chu, SY, Deaton, R and Cavanaugh, J (1992a). Absolute bioavailability of clarithromycin after oral administration in humans. *Antimicrob Agents Chemother* 36(5): 1147-50.
- Chu, SY, Granneman, GR, Pichotta, PJ, Decourt, JP, Girault, J and Fourtillan, JB (1993). Effect of moderate or severe hepatic impairment on clarithromycin pharmacokinetics. *J Clin Pharmacol* 33(5): 480-5.
- Chu, SY, Sennello, LT, Bunnell, ST, Varga, LL, Wilson, DS and Sonders, RC (1992b). Pharmacokinetics of clarithromycin, a new macrolide, after single ascending oral doses. *Antimicrob Agents Chemother* 36(11): 2447-53.
- Coakes, RL and Brubaker, RF (1979). Method of measuring aqueous humor flow and corneal endothelial permeability using a fluorophotometry nomogram. *Invest Ophthalmol Vis Sci* 18(3): 288-302.
- Cole, M, Boddy, AV, Kearns, P, Teh, KH, Price, L, Parry, A, Pearson, AD and Veal, GJ (2006). Potential clinical impact of taking multiple blood samples for research studies in paediatric oncology: how much do we really know? *Pediatr Blood Cancer* 46(7): 723-7.
- Conil, JM, Georges, B, Lavit, M, Seguin, T, Tack, I, Samii, K, Chabanon, G, Houin, G and Saivin, S (2007). Pharmacokinetics of ceftazidime and cefepime in burn patients: the importance of age and creatinine clearance. *Int J Clin Pharmacol Ther* 45(10): 529-38.

## REFERENCES:

- Cosson, V, Jorga, K and Fuseau, E (2007). Modeling of Metabolite Pharmacokinetics in a Large Pharmacokinetic Data Set: An Application. In: Ette EI, Williams PJ (ed.) *Pharmacometrics; the science of quantitative pharmacology*. John Wiley & Sons, Inc., New Jersey, pp1107-1136.
- Craig, WA, Kiem, S and Andes, DR (2002). Free Drug 24-Hr AUC/MIC is the PK/PD Target that Correlates with In Vivo Efficacy of Macrolides, Azalides, Ketolides and Clindamycin. Abstr. 42nd Intersci. Conf. Antimicrob. Agents Chemother., San Diego, CA, abstr. A-1264. American Society for Microbiology, Washington, DC.
- Csajka, C, Buclin, T, Fattinger, K, Brunner, HR and Biollaz, J (2002). Population pharmacokinetic-pharmacodynamic modelling of angiotensin receptor blockade in healthy volunteers. *Clin Pharmacokinet* 41(2): 137-52.
- Csajka, C, Drover, D and Verotta, D (2005). The use of a sum of inverse Gaussian functions to describe the absorption profile of drugs exhibiting complex absorption. *Pharm Res* 22(8): 1227-35.
- Cuffari, C, Dassopoulos, T, Turnbough, L, Thompson, RE and Bayless, TM (2004). Thiopurine methyltransferase activity influences clinical response to azathioprine in inflammatory bowel disease. *Clin Gastroenterol Hepatol* 2(5): 410-7.
- Cunha-Vaz, JG and Maurice, DM (1967). The active transport of fluorescein by the retinal vessels and the retina. *J Physiol* 191(3): 467-86.
- D'Andrea, G, D'Ambrosio, R and Margaglione, M (2008). Oral anticoagulants: Pharmacogenetics Relationship between genetic and non-genetic factors. *Blood Rev* 22(3): 127-40.
- D'Argenio, DZ and Schumitzky, A (2008). ADAPT 5 User's guide: Pharmacokinetic/Pharmacodynamic Systems Analysis Software. Biomedical Simulations Resource, Los Angeles.
- Danhof, M, Alvan, G, Dahl, SG, Kuhlmann, J and Paintaud, G (2005). Mechanism-based pharmacokinetic-pharmacodynamic modeling-a new classification of biomarkers. *Pharm Res* 22(9): 1432-7.
- Davey, PG (1991). The pharmacokinetics of clarithromycin and its 14-OH metabolite. *J Hosp Infect* 19 Suppl A: 29-37.
- Davidian, M and Giltinan, DM (1993). Some general estimation methods for nonlinear mixed-effects models. *J Biopharm Stat* 3(1): 23-55.
- Davies, NM (2000). Biopharmaceutical considerations in topical ocular drug delivery. *Clin Exp Pharmacol Physiol* 27(7): 558-62.
- Davies, NM, Farr, SJ, Hadgraft, J and Kellaway, IW (1992). Evaluation of mucoadhesive polymers in ocular drug delivery. II. Polymer-coated vesicles. *Pharm Res* 9(9): 1137-44.
- de Jonge, ME, Huitema, AD, van Dam, SM, Rodenhuis, S and Beijnen, JH (2005). Population pharmacokinetics of cyclophosphamide and its metabolites 4-hydroxycyclophosphamide, 2-dechloroethylcyclophosphamide, and phosphoramidate mustard in a high-dose combination with Thiotepa and Carboplatin. *Ther Drug Monit* 27(6): 756-65.
- De Paepe, P, Belpaire, FM and Buylaert, WA (2002). Pharmacokinetic and pharmacodynamic considerations when treating patients with sepsis and septic shock. *Clin Pharmacokinet* 41(14): 1135-51.
- de Vries, JX, Raedsch, R, Volker, U, Walter-Sack, I and Weber, E (1988). Biliary excretion of phenprocoumon and metabolites. *Eur J Clin Pharmacol* 35(4): 433-6.



## REFERENCES:

- de Vries, JX and Volker, U (1990). Determination of the plasma protein binding of the coumarin anticoagulants phenprocoumon and its metabolites, warfarin and acenocoumarol, by ultrafiltration and high-performance liquid chromatography. *J Chromatogr* 529(2): 479-85.
- Debord, J, Risco, E, Harel, M, Le Meur, Y, Buchler, M, Lachatre, G, Le Guellec, C and Marquet, P (2001). Application of a gamma model of absorption to oral cyclosporin. *Clin Pharmacokinet* 40(5): 375-82.
- Demirbas, S, Reyderman, L and Stavchansky, S (1998). Bioavailability of dextromethorphan (as dextrophan) from sustained release formulations in the presence of guaifenesin in human volunteers. *Biopharm Drug Dispos* 19(8): 541-5.
- Derendorf, H, Lesko, LJ, Chaikin, P, Colburn, WA, Lee, P, Miller, R, Powell, R, Rhodes, G, Stanski, D and Venitz, J (2000). Pharmacokinetic/pharmacodynamic modeling in drug research and development. *J Clin Pharmacol* 40(12 Pt 2): 1399-418.
- Diamond, JP (1997). Systemic adverse effects of topical ophthalmic agents. Implications for older patients. *Drugs Aging* 11(5): 352-60.
- Diestelhorst, M, Grunthal, S and Suverkrup, R (1999). Dry Drops: a new preservative-free drug delivery system. *Graefes Arch Clin Exp Ophthalmol* 237(5): 394-8.
- Ding, X and Kaminsky, LS (2003). Human extrahepatic cytochromes P450: function in xenobiotic metabolism and tissue-selective chemical toxicity in the respiratory and gastrointestinal tracts. *Annu Rev Pharmacol Toxicol* 43: 149-73.
- Dinslage, S, Diestelhorst, M, Weichselbaum, A and Suverkrup, R (2002). Lyophilisates for drug delivery in ophthalmology: pharmacokinetics of fluorescein in the human anterior segment. *Br J Ophthalmol* 86(10): 1114-7.
- Duedahl, TH, Dirks, J, Petersen, KB, Romsing, J, Larsen, NE and Dahl, JB (2005). Intravenous dextromethorphan to human volunteers: relationship between pharmacokinetics and anti-hyperalgesic effect. *Pain* 113(3): 360-8.
- Edelbroek, PM, van Kempen, GM, Hessing, TJ and de Wolff, FA (1990). Analysis of phenprocoumon and its hydroxylated and conjugated metabolites in human urine by high-performance liquid chromatography after solid-phase extraction. *J Chromatogr* 530(2): 347-58.
- Eichelbaum, M, Spannbrucker, N, Steincke, B and Dengler, HJ (1979). Defective N-oxidation of sparteine in man: a new pharmacogenetic defect. *Eur J Clin Pharmacol* 16(3): 183-7.
- El Desoky, ES, Derendorf, H and Klotz, U (2006). Variability in response to cardiovascular drugs. *Curr Clin Pharmacol* 1(1): 35-46.
- Ette, EI (1997). Stability and performance of a population pharmacokinetic model. *J Clin Pharmacol* 37(6): 486-95.
- Ette, EI, Kelman, AW, Howie, CA and Whiting, B (1995). Analysis of animal pharmacokinetic data: performance of the one point per animal design. *J Pharmacokinet Biopharm* 23(6): 551-66.
- Ette, EI and Ludden, TM (1995). Population pharmacokinetic modeling: the importance of informative graphics. *Pharm Res* 12(12): 1845-55.
- Ette, EI, Sun, H and Ludden, TM (1998). Balanced designs in longitudinal population pharmacokinetic studies. *J Clin Pharmacol* 38(5): 417-23.
- Ette, EI and Williams, PJ (2004). Population pharmacokinetics I: background, concepts, and models. *Ann Pharmacother* 38(10): 1702-6.
- Ette, EI and Williams, PJ (2007). *Pharmacometrics; the science of quantitative pharmacology*. John Wiley & Sons, Inc., New Jersey.

## REFERENCES:

- Ette, EI and Williams, PJ (2007). Pharmacometrics; the science of quantitative pharmacology. John Wiley & Sons, Inc., New Jersey.
- Ette, EI, Williams, PJ, Kim, YH, Lane, JR, Liu, MJ and Capparelli, EV (2003). Model appropriateness and population pharmacokinetic modeling. *J Clin Pharmacol* 43(6): 610-23.
- Ette, EI, Williams, PJ and Lane, JR (2004). Population pharmacokinetics III: design, analysis, and application of population pharmacokinetic Studies. *Ann Pharmacother* 38(12): 2136-44.
- Evans, ND, Godfrey, KR, Chapman, MJ, Chappell, MJ, Aarons, L and Duffull, SB (2001). An identifiability analysis of a parent-metabolite pharmacokinetic model for ivabradine. *J Pharmacokinetic Pharmacodyn* 28(1): 93-105.
- FDA (1999). Guidance for Industry: Population Pharmacokinetics. U.S. Department of Health and Human Services, FDA., Washington.
- Fernandes, PB, Bailer, R, Swanson, R, Hanson, CW, McDonald, E, Ramer, N, Hardy, D, Shipkowitz, N, Bower, RR and Gade, E (1986). In vitro and in vivo evaluation of A-56268 (TE-031), a new macrolide. *Antimicrob Agents Chemother* 30(6): 865-73.
- Ferrero, JL, Bopp, BA, Marsh, KC, Quigley, SC, Johnson, MJ, Anderson, DJ, Lamm, JE, Tolman, KG, Sanders, SW, Cavanaugh, JH and et al. (1990a). Metabolism and disposition of clarithromycin in man. *Drug Metab Dispos* 18(4): 441-6.
- Ferrero, JL, Bopp, BA, Marsh, KC, Quigley, SC, Johnson, MJ, Anderson, DJ, Lamm, JE, Tolman, KG, Sanders, SW, Cavanaugh, JH and Sonders, RC (1990b). Metabolism and disposition of clarithromycin in man. *Drug Metab Dispos* 18(4): 441-6.
- Fisher, JW, Mahle, D and Abbas, R (1998). A human physiologically based pharmacokinetic model for trichloroethylene and its metabolites, trichloroacetic acid and free trichloroethanol. *Toxicol Appl Pharmacol* 152(2): 339-59.
- Fisher, MB, Paine, MF, Strelevitz, TJ and Wrighton, SA (2001). The role of hepatic and extrahepatic UDP-glucuronosyltransferases in human drug metabolism. *Drug Metab Rev* 33(3-4): 273-97.
- Florence, AT and Attwood, D (2006). Physicochemical principles of pharmacy, 4th ed., Pharmaceutical Press, London, UK.
- Florence, AT and Attwood, D (2006). Physicochemical principles of pharmacy, 4th ed., Pharmaceutical Press, London, UK.
- Frame, B, Miller, R and Lalonde, RL (2003). Evaluation of mixture modeling with count data using NONMEM. *J Pharmacokinetic Pharmacodyn* 30(3): 167-83.
- Frank, D, Jaehde, U and Fuhr, U (2007). Evaluation of probe drugs and pharmacokinetic metrics for CYP2D6 phenotyping. *Eur J Clin Pharmacol* 63(4): 321-33.
- Fraschini, F, Scaglione, F and Demartini, G (1993). Clarithromycin clinical pharmacokinetics. *Clin Pharmacokinetic* 25(3): 189-204.
- Fraunfelder, FT and Meyer, SM (1987). Systemic side effects from ophthalmic timolol and their prevention. *J Ocul Pharmacol* 3(2): 177-84.
- Fraunfelder, FW (2006). Corneal toxicity from topical ocular and systemic medications. *Cornea* 25(10): 1133-8.
- Freedman, MD and Olatidoye, AG (1994). Clinically significant drug interactions with the oral anticoagulants. *Drug Saf* 10(5): 381-94.
- Freudenthaler, S, Meineke, I, Schreeb, KH, Boakye, E, Gundert-Remy, U and Gleiter, CH (1998). Influence of urine pH and urinary flow on the renal excretion of memantine. *Br J Clin Pharmacol* 46(6): 541-6.

## REFERENCES:

- Fuhr, U (2008). Improvement in the handling of drug-drug interactions. *Eur J Clin Pharmacol* 64(2): 167-71.
- Fuhr, U (2009). Pharmacogenetic-Based Clinical Scores – A Useful Simple Tool to Predict Tamoxifen Based CYP2D6 Phenotype? *J Clin Pharmacol* 2009 in press.
- Fuhr, U, Jetter, A and Kirchheiner, J (2007). Appropriate phenotyping procedures for drug metabolizing enzymes and transporters in humans and their simultaneous use in the "cocktail" approach. *Clin Pharmacol Ther* 81(2): 270-83.
- Furst, DE (1988). The basis for variability of response to anti-rheumatic drugs. *Baillieres Clin Rheumatol* 2(2): 395-424.
- Gaedigk, A, Simon, SD, Pearce, RE, Bradford, LD, Kennedy, MJ and Leeder, JS (2008). The CYP2D6 activity score: translating genotype information into a qualitative measure of phenotype. *Clin Pharmacol Ther* 83(2): 234-42.
- Gage, BF, Eby, C, Johnson, JA, Deych, E, Rieder, MJ, Ridker, PM, Milligan, PE, Grice, G, Lenzini, P, Rettie, AE, Aquilante, CL, Grosso, L, Marsh, S, Langae, T, Farnett, LE, Voora, D, Veenstra, DL, Glynn, RJ, Barrett, A and McLeod, HL (2008). Use of pharmacogenetic and clinical factors to predict the therapeutic dose of warfarin. *Clin Pharmacol Ther* 84(3): 326-31.
- Garrido, MJ, Habre, W, Rombout, F and Troconiz, IF (2006). Population pharmacokinetic/pharmacodynamic modelling of the analgesic effects of tramadol in pediatrics. *Pharm Res* 23(9): 2014-23.
- Gieschke, R and Steimer, JL (2000). Pharmacometrics: modelling and simulation tools to improve decision making in clinical drug development. *Eur J Drug Metab Pharmacokinet* 25(1): 49-58.
- Gobburu, JVS (2004). Population Pharmacokinetic and Pharmacodynamic Analysis. In: Sahajwalla CG (Ed.). *New Drug Development; Regulatory Paradigms for Clinical Pharmacology and Biopharmaceutics. Drugs and the pharmaceutical sciences.* pp 229-244. Marcel Dekker, Inc.
- Gorski, JC, Jones, DR, Haehner-Daniels, BD, Hamman, MA, O'Mara, EM, Jr. and Hall, SD (1998). The contribution of intestinal and hepatic CYP3A to the interaction between midazolam and clarithromycin. *Clin Pharmacol Ther* 64(2): 133-43.
- Grasela, TH, Dement, CW, Kolterman, OG, Fineman, MS, Grasela, DM, Honig, P, Antal, EJ, Bjornsson, TD and Loh, E (2007). Pharmacometrics and the transition to model-based development. *Clin Pharmacol Ther* 82(2): 137-42.
- Grasmader, K, Verwohlt, PL, Kuhn, KU, Dragicevic, A, von Widdern, O, Zobel, A, Hiemke, C, Rietschel, M, Maier, W, Jaehde, U and Rao, ML (2004). Population pharmacokinetic analysis of mirtazapine. *Eur J Clin Pharmacol* 60(7): 473-80.
- Gueorguieva, I, Nestorov, IA, Aarons, L and Rowland, M (2005). Uncertainty analysis in pharmacokinetics and pharmacodynamics: application to naratriptan. *Pharm Res* 22(10): 1614-26.
- Haefner, JW (1996). *Modeling Biological Systems: Principles and Applications.* Springer Publishers. NY.
- Hamberg, AK, Dahl, ML, Barban, M, Scordo, MG, Wadelius, M, Pengo, V, Padrini, R and Jonsson, EN (2007). A PK-PD model for predicting the impact of age, CYP2C9, and VKORC1 genotype on individualization of warfarin therapy. *Clin Pharmacol Ther* 81(4): 529-38.
- Harrington, DJ, Western, H, Seton-Jones, C, Rangarajan, S, Beynon, T and Shearer, MJ (2008). A study of the prevalence of vitamin K deficiency in patients with cancer referred to a

## REFERENCES:

- hospital palliative care team and its association with abnormal haemostasis. *J Clin Pathol* 61(4): 537-40.
- Hassan, M, Svensson, US, Ljungman, P, Bjorkstrand, B, Olsson, H, Bielenstein, M, Abdel-Rehim, M, Nilsson, C, Johansson, M and Karlsson, MO (1999). A mechanism-based pharmacokinetic-enzyme model for cyclophosphamide autoinduction in breast cancer patients. *Br J Clin Pharmacol* 48(5): 669-77.
- Hathout, RM, Mansour, S, Mortada, ND and Guinedi, AS (2007). Liposomes as an ocular delivery system for acetazolamide: in vitro and in vivo studies. *AAPS PharmSciTech* 8(1): 1.
- Haustein, KO and Huller, G (1994). Pharmacokinetics of phenprocoumon. *Int J Clin Pharmacol Ther* 32(4): 192-7.
- Hayreh, SS, Podhajsky, P and Zimmerman, MB (1999). Beta-blocker eyedrops and nocturnal arterial hypotension. *Am J Ophthalmol* 128(3): 301-9.
- He, M, Korzekwa, KR, Jones, JP, Rettie, AE and Trager, WF (1999). Structural forms of phenprocoumon and warfarin that are metabolized at the active site of CYP2C9. *Arch Biochem Biophys* 372(1): 16-28.
- Heller, T, Kirchheiner, J, Armstrong, VW, Luthe, H, Tzvetkov, M, Brockmoller, J and Oellerich, M (2006). AmpliChip CYP450 GeneChip: a new gene chip that allows rapid and accurate CYP2D6 genotyping. *Ther Drug Monit* 28(5): 673-7.
- Henningson, A, Marsh, S, Loos, WJ, Karlsson, MO, Garsa, A, Mross, K, Mielke, S, Vigano, L, Locatelli, A, Verweij, J, Sparreboom, A and McLeod, HL (2005). Association of CYP2C8, CYP3A4, CYP3A5, and ABCB1 polymorphisms with the pharmacokinetics of paclitaxel. *Clin Cancer Res* 11(22): 8097-104.
- Herd, DW, Anderson, BJ and Holford, NH (2007). Modeling the norketamine metabolite in children and the implications for analgesia. *Paediatr Anaesth* 17(9): 831-40.
- Hertrampf, R, Gundert-Remy, U, Beckmann, J, Hoppe, U, Elsasser, W and Stein, H (1991). Elimination of flecainide as a function of urinary flow rate and pH. *Eur J Clin Pharmacol* 41(1): 61-3.
- Higaki, K, Choe, SY, Lobenberg, R, Welage, LS and Amidon, GL (2008). Mechanistic understanding of time-dependent oral absorption based on gastric motor activity in humans. *Eur J Pharm Biopharm* 70(1): 313-25.
- Hirsh, J, Dalen, JE, Anderson, DR, Poller, L, Bussey, H, Ansell, J, Deykin, D and Brandt, JT (1998). Oral anticoagulants: mechanism of action, clinical effectiveness, and optimal therapeutic range. *Chest* 114(5 Suppl): 445S-469S.
- Hirt, D, Mentre, F, Tran, A, Rey, E, Auleley, S, Salmon, D, Duval, X and Treluyer, JM (2008). Effect of CYP2C19 polymorphism on nelfinavir to M8 biotransformation in HIV patients. *Br J Clin Pharmacol* 65(4): 548-57.
- Holford, N (2002). Input-output models. In: Kimko HC, Duffull SB, eds. *Simulation for Designing Clinical Trials: A Pharmacokinetic-Pharmacodynamic Perspective*. Vol. 125 New York, NY: Marcel Dekker, Pp 2-31.
- Holford, NH (1986). Clinical pharmacokinetics and pharmacodynamics of warfarin. Understanding the dose-effect relationship. *Clin Pharmacokinet* 11(6): 483-504.
- Holford, NH (2002). Input-output models. In: Kimko HC, Duffull SB, eds. *Simulation for Designing Clinical Trials: A Pharmacokinetic-Pharmacodynamic Perspective*. Vol. 125 New York, NY: Marcel Dekker, Pp 2-31.
- Holford, NH (2006). Dose response: Pharmacokinetic-pharmacodynamic approach. In Ting, N. (ed.) *Dose finding in drug development*. Springer, New York. pp . 73–88.

## REFERENCES:

- Hornof, M, Weyenberg, W, Ludwig, A and Bernkop-Schnurch, A (2003). Mucoadhesive ocular insert based on thiolated poly(acrylic acid): development and in vivo evaluation in humans. *J Control Release* 89(3): 419-28.
- Hughes, AR, Mosteller, M, Bansal, AT, Davies, K, Haneline, SA, Lai, EH, Nangle, K, Scott, T, Spreen, WR, Warren, LL and Roses, AD (2004). Association of genetic variations in HLA-B region with hypersensitivity to abacavir in some, but not all, populations. *Pharmacogenomics* 5(2): 203-11.
- Huitema, AD, Mathot, RA, Tibben, MM, Rodenhuis, S and Beijnen, JH (2001). A mechanism-based pharmacokinetic model for the cytochrome P450 drug-drug interaction between cyclophosphamide and thioTEPA and the autoinduction of cyclophosphamide. *J Pharmacokinet Pharmacodyn* 28(3): 211-30.
- Hummers-Pradier, E, Hess, S, Adham, IM, Papke, T, Pieske, B and Kochen, MM (2003). Determination of bleeding risk using genetic markers in patients taking phenprocoumon. *Eur J Clin Pharmacol* 59(3): 213-9.
- Hung, IF, Wu, AK, Cheng, VC, Tang, BS, To, KW, Yeung, CK, Woo, PC, Lau, SK, Cheung, BM and Yuen, KY (2005). Fatal interaction between clarithromycin and colchicine in patients with renal insufficiency: a retrospective study. *Clin Infect Dis* 41(3): 291-300.
- Irwin, S (1964). Determinants of Variability in Drug Response. *Psychosomatics* 5: 174-9.
- Ishii, K, Saito, Y, Itai, S, Nemoto, M, Takayama, K and Nagai, T (1998). Comparative study of pharmacokinetic parameters between clarithromycin and erythromycin stearate in relation to their physicochemical properties. *Drug Dev Ind Pharm* 24(2): 129-37.
- Jacqz-Aigrain, E, Funck-Brentano, C and Cresteil, T (1993). CYP2D6- and CYP3A-dependent metabolism of dextromethorphan in humans. *Pharmacogenetics* 3(4): 197-204.
- Jaenen, N, Baudouin, C, Pouliquen, P, Manni, G, Figueiredo, A and Zeyen, T (2007). Ocular symptoms and signs with preserved and preservative-free glaucoma medications. *Eur J Ophthalmol* 17(3): 341-9.
- Jelliffe, R, Schumitzky, A and Van Guilder, M (2000). Population pharmacokinetics/pharmacodynamics modeling: parametric and nonparametric methods. *Ther Drug Monit* 22(3): 354-65.
- Jones, RN, Erwin, ME and Barrett, MS (1990). In vitro activity of clarithromycin (TE-031, A-67268) and 14OH-clarithromycin alone and in combination against Legionella species. *Eur J Clin Microbiol Infect Dis* 9(11): 846-8.
- Jonsson, EN, Karlsson, MO and Milligan, PA (2007). Graphical displays for modeling population data. In: Ette EI, Williams PJ (ed.) *Pharmacometrics; the science of quantitative pharmacology*. John Wiley & Sons, Inc., New Jersey. pp 183-222.
- Kaila, N, Straka, RJ and Brundage, RC (2007). Mixture models and subpopulation classification: a pharmacokinetic simulation study and application to metoprolol CYP2D6 phenotype. *J Pharmacokinet Pharmacodyn* 34(2): 141-56.
- Kammerer, B, Kahlich, R, Ufer, M, Schenkel, A, Laufer, S and Gleiter, CH (2005). Stereospecific pharmacokinetic characterisation of phenprocoumon metabolites, and mass-spectrometric identification of two novel metabolites in human plasma and liver microsomes. *Anal Bioanal Chem* 383(6): 909-17.
- Karol, MD and Goodrich, S (1988). Metabolite formation pharmacokinetics: rate and extent of metabolite formation determined by deconvolution. *Pharm Res* 5(6): 347-51.
- Kazis, A, Kimiskidis, V and Niopas, I (1996). Pharmacokinetics of dextromethorphan and dextrorphan in epileptic patients. *Acta Neurol Scand* 93(2-3): 94-8.
- Kerbusch, T, Wahlby, U, Milligan, PA and Karlsson, MO (2003). Population pharmacokinetic modelling of darifenacin and its hydroxylated metabolite using pooled data,

## REFERENCES:

- incorporating saturable first-pass metabolism, CYP2D6 genotype and formulation-dependent bioavailability. *Br J Clin Pharmacol* 56(6): 639-52.
- Kimko, HC and Duffull, SB (2003). Simulation for designing clinical trials: A pharmacokinetic-pharmacodynamic modeling perspective. New York, NY: Marcel Dekker.
- Kinzig-Schippers, M, Tomalik-Scharte, D, Jetter, A, Scheidel, B, Jakob, V, Rodamer, M, Cascorbi, I, Doroshenko, O, Sorgel, F and Fuhr, U (2005). Should we use N-acetyltransferase type 2 genotyping to personalize isoniazid doses? *Antimicrob Agents Chemother* 49(5): 1733-8.
- Kirchheiner, J, Brosen, K, Dahl, ML, Gram, LF, Kasper, S, Roots, I, Sjoqvist, F, Spina, E and Brockmoller, J (2001). CYP2D6 and CYP2C19 genotype-based dose recommendations for antidepressants: a first step towards subpopulation-specific dosages. *Acta Psychiatr Scand* 104(3): 173-92.
- Kirchheiner, J, Fuhr, U and Brockmoller, J (2005). Pharmacogenetics-based therapeutic recommendations--ready for clinical practice? *Nat Rev Drug Discov* 4(8): 639-47.
- Kirchheiner, J, Heesch, C, Bauer, S, Meisel, C, Seringer, A, Goldammer, M, Tzvetkov, M, Meineke, I, Roots, I and Brockmoller, J (2004a). Impact of the ultrarapid metabolizer genotype of cytochrome P450 2D6 on metoprolol pharmacokinetics and pharmacodynamics. *Clin Pharmacol Ther* 76(4): 302-12.
- Kirchheiner, J, Keulen, JT, Bauer, S, Roots, I and Brockmoller, J (2008). Effects of the CYP2D6 gene duplication on the pharmacokinetics and pharmacodynamics of tramadol. *J Clin Psychopharmacol* 28(1): 78-83.
- Kirchheiner, J, Nickchen, K, Bauer, M, Wong, ML, Licinio, J, Roots, I and Brockmoller, J (2004b). Pharmacogenetics of antidepressants and antipsychotics: the contribution of allelic variations to the phenotype of drug response. *Mol Psychiatry* 9(5): 442-73.
- Kirchheiner, J, Schmidt, H, Tzvetkov, M, Keulen, JT, Lotsch, J, Roots, I and Brockmoller, J (2007). Pharmacokinetics of codeine and its metabolite morphine in ultra-rapid metabolizers due to CYP2D6 duplication. *Pharmacogenomics J* 7(4): 257-65.
- Kirchheiner, J, Ufer, M, Walter, EC, Kammerer, B, Kahlich, R, Meisel, C, Schwab, M, Gleiter, CH, Rane, A, Roots, I and Brockmoller, J (2004c). Effects of CYP2C9 polymorphisms on the pharmacokinetics of R- and S-phenprocoumon in healthy volunteers. *Pharmacogenetics* 14(1): 19-26.
- Kitteringham, NR, Bustgens, L, Brundert, E, Mineshita, S and Ohnhaus, EE (1984). The effect of liver cirrhosis on the pharmacokinetics of phenprocoumon. *Eur J Clin Pharmacol* 26(1): 65-70.
- Kitteringham, NR, Mineshita, S and Ohnhaus, EE (1985). The effect of wheat bran on the pharmacokinetics of phenprocoumon in normal volunteers. *Klin Wochenschr* 63(12): 537-9.
- Klaassen, T, Jetter, A, Tomalik-Scharte, D, Kasel, D, Kirchheiner, J, Jaehde, U and Fuhr, U (2008). Assessment of urinary mephenytoin metrics to phenotype for CYP2C19 and CYP2B6 activity. *Eur J Clin Pharmacol* 64(4): 387-98.
- Klein, TE, Altman, RB, Eriksson, N, Gage, BF, Kimmel, SE, Lee, MT, Limdi, NA, Page, D, Roden, DM, Wagner, MJ, Caldwell, MD and Johnson, JA (2009). Estimation of the warfarin dose with clinical and pharmacogenetic data. *N Engl J Med* 360(8): 753-64.
- Kleinbloesem, CH, van Brummelen, P, Danhof, M, Faber, H, Urquhart, J and Breimer, DD (1987). Rate of increase in the plasma concentration of nifedipine as a major determinant of its hemodynamic effects in humans. *Clin Pharmacol Ther* 41(1): 26-30.

## REFERENCES:

- Krishna, DR and Klotz, U (1994). Extrahepatic metabolism of drugs in humans. *Clin Pharmacokinet* 26(2): 144-60.
- Kupfer, A, Schmid, B, Preisig, R and Pfaff, G (1984). Dextromethorphan as a safe probe for debrisoquine hydroxylation polymorphism. *Lancet* 2(8401): 517-8.
- Kusama, M, Maeda, K, Chiba, K, Aoyama, A and Sugiyama, Y (2009). Prediction of the effects of genetic polymorphism on the pharmacokinetics of CYP2C9 substrates from in vitro data. *Pharm Res* 26(4): 822-35.
- Labbe, L, Sirois, C, Pilote, S, Arseneault, M, Robitaille, NM, Turgeon, J and Hamelin, BA (2000). Effect of gender, sex hormones, time variables and physiological urinary pH on apparent CYP2D6 activity as assessed by metabolic ratios of marker substrates. *Pharmacogenetics* 10(5): 425-38.
- Laika, B, Leucht, S, Heres, S and Steimer, W (2009). Intermediate metabolizer: increased side effects in psychoactive drug therapy. The key to cost-effectiveness of pretreatment CYP2D6 screening? *Pharmacogenomics J*.
- Lang, JC (1995). Ocular drug delivery conventional ocular formulations. *Adv Drug Delivery Rev* 16: 39-43.
- Langtry, HD and Brogden, RN (1997). Clarithromycin. A review of its efficacy in the treatment of respiratory tract infections in immunocompetent patients. *Drugs* 53(6): 973-1004.
- Lavielle, M and Mentre, F (2007). Estimation of population pharmacokinetic parameters of saquinavir in HIV patients with the MONOLIX software. *J Pharmacokinet Pharmacodyn* 34(2): 229-49.
- Lee, MS (2007). Role of genetic polymorphisms related to neurotransmitters and cytochrome P-450 enzymes in response to antidepressants. *Drugs Today (Barc)* 43(8): 569-81.
- Lee, PCL, Jawad, MS and Eccles, R (2000). Antitussive efficacy of dextromethorphan in cough associated with acute upper respiratory tract infection. *J Pharm Pharmacol* 52(9): 1137-42.
- Lee, SB, Geroski, DH, Prausnitz, MR and Edelhauser, HF (2004). Drug delivery through the sclera: effects of thickness, hydration, and sustained release systems. *Exp Eye Res* 78(3): 599-607.
- Lee, VH and Robinson, JR (1986). Topical ocular drug delivery: recent developments and future challenges. *J Ocul Pharmacol* 2(1): 67-108.
- Lee, VH, Urrea, PT, Smith, RE and Schanzlin, DJ (1985). Ocular drug bioavailability from topically applied liposomes. *Surv Ophthalmol* 29(5): 335-48.
- Lehr, T, Staab, A, Tillmann, C, Nielsen, EO, Trommeshauser, D, Schaefer, HG and Kloft, C (2008). Contribution of the active metabolite M1 to the pharmacological activity of tesofensine in vivo: a pharmacokinetic-pharmacodynamic modelling approach. *Br J Pharmacol* 153(1): 164-74.
- Lemuel-Diot, A, Laveille, C, Frey, N, Jochemsen, R and Mallet, A (2007). Mixture modeling for the detection of subpopulations in a pharmacokinetic/pharmacodynamic analysis. *J Pharmacokinet Pharmacodyn* 34(2): 157-81.
- Lessard, E, Yessine, MA, Hamelin, BA, O'Hara, G, LeBlanc, J and Turgeon, J (1999). Influence of CYP2D6 activity on the disposition and cardiovascular toxicity of the antidepressant agent venlafaxine in humans. *Pharmacogenetics* 9(4): 435-43.
- Levi, M, Dempsey, DA, Benowitz, NL and Sheiner, LB (2007). Population pharmacokinetics of nicotine and its metabolites I. Model development. *J Pharmacokinet Pharmacodyn* 34(1): 5-21.

## REFERENCES:

- Levitt, DG and Schoemaker, RC (2006). Human physiologically based pharmacokinetic model for ACE inhibitors: ramipril and ramiprilat. *BMC Clin Pharmacol* 6: 1.
- Limdi, NA, Arnett, DK, Goldstein, JA, Beasley, TM, McGwin, G, Adler, BK and Acton, RT (2008). Influence of CYP2C9 and VKORC1 on warfarin dose, anticoagulation attainment and maintenance among European-Americans and African-Americans. *Pharmacogenomics* 9(5): 511-26.
- Lin, JH (2006). CYP induction-mediated drug interactions: in vitro assessment and clinical implications. *Pharm Res* 23(6): 1089-116.
- Lin, JH and Lu, AY (2001). Interindividual variability in inhibition and induction of cytochrome P450 enzymes. *Annu Rev Pharmacol Toxicol* 41: 535-67.
- Lindauer, A, Siepmann, T, Oertel, R, Jung, A, Ziemssen, T, Jaehde, U, Kirch, W and Siepmann, M (2008). Pharmacokinetic/pharmacodynamic modelling of venlafaxine: pupillary light reflex as a test system for noradrenergic effects. *Clin Pharmacokinet* 47(11): 721-31.
- Linden, C and Alm, A (1997). Effect of consecutively applied fluorescein eye drops on corneal and aqueous concentrations of fluorescein. *Ophthalmic Res* 29(2): 57-60.
- Lindstrom, ML and Bates, DM (1990). Nonlinear mixed effects models for repeated measures data. *Biometrics* 46(3): 673-87.
- Logan, J (2003). A review of graphical methods for tracer studies and strategies to reduce bias. *Nucl Med Biol* 30(8): 833-44.
- Lu, AY (1998). Drug-metabolism research challenges in the new millennium: individual variability in drug therapy and drug safety. *Drug Metab Dispos* 26(12): 1217-22.
- Luck, H, Kinzig, M, Jetter, A, Fuhr, U and Sorgel, F (2009). Mesalazine pharmacokinetics and NAT2 phenotype. *Eur J Clin Pharmacol* 65(1): 47-54.
- Ludwig, A, van Haeringen, NJ, Bodelier, VM and Van Ooteghem, M (1992). Relationship between precorneal retention of viscous eye drops and tear fluid composition. *Int Ophthalmol* 16(1): 23-6.
- Lunn, DJ, Best, N, Thomas, A, Wakefield, J and Spiegelhalter, D (2002). Bayesian analysis of population PK/PD models: general concepts and software. *J Pharmacokinetic Pharmacodyn* 29(3): 271-307.
- Lux, A, Maier, S, Dinslage, S, Suverkrup, R and Diestelhorst, M (2003). A comparative bioavailability study of three conventional eye drops versus a single lyophilisate. *Br J Ophthalmol* 87(4): 436-40.
- Ma, JD, Nafziger, AN and Bertino, JS, Jr. (2004). Genetic polymorphisms of cytochrome P450 enzymes and the effect on interindividual, pharmacokinetic variability in extensive metabolizers. *J Clin Pharmacol* 44(5): 447-56.
- Macdonald, EA and Maurice, DM (1991). Loss of fluorescein across the conjunctiva. *Exp Eye Res* 53(4): 427-30.
- Macha, S, Hughes, PM and Mitra, AK (2003). Overview of ocular drug delivery. In: Mitra AK (ed) *Ophthalmic drug delivery system; drugs and the pharmaceutical sciences*, 2nd edn. Marcel Dekker, New York, pp 1-12.
- Mahesh Kumar, KN, Ramu, P, Rajan, S, Shewade, DG, Balachander, J and Adithan, C (2008). Genetic polymorphisms of beta1 adrenergic receptor and their influence on the cardiovascular responses to metoprolol in a South Indian population. *J Cardiovasc Pharmacol* 52(5): 459-66.
- Mahgoub, A, Idle, JR, Dring, LG, Lancaster, R and Smith, RL (1977). Polymorphic hydroxylation of Debrisoquine in man. *Lancet* 2(8038): 584-6.



## REFERENCES:

- Maitre, PO, Buhner, M, Thomson, D and Stanski, DR (1991). A three-step approach combining Bayesian regression and NONMEM population analysis: application to midazolam. *J Pharmacokinet Biopharm* 19(4): 377-84.
- Mallet, A, Mentre, F, Steimer, JL and Lokiec, F (1988). Nonparametric maximum likelihood estimation for population pharmacokinetics, with application to cyclosporine. *J Pharmacokinet Biopharm* 16(3): 311-27.
- Mandema, JW, Verotta, D and Sheiner, LB (1992). Building population pharmacokinetic--pharmacodynamic models. I. Models for covariate effects. *J Pharmacokinet Biopharm* 20(5): 511-28.
- Manivannan, A, Plskova, J, Farrow, A, McKay, S, Sharp, PF and Forrester, JV (2005). Ultra-wide-field fluorescein angiography of the ocular fundus. *Am J Ophthalmol* 140(3): 525-7.
- Marchant, B (1981). Pharmacokinetic factors influencing variability in human drug response. *Scand J Rheumatol Suppl* 39: 5-14.
- Marez, D, Legrand, M, Sabbagh, N, Guidice, JM, Spire, C, Lafitte, JJ, Meyer, UA and Broly, F (1997). Polymorphism of the cytochrome P450 CYP2D6 gene in a European population: characterization of 48 mutations and 53 alleles, their frequencies and evolution. *Pharmacogenetics* 7(3): 193-202.
- Martin, SJ, Garvin, CG, McBurney, CR and Sahloff, EG (2001). The activity of 14-hydroxy clarithromycin, alone and in combination with clarithromycin, against penicillin- and erythromycin-resistant *Streptococcus pneumoniae*. *J Antimicrob Chemother* 47(5): 581-7.
- Masche, UP, Rentsch, KM, von Felten, A, Meier, PJ and Fattinger, KE (1999). Opposite effects of lornoxicam co-administration on phenprocoumon pharmacokinetics and pharmacodynamics. *Eur J Clin Pharmacol* 54(11): 857-64.
- Maurice, DM (1967). The use of fluorescein in ophthalmological research. *Invest Ophthalmol* 6(5): 464-77.
- Maurice, DM and Mishima, S (1984). Ocular pharmacokinetics. In: Sears ML (ed) *Pharmacology of the eye, handbook of experimental Pharmacology*, vol. 69. Springer-Verlag, Berlin, pp 19–116.
- Mayhew, BS, Jones, DR and Hall, SD (2000). An in vitro model for predicting in vivo inhibition of cytochrome P450 3A4 by metabolic intermediate complex formation. *Drug Metab Dispos* 28(9): 1031-7.
- McGilveray, IJ (2005). Pharmacokinetics of cannabinoids. *Pain Res Manag* 10(A): 15A-22A.
- McLaren, JW, Ziai, N and Brubaker, RF (1993). A simple three-compartment model of anterior segment kinetics. *Exp Eye Res* 56(3): 355-66.
- Mega, JL, Close, SL, Wiviott, SD, Shen, L, Hockett, RD, Brandt, JT, Walker, JR, Antman, EM, Macias, W, Braunwald, E and Sabatine, MS (2009). Cytochrome p-450 polymorphisms and response to clopidogrel. *N Engl J Med* 360(4): 354-62.
- Mihara, K, Suzuki, A, Kondo, T, Yasui, N, Furukori, H, Nagashima, U, Otani, K, Kaneko, S and Inoue, Y (1999). Effects of the CYP2D6\*10 allele on the steady-state plasma concentrations of haloperidol and reduced haloperidol in Japanese patients with schizophrenia. *Clin Pharmacol Ther* 65(3): 291-4.
- Mishima, S (1981). Clinical pharmacokinetics of the eye. Proctor lecture. *Invest Ophthalmol Vis Sci* 21(4): 504-41.
- Mishima, S, Gasset, A, Klyce, SD, Jr. and Baum, JL (1966). Determination of tear volume and tear flow. *Invest Ophthalmol* 5(3): 264-76.

## REFERENCES:

- Mitra, AK (2003). Ophthalmic drug delivery system; drugs and the pharmaceutical sciences, 2nd edn. Marcel Dekker, New York.
- Mochizuki, H, Yamada, M, Hatou, S and Tsubota, K (2009). Turnover rate of tear-film lipid layer determined by fluorophotometry. *Br J Ophthalmol* 93(11): 1535-8.
- Moghadamnia, AA, Rostami-Hodjegan, A, Abdul-Manap, R, Wright, CE, Morice, AH and Tucker, GT (2003). Physiologically based modelling of inhibition of metabolism and assessment of the relative potency of drug and metabolite: dextromethorphan vs. dextrorphan using quinidine inhibition. *Br J Clin Pharmacol* 56(1): 57-67.
- Muszkat, M (2007). Interethnic differences in drug response: the contribution of genetic variability in beta adrenergic receptor and cytochrome P4502C9. *Clin Pharmacol Ther* 82(2): 215-8.
- Nelson, JD (1995). Simultaneous evaluation of tear turnover and corneal epithelial permeability by fluorophotometry in normal subjects and patients with keratoconjunctivitis sicca (KCS). *Trans Am Ophthalmol Soc* 93: 709-53.
- Nestorov, I (2001). Modelling and simulation of variability and uncertainty in toxicokinetics and pharmacokinetics. *Toxicol Lett* 120(1-3): 411-20.
- Nielsen, MD, Brosen, K and Gram, LF (1990). A dose-effect study of the in vivo inhibitory effect of quinidine on sparteine oxidation in man. *Br J Clin Pharmacol* 29(3): 299-304.
- Noecker, R (2001). Effects of common ophthalmic preservatives on ocular health. *Adv Ther* 18(5): 205-15.
- Noecker, RJ, Herrygers, LA and Anwaruddin, R (2004). Corneal and conjunctival changes caused by commonly used glaucoma medications. *Cornea* 23(5): 490-6.
- Nomura, K, Morikawa, N, Ikawa, K, Ikeda, K, Fujimoto, Y, Shimizu, D, Taniguchi, K, Shimura, K, Kanbayashi, Y, Komori, T, Matsumoto, Y, Fujita, N, Shimazaki, C and Taniwaki, M (2008). Optimized dosage and frequency of cefozopran for patients with febrile neutropenia based on population pharmacokinetic and pharmacodynamic analysis. *J Antimicrob Chemother* 61(4): 892-900.
- Noreddin, AM, Roberts, D, Nichol, K, Wierzbowski, A, Hoban, DJ and Zhanel, GG (2002). Pharmacodynamic modeling of clarithromycin against macrolide-resistant [PCR-positive *mef(A)* or *erm(B)*] *Streptococcus pneumoniae* simulating clinically achievable serum and epithelial lining fluid free-drug concentrations. *Antimicrob Agents Chemother* 46(12): 4029-34.
- Pacanowski, MA, Hopley, CW and Aquilante, CL (2008). Interindividual variability in oral antidiabetic drug disposition and response: the role of drug transporter polymorphisms. *Expert Opin Drug Metab Toxicol* 4(5): 529-44.
- Paine, MF, Khalighi, M, Fisher, JM, Shen, DD, Kunze, KL, Marsh, CL, Perkins, JD and Thummel, KE (1997). Characterization of interintestinal and intrainestinal variations in human CYP3A-dependent metabolism. *J Pharmacol Exp Ther* 283(3): 1552-62.
- Parvez, L, Vaidya, M, Sakhardande, A, Subburaj, S and Rajagopalan, TG (1996). Evaluation of antitussive agents in man. *Pulm Pharmacol* 9(5-6): 299-308.
- Patton, TF and Francoeur, M (1978). Ocular bioavailability and systemic loss of topically applied ophthalmic drugs. *Am J Ophthalmol* 85(2): 225-9.
- Peters, DH and Clissold, SP (1992). Clarithromycin. A review of its antimicrobial activity, pharmacokinetic properties and therapeutic potential. *Drugs* 44(1): 117-64.
- Petricoul O, CV, Fuseau E and Marchand M (2007). Population models for drug absorption and enterohepatic recycling. pp345-382. In E. I. Ette, and P. J. Williams (ed.), *Pharmacometrics: the science of quantitative pharmacology*, 1st ed., John Wiley & Sons, New Jersey.

## REFERENCES:

- Petricoulo, CV, Fuseau, E and Marchand, M (2007). Population models for drug absorption and enterohepatic recycling. In: Ette EI and Williams (ed) *Pharmacometrics; the science of quantitative pharmacology*, 1st edn. John Wiley & Sons, New Jersey, pp345-382.
- Pinto, AG, Horlander, J, Chalasani, N, Hamman, M, Asghar, A, Kolwankar, D and Hall, SD (2005a). Diltiazem inhibits human intestinal cytochrome P450 3A (CYP3A) activity in vivo without altering the expression of intestinal mRNA or protein. *Br J Clin Pharmacol* 59(4): 440-6.
- Pinto, AG, Wang, YH, Chalasani, N, Skaar, T, Kolwankar, D, Gorski, JC, Liangpunsakul, S, Hamman, MA, Arefayene, M and Hall, SD (2005b). Inhibition of human intestinal wall metabolism by macrolide antibiotics: effect of clarithromycin on cytochrome P450 3A4/5 activity and expression. *Clin Pharmacol Ther* 77(3): 178-88.
- Piotrovskij, V, Van Peer, A. (1997). A model with separate hepato-portal compartment ("first-pass" model): fitting to plasma concentration-time profiles in humans. *Pharm Res* 14: 230-7.
- Piotrovskij, VK, Paintaud, G, Alvan, G and Trnovec, T (1994). Modeling of the saturable time-constrained amoxicillin absorption in humans. *Pharm Res* 11(9): 1346-51.
- Pisella, PJ, Pouliquen, P and Baudouin, C (2002). Prevalence of ocular symptoms and signs with preserved and preservative free glaucoma medication. *Br J Ophthalmol* 86(4): 418-23.
- Plock, N, Buerger, C, Joukhadar, C, Kljucar, S and Kloft, C (2007). Does linezolid inhibit its own metabolism? Population pharmacokinetics as a tool to explain the observed nonlinearity in both healthy volunteers and septic patients. *Drug Metab Dispos* 35(10): 1816-23.
- Pontes de Carvalho, RA, Krausse, ML, Murphree, AL, Schmitt, EE, Campochiaro, PA and Maumenee, IH (2006). Delivery from episcleral explants. *Invest Ophthalmol Vis Sci* 47(10): 4532-9.
- Pope, LE, Khalil, MH, Berg, JE, Stiles, M, Yakatan, GJ and Sellers, EM (2004). Pharmacokinetics of dextromethorphan after single or multiple dosing in combination with quinidine in extensive and poor metabolizers. *J Clin Pharmacol* 44(10): 1132-42.
- Post, TM, Freijer, JI, Ploeger, BA and Danhof, M (2008). Extensions to the visual predictive check to facilitate model performance evaluation. *J Pharmacokinetic Pharmacodyn* 35(2): 185-202.
- Qazim, B, Stollberger, C, Krugluger, W, Dossenbach-Glaninger, A and Finsterer, J (2008). Dependency of phenprocoumon dosage on polymorphisms in the VKORC1 and CYP2C9 genes. *J Thromb Thrombolysis*.
- Quinney, SK, Galinsky, RE, Jiyamapa-Serna, VA, Chen, Y, Hamman, MA, Hall, SD and Kimura, RE (2008). Hydroxyitraconazole, formed during intestinal first-pass metabolism of itraconazole, controls the time course of hepatic CYP3A inhibition and the bioavailability of itraconazole in rats. *Drug Metab Dispos* 36(6): 1097-101.
- Raimundo, S, Fischer, J, Eichelbaum, M, Griese, EU, Schwab, M and Zanger, UM (2000). Elucidation of the genetic basis of the common 'intermediate metabolizer' phenotype for drug oxidation by CYP2D6. *Pharmacogenetics* 10(7): 577-81.
- Rebsamen, MC, Desmeules, J, Daali, Y, Chiappe, A, Diemand, A, Rey, C, Chabert, J, Dayer, P, Hochstrasser, D and Rossier, MF (2008). The AmpliChip CYP450 test: cytochrome P450 2D6 genotype assessment and phenotype prediction. *Pharmacogenomics J*.
- Reidy, JJ, Limberg, M and Kaufman, HE (1990). Delivery of fluorescein to the anterior chamber using the corneal collagen shield. *Ophthalmology* 97(9): 1201-3.

## REFERENCES:

- Reitsma, PH, van der Heijden, JF, Groot, AP, Rosendaal, FR and Buller, HR (2005). A C1173T dimorphism in the VKORC1 gene determines coumarin sensitivity and bleeding risk. *PLoS Med* 2(10): e312.
- Rodrigues, AD, Roberts, EM, Mulford, DJ, Yao, Y and Ouellet, D (1997). Oxidative metabolism of clarithromycin in the presence of human liver microsomes. Major role for the cytochrome P4503A (CYP3A) subfamily. *Drug Metab Dispos* 25(5): 623-30.
- Rodvold, KA (1999). Clinical pharmacokinetics of clarithromycin. *Clin Pharmacokinet* 37(5): 385-98.
- Roos, JF, Kirkpatrick, CM, Tett, SE, McLachlan, AJ and Duffull, SB (2008). Development of a sufficient design for estimation of fluconazole pharmacokinetics in people with HIV infection. *Br J Clin Pharmacol* 66(4): 455-66.
- Roskopf, D and Michel, MC (2008). Pharmacogenomics of G Protein-Coupled Receptor Ligands in Cardiovascular Medicine. *Pharmacol Rev*.
- Rougier, F, Claude, D, Maurin, M, Sedoglavic, A, Ducher, M, Corvaisier, S, Jelliffe, R and Maire, P (2003). Aminoglycoside nephrotoxicity: modeling, simulation, and control. *Antimicrob Agents Chemother* 47(3): 1010-6.
- Rousseau, A, Leger, F, Le Meur, Y, Saint-Marcoux, F, Paintaud, G, Buchler, M and Marquet, P (2004). Population pharmacokinetic modeling of oral cyclosporin using NONMEM: comparison of absorption pharmacokinetic models and design of a Bayesian estimator. *Ther Drug Monit* 26(1): 23-30.
- Rowland, M and Tozer, TN (1989). Clinical Pharmacokinetics: Concepts and Applications, 2nd edn. Lea & Febiger, Philadelphia, PA.
- Roy, SD, Hawes, EM and Midha, KK (1987). Influence of urinary pH on the disposition of methoxyphenamine and three metabolites in humans. *J Pharm Sci* 76(6): 427-32.
- Rubinstein, E and Camm, J (2002). Cardiotoxicity of fluoroquinolones. *J Antimicrob Chemother* 49(4): 593-6.
- Russmann, S, Dilger, K, Trenk, D, Nagyivanyi, P and Jahnchen, E (2001). Effect of lysine clonixinate on the pharmacokinetics and anticoagulant activity of phenprocoumon. *Arzneimittelforschung* 51(11): 891-5.
- Sachse, C, Brockmoller, J, Bauer, S and Roots, I (1997). Cytochrome P450 2D6 variants in a Caucasian population: allele frequencies and phenotypic consequences. *Am J Hum Genet* 60(2): 284-95.
- Schalekamp, T, Brasse, BP, Roijers, JF, Chahid, Y, van Geest-Daalderop, JH, de Vries-Goldschmeding, H, van Wijk, EM, Egberts, AC and de Boer, A (2006). VKORC1 and CYP2C9 genotypes and acenocoumarol anticoagulation status: interaction between both genotypes affects overanticoagulation. *Clin Pharmacol Ther* 80(1): 13-22.
- Schalekamp, T, Brasse, BP, Roijers, JF, van Meegen, E, van der Meer, FJ, van Wijk, EM, Egberts, AC and de Boer, A (2007). VKORC1 and CYP2C9 genotypes and phenprocoumon anticoagulation status: interaction between both genotypes affects dose requirement. *Clin Pharmacol Ther* 81(2): 185-93.
- Schalekamp, T, Oosterhof, M, van Meegen, E, van Der Meer, FJ, Conemans, J, Hermans, M, Meijerman, I and de Boer, A (2004). Effects of cytochrome P450 2C9 polymorphisms on phenprocoumon anticoagulation status. *Clin Pharmacol Ther* 76(5): 409-17.
- Schmider, J, Greenblatt, DJ, Fogelman, SM, von Moltke, LL and Shader, RI (1997). Metabolism of dextromethorphan in vitro: involvement of cytochromes P450 2D6 and 3A3/4, with a possible role of 2E1. *Biopharm Drug Dispos* 18(3): 227-40.
- Schoemaker, RC and Cohen, AF (1996). Estimating impossible curves using NONMEM. *Br J Clin Pharmacol* 42(3): 283-90.

## REFERENCES:

- Schoenwald, RD (1990). Ocular drug delivery. Pharmacokinetic considerations. *Clin Pharmacokinet* 18(4): 255-69.
- Schraermeyer, U, Diestelhorst, M, Bieker, A, Theisohn, M, Mietz, H, Ustundag, C, Joseph, G and Krieglstein, GK (1999). Morphologic proof of the toxicity of mitomycin C on the ciliary body in relation to different application methods. *Graefes Arch Clin Exp Ophthalmol* 237(7): 593-600.
- Sconce, EA, Khan, TI, Wynne, HA, Avery, P, Monkhouse, L, King, BP, Wood, P, Kesteven, P, Daly, AK and Kamali, F (2005). The impact of CYP2C9 and VKORC1 genetic polymorphism and patient characteristics upon warfarin dose requirements: proposal for a new dosing regimen. *Blood* 106(7): 2329-33.
- Scordo, MG and Spina, E (2002). Cytochrome P450 polymorphisms and response to antipsychotic therapy. *Pharmacogenomics* 3(2): 201-18.
- Seeringer, A and Kirchheiner, J (2008). Pharmacogenetics-guided dose modifications of antidepressants. *Clin Lab Med* 28(4): 619-26.
- Sheiner, LB (1969). Computer-aided long-term anticoagulation therapy. *Comput Biomed Res* 2(6): 507-18.
- Sheiner, LB and Beal, SL (1980). Evaluation of methods for estimating population pharmacokinetics parameters. I. Michaelis-Menten model: routine clinical pharmacokinetic data. *J Pharmacokinet Biopharm* 8(6): 553-71.
- Sheiner, LB and Ludden, TM (1992). Population pharmacokinetics/dynamics. *Annu Rev Pharmacol Toxicol* 32: 185-209.
- Shen, H, He, MM, Liu, H, Wrighton, SA, Wang, L, Guo, B and Li, C (2007). Comparative metabolic capabilities and inhibitory profiles of CYP2D6.1, CYP2D6.10, and CYP2D6.17. *Drug Metab Dispos* 35(8): 1292-300.
- Silvasti, M, Karttunen, P, Tukiainen, H, Kokkonen, P, Hanninen, U and Nykanen, S (1987). Pharmacokinetics of dextromethorphan and dextrorphan: a single dose comparison of three preparations in human volunteers. *Int J Clin Pharmacol Ther Toxicol* 25(9): 493-7.
- Sistonen, J, Sajantila, A, Lao, O, Corander, J, Barbuajani, G and Fuselli, S (2007). CYP2D6 worldwide genetic variation shows high frequency of altered activity variants and no continental structure. *Pharmacogenet Genomics* 17(2): 93-101.
- Spreafico, M, Lodigiani, C, van Leeuwen, Y, Pizzotti, D, Rota, LL, Rosendaal, F, Mannucci, PM and Peyvandi, F (2008). Effects of CYP2C9 and VKORC1 on INR variations and dose requirements during initial phase of anticoagulant therapy. *Pharmacogenomics* 9(9): 1237-50.
- Stehle, S, Kirchheiner, J, Lazar, A and Fuhr, U (2008). Pharmacogenetics of oral anticoagulants: a basis for dose individualization. *Clin Pharmacokinet* 47(9): 565-94.
- Steimer, W, Zopf, K, von Amelunxen, S, Pfeiffer, H, Bachofer, J, Popp, J, Messner, B, Kissling, W and Leucht, S (2004). Allele-specific change of concentration and functional gene dose for the prediction of steady-state serum concentrations of amitriptyline and nortriptyline in CYP2C19 and CYP2D6 extensive and intermediate metabolizers. *Clin Chem* 50(9): 1623-33.
- Steinfeld, A, Lux, A, Maier, S, Suverkrup, R and Diestelhorst, M (2004). Bioavailability of fluorescein from a new drug delivery system in human eyes. *Br J Ophthalmol* 88(1): 48-53.
- Sturgill, MG and Rapp, RP (1992). Clarithromycin: review of a new macrolide antibiotic with improved microbiologic spectrum and favorable pharmacokinetic and adverse effect profiles. *Ann Pharmacother* 26(9): 1099-108.

## REFERENCES:

- Sutherland, S (2005). Massive variability in a stable binding protein. *Drug Discov Today* 10(23-24): 1580.
- Suverkrup, R (1985). Segmentally continuous input functions in linear multicompartement systems. *J Pharm Sci* 74(2): 136-41.
- Suverkrup, R, Grunthal, S, Krasichkova, O, Maier, S, Weichselbaum, A, Neff, B, Diestelhorst, M, Dinslage, S and Lux, A (2004). The ophthalmic lyophilisate carrier system (OLCS): development of a novel dosage form, freeze-drying technique, and in vitro quality control tests. *Eur J Pharm Biopharm* 57(2): 269-77.
- Suverkrup, R, Weichselbaum, A and Diestelhorst, M (1999). Pilocarpine dry drops: miotic effect and discomfort upon administration compared to conventional eye drops. *IOVS Supl* 40(4):85.
- Suzuki, A, Iida, I, Hirota, M, Akimoto, M, Higuchi, S, Suwa, T, Tani, M, Ishizaki, T and Chiba, K (2003). CYP isoforms involved in the metabolism of clarithromycin in vitro: comparison between the identification from disappearance rate and that from formation rate of metabolites. *Drug Metab Pharmacokinet* 18(2): 104-13.
- Taft, DR, Iyer, GR, Behar, L and DiGregorio, RV (1997). Application of a first-pass effect model to characterize the pharmacokinetic disposition of venlafaxine after oral administration to human subjects. *Drug Metab Dispos* 25(10): 1215-8.
- Tang-Liu, DD, Liu, S, Neff, J and Sandri, R (1987). Disposition of levobunolol after an ophthalmic dose to rabbits. *J Pharm Sci* 76(10): 780-3.
- Tang-Liu, DD, Liu, SS and Weinkam, RJ (1984). Ocular and systemic bioavailability of ophthalmic flurbiprofen. *J Pharmacokinet Biopharm* 12(6): 611-26.
- Taniguchi, T and Kitazawa, Y (1997). The potential systemic effect of topically applied beta-blockers in glaucoma therapy. *Curr Opin Ophthalmol* 8(2): 55-8.
- Taravella, MJ, Balentine, J, Young, DA and Stepp, P (1999). Collagen shield delivery of ofloxacin to the human eye. *J Cataract Refract Surg* 25(4): 562-5.
- Teichert, M, van Schaik, RH, Hofman, A, Uitterlinden, AG, de Smet, PA, Stricker, BH and Visser, LE (2009). Genotypes associated with reduced activity of VKORC1 and CYP2C9 and their modification of acenocoumarol anticoagulation during the initial treatment period. *Clin Pharmacol Ther* 85(4): 379-86.
- Tessier, PR, Kim, MK, Zhou, W, Xuan, D, Li, C, Ye, M, Nightingale, CH and Nicolau, DP (2002). Pharmacodynamic assessment of clarithromycin in a murine model of pneumococcal pneumonia. *Antimicrob Agents Chemother* 46(5): 1425-34.
- Thakur, AK (1991). Model: mechanistic vs. empirical. In: Rescigno A, Thakur AK, eds. *New Trends in Pharmacokinetics*, New York: Plenum Press. pp41-51.
- Thummel, KE, O'Shea, D, Paine, MF, Shen, DD, Kunze, KL, Perkins, JD and Wilkinson, GR (1996). Oral first-pass elimination of midazolam involves both gastrointestinal and hepatic CYP3A-mediated metabolism. *Clin Pharmacol Ther* 59(5): 491-502.
- Tomalik-Scharte, D, Lutjohann, D, Doroshenko, O, Frank, D, Jetter, A and Fuhr, U (2009). Plasma 4beta-hydroxycholesterol: an endogenous CYP3A metric? *Clin Pharmacol Ther* 86(2): 147-53.
- Toon, S, Heimark, LD, Trager, WF and O'Reilly, RA (1985). Metabolic fate of phenprocoumon in humans. *J Pharm Sci* 74(10): 1037-40.
- Traunmuller, F, Zeitlinger, M, Zeleny, P, Muller, M and Joukhadar, C (2007). Pharmacokinetics of single- and multiple-dose oral clarithromycin in soft tissues determined by microdialysis. *Antimicrob Agents Chemother* 51(9): 3185-9.

## REFERENCES:

- Trenk, D, Althen, H, Jahnchen, E, Meinertz, T and Oie, S (1987). Factors responsible for interindividual differences in the dose requirement of phenprocoumon. *Eur J Clin Pharmacol* 33(1): 49-54.
- Tucker, GT (2000). Advances in understanding drug metabolism and its contribution to variability in patient response. *Ther Drug Monit* 22(1): 110-3.
- Ufer, M (2005a). Comparative pharmacokinetics of vitamin K antagonists: warfarin, phenprocoumon and acenocoumarol. *Clin Pharmacokinet* 44(12): 1227-46.
- Ufer, M (2005b). Effects of CYP2C9 polymorphisms on phenprocoumon anticoagulation status. *Clin Pharmacol Ther* 77(4): 335-6; author reply 336.
- Ufer, M, Kammerer, B, Kahlich, R, Kirchheiner, J, Yasar, U, Brockmoller, J and Rane, A (2004a). Genetic polymorphisms of cytochrome P450 2C9 causing reduced phenprocoumon (S)-7-hydroxylation in vitro and in vivo. *Xenobiotica* 34(9): 847-59.
- Ufer, M, Kammerer, B, Kirchheiner, J, Rane, A and Svensson, JO (2004b). Determination of phenprocoumon, warfarin and their monohydroxylated metabolites in human plasma and urine by liquid chromatography-mass spectrometry after solid-phase extraction. *J Chromatogr B Analyt Technol Biomed Life Sci* 809(2): 217-26.
- Ufer, M, Svensson, JO, Krausz, KW, Gelboin, HV, Rane, A and Tybring, G (2004c). Identification of cytochromes P450 2C9 and 3A4 as the major catalysts of phenprocoumon hydroxylation in vitro. *Eur J Clin Pharmacol* 60(3): 173-82.
- Urtti, A (2006). Challenges and obstacles of ocular pharmacokinetics and drug delivery. *Adv Drug Deliv Rev* 58(11): 1131-5.
- Urtti, A, Pipkin, JD, Rork, G and Repta, AJ (1990). Controlled drug delivery devices for experimental ocular studies with timolol. 1. In vitro release studies. *Int J Pharm* 61:235-240. *Int J Pharm* 61: 235-240.
- Ushiyama, H, Echizen, H, Nachi, S and Ohnishi, A (2002). Dose-dependent inhibition of CYP3A activity by clarithromycin during *Helicobacter pylori* eradication therapy assessed by changes in plasma lansoprazole levels and partial cortisol clearance to 6beta-hydroxycortisol. *Clin Pharmacol Ther* 72(1): 33-43.
- Van de Waterbeemd, H, Lennernäs, H and Artursson, P (2004). Drug Bioavailability. Estimation of Solubility, Permeability, Absorption, and Bioavailability. Vol. 18. Wiley-VCH, Hoboken, NJ.
- van der Marel, CD, Anderson, BJ, van Lingen, RA, Holford, NH, Pluim, MA, Jansman, FG, van den Anker, JN and Tibboel, D (2003). Paracetamol and metabolite pharmacokinetics in infants. *Eur J Clin Pharmacol* 59(3): 243-51.
- Verotta, D, Beal, SL and Sheiner, LB (1989). Semiparametric approach to pharmacokinetic-pharmacodynamic data. *Am J Physiol* 256(4 Pt 2): R1005-10.
- Vincent, JL, Spapen, HD, Creteur, J, Piagnerelli, M, Hubloue, I, Diltoer, M, Roman, A, Stevens, E, Vercammen, E and Beaver, JS (2006). Pharmacokinetics and pharmacodynamics of once-weekly subcutaneous epoetin alfa in critically ill patients: results of a randomized, double-blind, placebo-controlled trial. *Crit Care Med* 34(6): 1661-7.
- Wade, JR, Kelman, AW, Howie, CA and Whiting, B (1993). Effect of misspecification of the absorption process on subsequent parameter estimation in population analysis. *J Pharmacokinet Biopharm* 21(2): 209-22.
- Wadelius, M, Chen, LY, Lindh, JD, Eriksson, N, Ghori, MJ, Bumpstead, S, Holm, L, McGinnis, R, Rane, A and Deloukas, P (2009). The largest prospective warfarin-treated cohort supports genetic forecasting. *Blood* 113(4): 784-92.

## REFERENCES:

- Wang, J, Weiss, M and D'Argenio, DZ (2008). A note on population analysis of dissolution-absorption models using the inverse Gaussian function. *J Clin Pharmacol* 48(6): 719-25.
- Wang, Y, Eskridge, KM and Zhang, S (2008). Semiparametric mixed-effects analysis of PK/PD models using differential equations. *J Pharmacokinet Pharmacodyn* 35(4): 443-63.
- Wang, YM and Reuning, RH (1992). An experimental design strategy for quantitating complex pharmacokinetic models: enterohepatic circulation with time-varying gallbladder emptying as an example. *Pharm Res* 9(2): 169-77.
- Wang, ZJ, Yin, OQ, Tomlinson, B and Chow, MS (2008). OCT2 polymorphisms and in-vivo renal functional consequence: studies with metformin and cimetidine. *Pharmacogenet Genomics* 18(7): 637-45.
- Weiss, M (1988). A general model of metabolite kinetics following intravenous and oral administration of the parent drug. *Biopharm Drug Dispos* 9(2): 159-76.
- Weiss, M (1998). Analysis of metabolite formation pharmacokinetics after intravenous and oral administration of the parent drug using inverse Laplace transformation. *Drug Metab Dispos* 26(6): 562-5.
- Werner, D, Werner, U, Meybaum, A, Schmidt, B, Umbreen, S, Grosch, A, Lestin, HG, Graf, B, Zolk, O and Fromm, MF (2008). Determinants of steady-state torasemide pharmacokinetics: impact of pharmacogenetic factors, gender and angiotensin II receptor blockers. *Clin Pharmacokinet* 47(5): 323-32.
- Werner, D, Werner, U, Wuerfel, A, Grosch, A, Lestin, HG, Eschenhagen, T and Rau, T (2009). Pharmacogenetic characteristics of patients with complicated phenprocoumon dosing. *Eur J Clin Pharmacol*.
- Williams, PJ and Ette, EI (2007). Pharmacometrics: impacting drug development and pharmacotherapy. In: Ette EI, Williams PJ (ed.) *Pharmacometrics; the science of quantitative pharmacology*. John Wiley & Sons, Inc., New Jersey. pp. 1-21.
- Williams, PJ, Kim, YH and Ette, EI (2007). The epistemology of pharmacometrics. In: Ette EI, Williams PJ (ed.) *Pharmacometrics; the science of quantitative pharmacology*. John Wiley & Sons, Inc., New Jersey. pp. 223-244.
- Williams, PJ, Lane, JR, Turkel, CC, Capparelli, EV, Dziewanowska, Z and Fox, AW (2001). Dichloroacetate: population pharmacokinetics with a pharmacodynamic sequential link model. *J Clin Pharmacol* 41(3): 259-67.
- Willmann, S, Schmitt, W, Keldenich, J, Lippert, J and Dressman, JB (2004). A physiological model for the estimation of the fraction dose absorbed in humans. *J Med Chem* 47(16): 4022-31.
- Wyen, C, Fuhr, U, Frank, D, Aarnoutse, R, Klaassen, T, Lazar, A, Seeringer, A, Doroshenko, O, Kirchheiner, J, Abdulrazik, F, Schmeisser, N, Lehmann, C, Hein, W, Schomig, E, Burger, D, Fatkenheuer, G and Jetter, A (2008). Effect of an Antiretroviral Regimen Containing Ritonavir Boosted Lopinavir on Intestinal and Hepatic CYP3A, CYP2D6 and P-glycoprotein in HIV-infected Patients. *Clin Pharmacol Ther*.
- Yamamoto, F, Harada, S, Mitsuyama, T, Harada, Y, Kitahara, Y, Yoshida, M and Nakanishi, Y (2004). Concentration of clarithromycin and 14-R-hydroxy-clarithromycin in plasma of patients with Mycobacterium avium complex infection, before and after the addition of rifampicin. *Jpn J Antibiot* 57(1): 124-33.
- Yeh, GC, Tao, PL, Ho, HO, Lee, YJ, Chen, JY and Sheu, MT (2003). Analysis of pharmacokinetic parameters for assessment of dextromethorphan metabolic phenotypes. *J Biomed Sci* 10(5): 552-64.



## REFERENCES:

- Yin, OQ, Tomlinson, B and Chow, MS (2006). Variability in renal clearance of substrates for renal transporters in Chinese subjects. *J Clin Pharmacol* 46(2): 157-63.
- Yu, A and Haining, R (2001). Comparative contribution to dextromethorphan metabolism by cytochrome P450 isoforms in vitro: can dextromethorphan be used as a dual probe for both CYP2D6 and CYP3A activities. *Drug Metab Dispos* 29(11): 1514-20.
- Yu, A and Haining, RL (2001). Comparative contribution to dextromethorphan metabolism by cytochrome P450 isoforms in vitro: can dextromethorphan be used as a dual probe for both CYP2D6 and CYP3A activities? *Drug Metab Dispos* 29(11): 1514-20.
- Yue, QY, Zhong, ZH, Tybring, G, Dalen, P, Dahl, ML, Bertilsson, L and Sjoqvist, F (1998). Pharmacokinetics of nortriptyline and its 10-hydroxy metabolite in Chinese subjects of different CYP2D6 genotypes. *Clin Pharmacol Ther* 64(4): 384-90.
- Yukawa, E and Mamiya, K (2006). Effect of CYP2C19 genetic polymorphism on pharmacokinetics of phenytoin and phenobarbital in Japanese epileptic patients using Non-linear Mixed Effects Model approach. *J Clin Pharm Ther* 31(3): 275-82.
- Yzet, T, Bouzerar, R, Baledent, O, Renard, C, Lumbala, DM, Nguyen-Khac, E, Regimbeau, JM, Meyer, ME and Deramond, H (2008). Dynamic measurements of total hepatic blood flow with Phase Contrast MRI. *Eur J Radiol*.
- Zandvliet, AS, Huitema, AD, de Jonge, ME, den Hoed, R, Sparidans, RW, Hendriks, VM, van den Brink, W, van Ree, JM and Beijnen, JH (2005). Population pharmacokinetics of caffeine and its metabolites theobromine, paraxanthine and theophylline after inhalation in combination with diacetylmorphine. *Basic Clin Pharmacol Toxicol* 96(1): 71-9.
- Zhang, L, Beal, SL and Sheiner, LB (2003a). Simultaneous vs. sequential analysis for population PK/PD data I: best-case performance. *J Pharmacokinetic Pharmacodyn* 30(6): 387-404.
- Zhang, L, Beal, SL and Sheiner, LB (2003b). Simultaneous vs. sequential analysis for population PK/PD data II: robustness of methods. *J Pharmacokinetic Pharmacodyn* 30(6): 405-16.
- Zhang, Y, Britto, MR, Valderhaug, KL, Wedlund, PJ and Smith, RA (1992). Dextromethorphan: enhancing its systemic availability by way of low-dose quinidine-mediated inhibition of cytochrome P450 2D6. *Clin Pharmacol Ther* 51(6): 647-55.
- Zhou, H (2003). Pharmacokinetic strategies in deciphering atypical drug absorption profiles. *J Clin Pharmacol* 43(3): 211-27.
- Zhou, S, Yung Chan, S, Cher Goh, B, Chan, E, Duan, W, Huang, M and McLeod, HL (2005). Mechanism-based inhibition of cytochrome P450 3A4 by therapeutic drugs. *Clin Pharmacokinetic* 44(3): 279-304.
- Zhou, SF, Liu, JP and Chowbay, B (2009). Polymorphism of human cytochrome P450 enzymes and its clinical impact. *Drug Metab Rev* 41(2): 89-295.
- Zimmerman, TJ, Kooner, KS, Kandarakis, AS and Ziegler, LP (1984). Improving the therapeutic index of topically applied ocular drugs. *Arch Ophthalmol* 102(4): 551-3.

## 8 ACKNOWLEDGMENTS

This work has been carried out in the Department of Pharmacology, University of Cologne during the years 2006-2008.

I wish to express my deepest gratitude to my supervisor Prof. Dr. Uwe Fuhr, without whom this work would never have been possible. I thank him for introducing me to the fascinating world of population pharmacokinetics and pharmacodynamics and for the guidance, encouragement, patience, and brilliant ideas he has provided for me throughout my work. He created an enjoyable work atmosphere that was incomparable. I would like to thank him for optimizing the content of this work and for the helpful suggestions he provided. I thank him again for his advice, constant support and for making me and my family feel at home in Germany.

I am deeply grateful to Prof. Dr. Richard Süverkrüp, who gave me the opportunity to attain my PhD degree in Pharmacy from the University of Bonn, where I had the privilege to enjoy excellent working facilities and his expertise. He is also gratefully acknowledged for welcoming me as a student under his supervision. I will never forget his valuable advice and all the amusing conversations we had. He is acknowledged for his careful review and valuable comments that led to considerable improvements of this thesis.

My sincere thanks also go to Prof. Dr. Michael Diestelhorst (Department of Ophthalmology, University of Cologne; Germany) and Prof. Fritz Sörgel (Institute for Biomedical and Pharmaceutical Research, Nürnberg-Heroldsberg; Germany) for giving me access to their clinical data for fluorescein and clarithromycin. In addition, I wish to thank Dr. Jurgen Bulitta for his helpful Perl script, which I used during evaluation and improvement of the developed models.

I also wish to thank all my colleagues at the institute of pharmacology, university of Cologne for their assistance during my work and for providing me with the necessary breaks from

## ACKNOWLEDGMENTS

work. Thanks also to Dr. Helen Cubitt, for valuable proofreading and elimination of potential grammatical errors.

Last but not least, my warmest thanks go to my parents for their patience and tolerance of my frequent and long absences. Most of all, I thank my wife, for her patience and support during these years of hard work and for reminding me that there is life outside of "Population Pharmacokinetics".

## 9 CURRICULUM VITAE

**Full name:** Khaled Mohammed Abdulwahab Abduljalil

### Education & Qualifications:

#### **12/2008 – Present**

SimCYP Ltd, Research Scientist:

SimCYP's *in vitro-in vivo* extrapolation intensive educational program (hands-on workshops)

MSc course in modelling and simulation in pharmacokinetics and pharmacodynamics (launched by Sheffield University)

#### **2006- 2008**

PhD-Student, Bonn University, Germany

Working place: Institute of Pharmacology, Cologne University

Doctoral Thesis: "Advanced Pharmacokinetic Modelling to Quality Selected Characteristics of Drugs"

#### **2004-2005**

Diploma in Pharmacy, Bonn University, Germany

#### **2001-2003**

Pharmacology Demonstrator, Faculty of Medicine, Tamar University, Yemen

#### **1995-2000**

Bachelor's Degree of Pharmacy, Sana'a University, Yemen

### Original Articles

**Abduljalil K**, Diestelhorst M, Doroshyenko O, Lux A, Steinfeld A, Dinslage S, Süverkrüp R, Fuhr U. Modelling ocular pharmacokinetics of fluorescein administered as lyophilisate or conventional eye drops. *Eur J Clin Pharmacol*. 2008;64(5):521-9.

**Abduljalil K**, Kinzig M, Bulitta J, Horkovics-Kovats S, Sörgel F, Rodamer M, Fuhr U. Modeling the autoinhibition of clarithromycin metabolism during repeated oral administration. *Antimicrob Agents Chemother*. 2009;53(7):2892-901.

Kohl V, Mueller C, Cornely OA, **Abduljalil K**, Fuhr U, Vehreschild JJ, Scheid C, Hallek M, Rueping MJGT. Factors influencing pharmacokinetics of prophylactic posaconazole in patients undergoing allogeneic stem cell transplantation. *Antimicrob Agents Chemother*. 2010;54(1):207-12.

## CURRICULUM VITAE

**Abduljalil K**, Frank D, Gaedigk A, Klaasse T, Tomalik-Scharte D, Jetter A, Jaehde U, Kirchheiner J, Fuhr U. Activity assessment for individual CYP2D6 alleles by population pharmacokinetics of dextromethorphan. To be submitted to Clin Pharmacol Ther

**Abduljalil K**, Stehle S, Zadoyan G, Schwab M, Lazar A, Tomalik-Scharte D, Kirchheiner J, Gleiter C, Harenberg J, Wu W, Fuhr U. Prospective evaluation of the pharmacogenetic component in pharmacokinetics and pharmacodynamics of steady state phenprocoumon. To be submitted to Clin Pharmacol Ther

### **Work Experience:**

**2000** Aloin and Emodin, extraction, antimicrobial activity and wound healing (BA graduate project).

**2001-2003** Pharmacology Demonstrator, Faculty of Medicine, Tamar University, Yemen

**2003** Medical Plants in Yemen; active constituents and pharmacological effects (Seminar, Tamar University).

**2004-2005:** The absorption window of Digoxin; A deconvolution study using WinNonlin program (Diploma Thesis).

**2006-2008:** Population pharmacokinetics and data fitting (Cologne University, Germany)

### **2008-present:**

Different duties including

- PK-PD evaluations and simulations for different population
- Drug-drug interaction and clinical trial simulations
- SimCYP simulator development and validations,
- Consultancy services to clients,
- Extrapolating data from in vitro studies, and
- Development of PBPK models for pregnancy and paediatrics

### **Seminars**

**12.01.2006:** Interpretation of digoxin absorption profiles (Seminar, Bonn University)

**15.07.2007:** Ophthalmic population pharmacokinetic model for fluorescein in man (Seminar, Cologne University)

**17.06.2008:** Application of modelling complex pharmacokinetic processes; a population pharmacokinetic study of clarithromycin (Seminar, Cologne University)

**18.11.2008:** Quantifying Individual CYP2D6 Alleles Activity Using Dextromethorphan as Model Probe; A population pharmacokinetic analysis (Seminar, Cologne University)

**20.12.2009:** Phenprocoumon population PK-PD; preliminary results from a prospective study.

(Seminar, Cologne University)

**02.07.2009:** Assessing CYP2D6 enzyme activity in vivo; different metric systems and clinical consequences. (Seminar, SIMCYP, UK)

**12.09.2009:** Prediction of plasma concentration profiles of CYP450s substrates from in vitro studies; the role of individual pharmacogenetics. (Seminar, SIMCYP consortium meeting, UK)

**Additional Information:**

**Languages:**

Arabic: Mother Language

English: very good

German: good

**Computer Knowledge:**

Experienced user of Microsoft office

Essential Programming skills: Python, S-language, Fortran, R

**Softwares:**

NONMEM: more than three years working knowledge

WinNonlin: more than three years working knowledge

SIMCYP: more than one year working knowledge

Others: ADAPT, PDx-MCPEM, PadPrism, Monolix, SPSS, S-Plus, SigmaPlot, Enzyme Kinetics,